UNIVERSITÀ
POLITECNICA
DELLE MARCHE

Department of Life and Environmental Sciences

PhD course in Life and Environmental Sciences
Marine Biology and Ecology
XV cycle

Heavy metals in the Antarctic marine environment and correlated systems

PhD student
Giulia Libani

Tutor
Prof.ssa Cristina Truzzi

Co-tutor
Prof. Giuseppe Scarponi

Dr.ssa Silvia Illuminati

Academic years 2013-2016

TABLE OF CONTENTS

Abstract

Within the framework of the Italian Antarctic Programme, this work focuses on the evaluation of metal distribution in seawater with particularly attention paid to phytoplankton and to the processes that regulate this distribution, considering also the influences of other matrices (e.g. atmospheric aerosol).

Heavy metals can be transported over long distances and once they reach ocean's surface, their distributions are controlled by their interaction with particulate matter suspended in water column. In particular, the distribution can be influenced by the presence of the algal component.

Cd, Pb and Cu have been selected for this work because two of them (Cd and Pb) are considered priority pollutants (PP) by regulation in force (European Parliament and Council of European Union, Directive 2000/60/EC) and the third one (Cu) is an element of interest, being a micronutrient for phytoplankton and so with potential differences on bioaccumulation in comparison to Cd and Pb.

During the XXIX Italian Antarctic Expedition (austral summer 2013-2014) samples of seawater were collected in the Gerlache Inlet area, Terra Nova Bay (TNB), from about mid-November 2013 to mid-February 2014. Seawater samples were divided in aliquots subjected to different treatments for the determination of total metal concentration, and of the principal metal fractions (metal dissolved fraction, total metal particulate fraction and metal fraction associated to phytoplankton). The metal fraction associated to phytoplankton was obtained through a procedure previously set-up based on a physical separation of phytoplanktonic cells from the raw sea water samples using an inverted optical microscope. After microwave digestion (MW) the determination of Cd, Pb and Cu in seawater and phytoplankton samples were carried out by Square Wave Anodic Stripping Voltammetry (SWASV). To better characterize the seawater column, several hydrologic parameters were determined along the water column and nutrients [NO_3^-, NO_2^-, NH_4^+, PO_4^{3-}, $Si(OH)_4$] in seawater samples were measured with colorimetric and spectrophotometric methods.

Six samples of atmospheric particulate matter (PM10) and five blank filters were collected every 10 days from the beginning of December 2013 to the beginning of February 2014, at Faraglione Camp. Aliquots of the original filters were subjected to a sequential extraction procedure to determine two different metal fractions (water soluble and insoluble) correlated to different metal sources. After MW digestion Cd, Pb and Cu were measured by Graphite Furnace Atomic Absorption Spectrometry (GFAAS). To test the additivity measurements of the two metal fractions with respect to the total content, another aliquot of the original filters was directly MW digested to obtain the total metal content.

The separation of the algal fraction from the particulate phase let us to better understand heavy metals distribution between dissolved and particulate fractions along the water column. In general, metals associated to the algal particulate varied with depth and during the season and the highest values were measured at the surface and in presence of the phytoplankton bloom. In seawater cadmium was dominated by its dissolved species and its vertical distribution was a typical nutrient-like profile, with a surface depletion of Cd by phytoplankton and a recycling along the water column. Copper distribution was also strongly affected by phytoplankton: in fact in November it showed a quite homogenous vertical profile, with the dominance of the dissolved fraction. Starting from December, when Chl-*a* started to increase (as a result of phytoplankton activity), it showed a net decrease in the surface (similar to a nutrient-like element) but no evidence for a maximum in deep layers (recycling), highlighting a hybrid profile. Lead (for which we suspect sample contamination in a few cases) features the typical distribution of a scavenged element, at least at the end of the season, with the particulate fraction generally prevailing. Its distribution was affected by several factors, with the phytoplankton which influenced its behaviour only partially.

Metal distributions were affected to some extent also by atmospheric aerosol input.

1. Introduction

1.1 Antarctica: geographical and climate aspects of the continent

Antarctica is one of the most pristine areas in the word, it is situated in the Antarctic region of the Southern hemisphere, surrounded by the Southern Ocean. It can be divided into three major areas: West Antarctica, East Antarctica and the Antarctic Peninsula, and running along the length of the peninsula, there is a mountain known as the Transantarctic Mountains, which divides the East and West Antarctic ice sheets. Antarctic surface has an area of 13.8 million km^2, covered for 98% of ice, with a total volume today of 27 million km^3. Antarctica is covered by a sheet of ice that is, on average, a mile thick or more (2.45 km), and contains 90% of the world's ice and more than 70% of its fresh water, which regulates the sea level, the ocean currents, the atmospheric dynamics and affects the climate on global scale. It is warming rapidly, this is particularly evident around the Antarctic Peninsula, but also across the West Antarctic Ice Sheet. This warming is associated with the increase of ocean temperatures, changes to atmospheric circulation, and incursions of warm circumpolar deep water into the continental shelf. The Antarctic Peninsula is one of the most rapidly warming locations on Earth. The highest temperature ever recorded in Antarctica was 17.5 °C (63.5 °F) at Hope Bay on 24 March 2015, the lowest one of −89.2 °C was on 21 July 1983 at Vostok Station. East Antarctica is colder than West Antarctica because of its higher elevation, on the other way the Antarctic Peninsula has a most moderate climate. The strong winds, called katabatic, formed by cold, dense air flowing out from the polar plateau down the steep vertical drops along the coast, reach up to 300 km/h and become frequent during spring season.

Katabatic winds, which originate over the Antarctic continental plateau and blown offshore, form the wind-driven flaw polynya as they shift the newly-formed ice far from the coasts.

For the minimum precipitations, the lowest temperatures, the strong winds, the great ice sheets and floating sea ice extension, and the high dryness air, this continent is classified as a desert, making it the most inhospitable place in the world. The limit of this region coincides with the Antarctic convergence, defined as the line at the surface along which Antarctic surface water sinks below the less dense sub-Antarctic water, and it is distinguished by a more or less sharp change of temperature at the surface (Marckintosh, 1946). The Antarctic convergence is not stationary, although its position varies within narrow margins (about 100 km), it is a natural boundary, which contributes actively to the biological isolation and, on the other way, the dispersal larvae is quite limited; some studies on invertebrates showed that the most effective dispersal mechanism are pelagic-benthic modes, rafting, and less extent from anthropogenic transport (Thatje, 2012).

1.2 The Southern Ocean and the Ross Sea

The Southern Ocean consists of the ocean surrounding Antarctica across all degrees of longitude and up to a northern boundary at 60° South latitude. It is an enormous body of water that surrounds the entire continent of Antarctica and reaches Australia and the southern end of South America.

This ocean is a smaller body of water compared to the Pacific, Atlantic and Indian Oceans, but is bigger than the Arctic Ocean. It covers approximately 4% of the earth's surface. It includes Amundsen Sea, Bellingshausen Sea, part of the Drake Passage, Ross Sea, a small part of the Scotia Sea, Weddell Sea, and other water bodies. The Southern Ocean has typical depths of 4000 and 5000 m, with the greatest depth of 7235 m. The Antarctic ice is ticker with the advance of the winter season for gradual freezing of the water layer at the interface between sea and ice already consolidated. During the phase of the "pack", the ice begins to form near the coast, going to expand later to sea. The ecology and the biogeography of the Southern Ocean are influenced strongly by the Antarctic circumpolar current (ACC), a system of ocean currents which flows from west to east, mainly or entirely wind-driven (Colton and Chase, 1985), and where its path is considered to be influenced by seabed topography (Lazarus and Caulet, 1993); it has a mean transport of 100-150 Sverdrup, making it the largest ocean current (Smith et al. 2003). ACC**,** which continuously surrounds the continent, is the current that moves the greater mass of the planet's water reaching depths between the 2000 and the 4000 meters and a width of about 2000 km. Along the circumpolar current there is an energy exchange, and the area that best expresses these phenomena is the Antarctic Convergence where the very cold Antarctic surface water, but of lesser salinity, meets the surface sub-antarctic water warmer and saltier**.** Since there are no continental barriers in this region, standard Sverdrup dynamics, describing gyre circulations in other ocean, are difficult to apply in this region, and when the current flows within the Drake passage (between Cape Horn and Antarctic Peninsula) because of the physical constriction of the passage, the current increases rapidly in velocity, indeed it has been report a mean transport through Drake Passage of 134 Sv (Whitworth and Peterson, 1986). Oceanic phytoplankton account for about half of the global primary production, and one area with great importance for increasing primary production is the Antarctic Circumpolar Current (ACC). As concentrations of nitrate and phosphate are high, thanks to upwelling, primary production is limited by other factors (Moore et al., 2000, Priddle et al., 1992), productivity is thought to be controlled by light availability (Mitchell and Brody, 1991), iron supply (Martin, 1990), silicate limitation (Brzezinski et al., 2003) and the effect of grazing (Atkinson et al., 2001, Dubischar and Bathmann 1997). The knowledge of potential factors controlling bloom dynamics are complicated by the fact that these different factors tend to co-vary and also interact

with each other (e.g. iron limitation decreases photo adaptive capabilities, thereby affecting light limitation) (Sunda and Huntsman 1997, Petrou et al., 2014).

Antarctica is poor in iron because this metal generally comes from continental erosion and wind transport, but in this continent the rock erosion is prevented by the ice cover, indeed the term "Antarctic paradox" is used to describe the phenomenon of vast areas of the Southern Ocean that contain plenty of nutrients for phytoplankton, but still they are low and constant in spite of high macro-nutrient concentrations. These areas are called as HNLC (high nutrient, low chlorophyll).

The Ross Sea is a deep bay of the Southern Ocean, of which the southernmost part is covered by the Ross Ice Shelf, the largest in the world, with an area of 182000 square miles (472000 km^2). The front of the Ross Ice Shelf has an average thickness of 330 meters, reaching 700 meters to the coast. The Ross Ice Shelf pushes out into the sea at the rate of between 1.5 and 3 m a day. This is one of the less cold seas of Antarctica, with a temperature that ranges between -1 °C and +1 °C, while the salinity varies depending on the water depth between 33 and 34.7 psu (Corami et al., 2005). The western part of the Ross Sea is constantly hit by katabatic winds that descend from the Antarctic plateau and pushing off the ice as in the case of Terra Nova Bay. In this area, the colder water masses with a high salinity sink because of their greater density. Physical forcing, including advective circulation, vertical mixing, and vertical stratification, may be the primary factor producing observed vertical and horizontal variability in phytoplankton distribution as well as primary production in the Ross Sea. The dynamics of the waters of the Ross sea has a high complexity due to the variable shape of the seabed and for the remix of different types of water.

1.3 Phytoplankton in the Ross Sea

The term plankton was coined by Victor Hensen to identify all the microorganism that are not capable of independent movement. Phytoplankton is the autotrophic component of the plankton community, it is the key of the ocean, thanks to their primary production (PP). Through PP phytoplankton use solar energy to combine water and carbon dioxide into organic compounds that will be available to higher trophic levels. The photosynthesis process essentially consists of a series of reactions that are dependent on light (the conversion of solar radiation into chemical energy, “light” reactions) and others independent of light (“dark” reactions) in which organic compounds are formed. They are photosynthesizing microscopic organisms that inhabit the upper layer (“photic zone”) of almost all oceans and bodies of fresh water. The photic zone is not defined by its vertical extension in meters but rather by the amount of available solar radiation. The lower limit of the photic zone is the depth were the penetrating light decreases to 1 % of the surface irradiation.

Phytoplankton organisms use active mechanisms to move to and stay in the photic zone: some have flagella or cilia and actively move in the water column in search of optimal conditions for growth and reproduction. Others use buoyancy for vertical migrations producing oil droplets within their cytoplasm or gas vacuoles produced by the body itself. Some of these movements follow a circadian rhythm with organisms moving down at night and toward the surface before and during daytime. Unlike most land plants, they can absorb water and nutrients directly from their environment. Phytoplankton have a great variety of unique patterns, shapes, and forms. Instead of leafs and blades they have developed numerous pores, spines, and other projections. The function of these projections is to increase the surface area of the plant body itself, reduce the sinking rate, facilitate absorption of nutrients and increased exposure to sunlight for photosynthesis.

The Southern Ocean is the largest high-nutrient, low-chlorophyll (HNLC) region although biomass is higher in coastal, shelf, frontal and ice-edge regions (Moore and Abbott, 2000, Sullivan et al., 1993). In spring, phytoplankton growth is limited by irradiance (Smith et al., 2000), but in summer it may be limited by iron, even on the continental shelf (Olson et al., 2000, Sedwick and Di Tullio, 1997). Deposition of iron is limited in this area (Fung et al., 2000), and biomass in spring is approximately four times higher than in summer. The distribution of flowering is not uniform throughout the Southern Ocean but is localized in three regions: in the shallow waters near the coast, in the areas of polynya near the sea ice and in marine areas downwind near the coast, where disrupts flows of the main currents in the sub Antarctic circumpolar and polar (Sullivan et al., 1993). In fact, zones of intense flowering (>3 g/m^3 of carbon) are found in Antarctica in areas where the continental shelf is less depth and in the regions of upwelling along the area of polar Antarctic front (Fitzwater et al., 2000). It has been proposed that the primary production of this ocean is determined by the availability of iron present in solution and that this metal derives from the iceberg, by the melting of sea ice and sediments coming from continental shelf (Fitzwater et al., 2000, Sullivan et al., 1993). The Ross Sea is a particularly productive region of the Southern Ocean system and supports a predictable phytoplankton bloom (Comiso et al., 1993). Thanks to the phenomenon of the Antarctic Circumpolar Current and these effects, the Ross Sea is highly productive, especially during the period of the retreat of sea ice, when the concentration of chlorophyll during the austral summer may reach 6 mg/l. In this area, indeed, there are large concentrations of organic matter (Peloquin et al., 2007, Smith et al., 2000).

The Ross Sea has been characterized by taxonomic heterogeneity, with phytoplankton having distinctly different composition in two separated regions. *Phaeocystis antarctica*, a haptophyte, that typically dominates the south-central portion of the Ross Sea, whereas diatoms often dominate along the west coast (Peloquin et al., 2007). These trends have not been attributed to a single

nutrient or physical feature (Arrigo et al., 2000, Olson et al., 2000, Van Hilst and Smith, 2002). Some studies found deeper mixed layers in areas dominated by *P. antarctica* and shallower ones in those dominated by diatoms (Arrigo et al., 2000, Smith and Asper, 2001); they believed that the taxonomic variability was primarily driven by the efficiency of light. The availability of light and iron, therefore, are the first order controls on rates of NNP (net primary production). Diatoms can grow well even at low concentrations of iron and other species such as *Phaeocystis Antarctica*, most affected by arresting their development, in fact generally *P. Antarctica* is more abundant in the early spring because there are higher concentrations of iron (Peloquin et al., 2007). Regarding the numerical abudance, diatoms are always higher than the other groups of phytoplankton cells, the high density of diatoms is probably due to the characteristic of the ice at Terra Nova Bay (Fonda Umani et al., 2002).

1.4 Atmospheric particulate matter in Antarctica

The atmospheric particulate matter is a suspension of solid or liquid particles in a medium gaseous (McNaught et al., 1990), it is the set of all the solid particles of insoluble and soluble solid material suspended in the atmosphere (Gadhavi et al., 2004) that range a size from few nanometres to tens of micron. The composition depends on the area of origin and the type of the emission source. In general, the effects of climatic and environmental aerosols depend on their atmospheric concentration, on the size of the particles and on the chemical composition. The size and mass of the particles mainly affect the deposition, the residence time, the dispersion, the transport of the particles and the processes of inhalation, while the chemical composition and the “speciation”, in particular for heavy metal traces, affect the mobility, bioavailability and potential toxicity of the suspended trapped (Giere and Querol., 2010).

Today there is a growing interest from the scientific community in the study of the chemical composition of the aerosol for its implications for human health and environmental protection; the particles interact with the transfer of sunlight radiation through the atmosphere and the ratio soluble/insoluble plays a key role in Earth’s climate system (Li et al., 1996).

Their sources can be natural or anthropogenic: natural sources are basically sea salt and crustal dust generated and transported by winds; smaller sources can be traced to forest fires, volcanic emissions and meteorites. The marine aerosol is formed by direct mechanical action of the wind on the water surface and for braking the air bubbles trapped in the water. Anthropogenic sources are mainly due to emissions from combustion processes such as vehicle traffic, use of fuels (coal, oil, wood, waste, agricultural waste), industrial emissions (cement factories, foundries, mines).

The Antarctic atmospheric aerosol is undoubtedly the most rarefied and cleanest on Heart.

Because 99% of the surface of the continent is covered by snow and ice, there are few local sources of natural aerosol particles. Human activities in the region are mainly limited to the maintenance of a few bases, primarily for scientific research, and there is generally thought to be little significant local pollution. Nevertheless, knowledge of Antarctic atmosphere aerosol content and chemical composition is essential, e.g., to discover the origin, transport pathways, and deposition processes of substances reaching the continent (the most isolated on the globe), to interpret ice core chemical data (e.g., to correlate observed past atmospheric variations to natural or anthropogenic changes), and to understand the climatic role of atmospheric particulate matter in areas of highly reflective surface.

In particular, as regards trace heavy metals, there is at present no information available in the literature, with the exception of our previous works (Annibaldi et al., 2007/2013), with reference to their distribution between the soluble and the insoluble fractions in aerosol, possibly due to difficulties in the treatment and analysis of samples under uncontaminated conditions and with sufficient sensitivity (Boutron 1995; Planchon et al., 2003). However, the global climatic and environmental changes which occurred in past glacial/interglacial cycles were always accompanied by substantial variations in the content of the atmospheric aerosol and, at the same time, in the distribution between soluble and insoluble phases in the Antarctic ice (Laj et al., 1997, Marino et al., 2003). Although the solubility depends on the chemical nature of particles and on the operative dissolution conditions (Colin et al; 1990, Losno et al., 1993), the soluble/insoluble discrimination of impurities present in the aerosol and deposited on the polar ice caps is an important tool for identifying the sources of chemical substances and detecting the changes that have taken place due to the climatic changes of the past.

In this work the atmospheric aerosol was studied for its important contribution in the deposition of particulate matter from atmosphere, also from remote areas, involving a wet and/or dry deposition in the seawater layer.

1.5 Biogeochemical cycles of heavy metals in the Antarctic ecosystem

Antarctica is one of the most pristine areas in the word and it is a privileged observatory for research on global changes. The distance from densely populated areas and its peculiar characteristics make Antarctica a very important area for studying the transport and accumulation of potentially toxic substances. The biogeochemical cycle of heavy metals is associated to the various and complex interactions among the different matrices which constitute this particular ecosystem. These include:

- The sea-water column, where scavenging processes affect dissolved and particulate metal concentrations.
- The pack ice, which covers the sea surface for a long period of the year and causes the metal to enter the water column during its dissolution
- The marine microlayer and aerosol that play an important role in transporting the metal from the atmosphere to the sea-water (Cincinelli et al., 2001, Grammatica&Zimmerman 2001)
- The marine sediment, which is the principal sink for heavy metals in aquatic environment
- The organisms, which can accumulate toxic elements in specific target organs.

Certain trace metals show profiles that are nutrient-like, like cadmium and copper, which is indicative of their involvement in biological cycles (Boyle, 1988; Boyle and Edmond, 1975). In contrast, other metals have a scavenged-type behaviour, like lead (Flegal and Patterson, 1983) or behave in a conservative manner like uranium (Bruland and Lohan, 2003). Elements such as manganese (Mn) can be considered hybrid-type metals at high latitudes, as their distribution is controlled by both biological uptake and scavenging processes (Bruland and Lohan, 2003).

Furthermore, the oceanic behaviour of other trace elements like silver (Ag) is still not well understood, with little data on Ag distribution in the global ocean, notably in the Southern Hemisphere (Zhang et al., 2004). Despite major advances on the biological involvement of trace metals and their geochemical dynamics in the ocean, basic knowledge is still lacking on their biogeochemical cycles. For instance, there are only few comprehensive datasets of Mn (Middag et al., 2011), and of Cd, Pb and Cu (Ellwood, 2008, Losher, 1999) for the Southern Ocean. Biogeochemical cycles are sensitive to atmospheric dust inputs (Cassar et al., 2007; Dixon, 2008). The transport and deposition of atmospheric aerosol is a significant source of trace metals to the surface ocean (Jickells et al., 2005) and, in large areas of the open ocean, may represent the dominant supply route for certain elements (Ussher et al., 2013).

The dissolution of these natural and anthropogenic particles in the upper layer of the ocean can vary with their origin, their elemental composition and the possible transformation which can occur in acid clouds of the atmosphere and/or by UV irradiation. For instance, metals contained in carbonated dusts are more easily dissolved in water than those present in alumina-silicate particles due to different binding strength of the metal to the mould (Desboeufs et al., 2005). Bio-available trace metals can regulate the growth of the phytoplankton influencing the primary production and the carbon cycle (Sunda and Huntsman, 1995). The nutritive metals contained in dust can be available for phytoplankton after their dissolution in seawater. Among these micro-nutrients, cobalt (Co) and zinc (Zn) have a potential key role in phytoplankton physiology and productivity. (Thuroczy et al., 2010).

In any case this research is extremely arduous, due to both the peculiarity of the Antarctic ecosystem and the difficulty to obtain uncontaminated seawater samples and accurate analytical data. Another difficulty arises from the specific chemical properties of each metal, which leads to a different speciation both in the dissolved and particulate phase and, as a consequence, to a different bio-availability. Concerning phytoplankton, its concentrations in oceanic waters can be extremely low, requiring processing of large volume or, alternatively, the analytical challenge of working with small sample sizes. Because of the difficulty in obtaining accurate and significant data, the knowledge of trace metal distribution and speciation in the Southern Ocean is hence limited; consequently, the complete understanding of their natural cycle and their importance in regulating oceanic primary production is far from clear.

Cd, Pb and Cu have been selected for this study because two of them (Cd and Pb) are considered priority pollutants (PP) by regulation in force (European Parliament and Council of European Union, Directive 2000/60/EC) and the third one (Cu) is an element of interest, being a micronutrient for phytoplankton and so with potential differences on bioaccumulation in comparison to Cd and Pb.

1.5.1 Definition of Heavy Metals

Over the past two decades, the term "heavy metals" has been used increasingly in various publications and in legislation related to chemical hazards and the safe use of chemicals. It is often used as a group name for metals and semimetals (metalloids) that have been associated with contamination and potential toxicity or ecotoxicity. Bjerrum's definition of heavy metals is based on the density of the elemental form of the metal, and he classifies heavy metals as those metals with elemental densities above 7 g/cm^3. Over the years, this definition has been modified by various authors. Some editors included heavy metals with a specific gravity. At one point in the history of the term, it has been realized that density or specific gravity is not of great significance in relation to the reactivity of a metal. Accordingly, definitions have been formulated in terms of atomic weight or mass. Another group of definitions is based on atomic number. Here there is more internal consistency because three of the definitions cite heavy metals as having atomic numbers above 11, that of sodium (Lyman, 1995, Rand et al., 1995). The problem with citing metals of atomic number greater than sodium as being "heavy" is that includes essential metals, such as magnesium and potassium, and this is in contrast with the definition linked to the density or specific gravity. For all those reason, the term "heavy metals" has never been defined by any authoritative body such as IUPAC. However, it can be stated that the group of "heavy metals" is intended to include both the transition elements (d-block) and the elements with the metallic features of the p-block (Fig. 1).

Heavy metals are naturally elements that are found throughout the earth's crust, most environmental contamination and human exposure result from anthropogenic activities such as mining and smelting operations, industrial production and use, and domestic and agricultural use of metals and metal-containing compounds (Shallari, et al., 1998). Natural phenomena such as weathering and volcanic eruptions contributed significantly to heavy metal pollution.

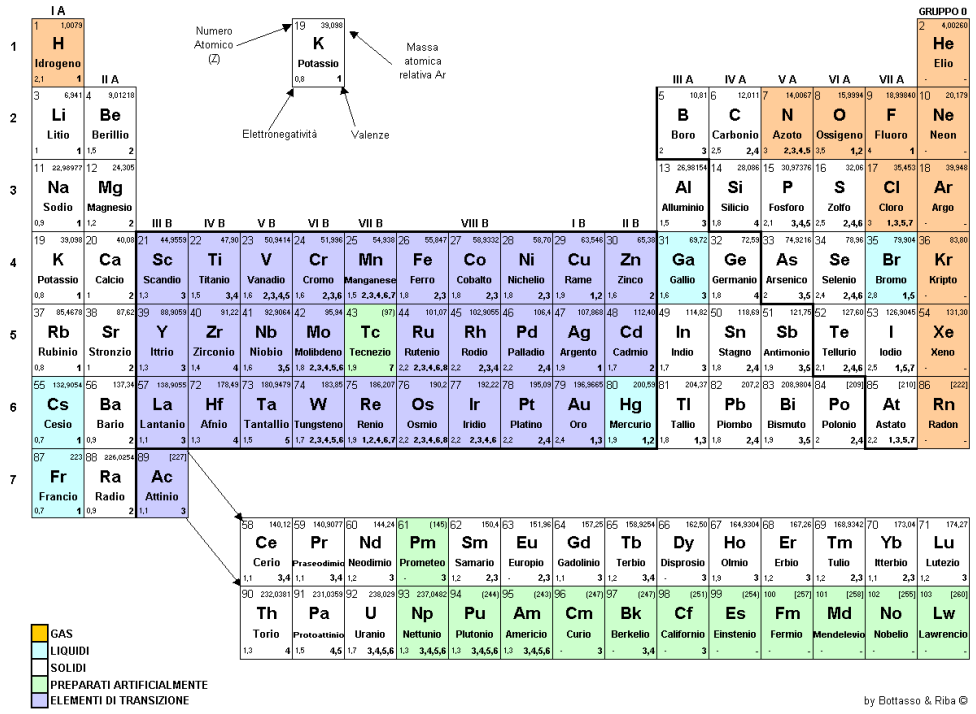

Fig. 1. Periodic table of elements, heavy metals are defined by the bold line.

1.5.2 Cadmium, Lead and Copper in Antarctic ecosystem

Cadmium

Cadmium occurs naturally in the earths'crust at an average concentration of about 0.15-0.20 mg/kg (Sadiq, 1992) and it is found in different concentrations in all components of freshwater, marine and terrestrial ecosystems. Because of its many industrial uses (plating, pigments, batteries, stabilizers for plastics, metal alloys, etc...), the main source of cadmium contamination is anthropogenic; it affects the marine environment through precipitation, discharges and effluents near the coast. This metal is generally found in aquatic environments in the oxidation state of [Cd (II)]. It has a strong affinity with halogen ions; indeed, in seawater it forms strong complexes with the chlorine and also it can form complexes with organic ions. It is important to emphasize that the degree of complexation affects its bioaccumulation and toxicity in the marine environment (Langston, 1986). The sediments, therefore, are important reservoirs of Cd (Santschi et al., 1980); in fact, if the physical-chemical conditions change, the Cd bound to the sediment can be released into the interstitial. For their ability to release and accumulate metals, sediments have a central role in the concentration of Cd in seawater. The average concentration of cadmium in sediments from Terra Nova Bay is ~0.26 mg/kg; highest concentrations are associated with-fine grained sediment fraction (Giordano et al., 1999).

Although information on heavy metals in the Antarctic Ocean is very scarce, there are indications that cadmium concentrations in surface waters, especially before the algal blooms, are higher than those in the central gyres of the Atlantic and Pacific Oceans (Bargagli, 1995). These higher values might be due to the upwelling of Cd-enriched deep waters to the surface. Cadmium, which is generally thought to be universally deleterious to living organisms, has a nutrient-like profile (Bruland, 1980). The vertical distribution of Cd in the oceanic water column resembles profiles of phytoplankton nutrients, with minimum concentrations at the surface that increase to maximum values in the main thermocline and remain relatively constant until the ocean bottom. Cd has a similar spatial distribution patterns to phosphate in Open Ocean deep and surface waters (Boyle, 1988). The exact nature of the relationship between Cd and P has remain elusive. It has been demonstrated that the non-linear relationship between Cd and PO_4^{3-} in seawater can be explained by a combination of water mass mixing, differential biological fractionation due to variation in micronutrient concentration and changes in phytoplankton community structure, which can vary within a season (Hendry K et al., 2008).

It has been widely thought that abiotic processes, such as adsorption onto organic particles, modulate the distribution of this metal. It has been proposed that the depletion of Cd from surface seawater is caused by its use by marine phytoplankton (Price & Morel, 1990). Particulate Cd

concentrations are significantly lower and are, conversely, maximal in surface waters. This distribution reflects the uptake of Cd by photosynthetic plankton at the surface and the sinking and subsequent decomposition of particulate matter in the water column. Laboratories studies have shown that the uptake of Cd by phytoplankton is directly proportional to dissolved Cd concentrations and indirectly proportional to dissolved Zn and Mn concentrations. Under conditions of Zn limitation, Cd enhances the growth rate of some marine phytoplankton in culture (Price, N.M. & Morel, F.M.M; 1990) and it thus seems that Cd may replace Zn in some essential biochemical function. *Thalassiosiraweissflogii* express a Cd-specific carbonic anhydrase, which, particularly under conditions of Zn limitation, can replace the Zn enzyme TWCA in its carbon-concentrating mechanism (Todd W.Lane & Morel F.M.M, 1999).

The ocean receives Cd mobilized from the crust through atmospheric input. The concentration of dissolved Cd in coastal surface waters is higher than oceanic waters and in the range of 0.2-0.9 nmol/kg. These high values represent terrestrial inputs of the metal from riverine and atmospheric sources, as well as wind driven upwelling of high nutrient and high Cd subsurface waters along the coast.

Copper

Copper (Cu) is widely spread in nature, especially in sulphides, arsenic, chlorides and carbonates deposits. It is one of the most common pollutants of the environment and the source of contamination is therefore anthropogenic (Nriagu, 1979). Copper is introduced into the aquatic environment from many sources: minerals in soil and weathered rock that form the sediments and suspended particles in the water, extraction from rock, biological particles, including both living and dead organic material, hydrothermal systems (volcanic action a thermal vents), input from sediments, anthropogenic input and deposition from the atmosphere. The most bioavailable and therefore most toxic form, as the other metals, is the cupric ion (Cu^{2+}) (Flemming et al., 1989; Sunda et al., 1984). It can be also complexed with inorganic anions or organic ligands or as suspended particles when present as a precipitate or adsorbed to organic matter (Mance et al., 1984). Complexes formed by copper with natural organic compounds are generally more stable than other metals such as cadmium, lead and zinc. Copper concentration in marine sediments varies widely between 0.3 and 1200 mg/kg (Libes, 1992). Copper displayed nutrient-like behaviour with lower concentrations in surface waters and increasing levels with depth (Boyle et al.; 2012). This behaviour of copper as a micronutrient has been investigate even if data on this metal in the Southern Ocean are scarce (Morel and Prince, 2003). Copper is an essential micronutrient for phytoplankton communities, it is involved in photosynthesis and in iron pathways, essential for cell growth (Peers et al., 2005). However, copper may have a negative effect on bacteria (Kim, 1985),

on phytoplankton (Sunda and Guillard, 1976) and on the production and the survival of marine copepods (Sunda et al., 1987). Various metabolic functions for copper have been identified: at least one oceanic diatom uses plastocyanin, a Cu-containing protein, to shuttle electrons between photosystem II and I (Peers and Price, 2006), and high affinity iron uptake in numerous diatom species is mediated by a multi-copper oxidase (Maldonaldo et al., 2006; Kustka et al., 2007), resulting in a high biological demand for copper by laboratory monocultures (Annett et al., 2008), and by field phytoplankton communities (Semeniuk et al.,2009).

Concerning phytoplankton, most studies show that biological activity is proportional to free Cu^{2+} concentration (Sunda and Guillard, 1976, Sunda and Huntsman, 1995), but some recent observations suggest that organic complexes may also be used (Quigg et al., 2006, Semeniuk et al., 2009). Diatoms are able to reduce Cu^{2+} bound to organic ligands (Jones et al., 1987) and may be able to use these species of Cu for growth just as they do for Fe. As with other bioactive trace elements (Fe, Zn), 98% of Cu is complexed by organic ligands, presumably of biological origin, resulting in low inorganic metal concentrations (Van den Berg, 1984, Mofflett, 1995). Recent studies suggest that Cu requirements may be higher when the organisms experience Fe-limitation.

In fact, Fe-limited marine diatoms possess a high affinity transport system with Cu-dependent cell surface oxidases which allows them to access Fe bound within strong organic complexes (Maldonado et al., 2006). It is reported that the sensitivity of phytoplankton to copper varies among algal species (Thomas and Seibert, 1997). Although there are exceptions, dinoflagellates and cyanophytes are more copper sensitive groups, and green flagellates (Gustavon and Wanberg, 1995) and diatoms (Stauber and Davis, 2000) are more resistant. Cyanobacteria are one of the most sensitive phytoplankton group to copper toxicity (Brand et al., 1986, Broise and Palenik, 2007, Le Jeune et al., 2006). Atmospheric copper deposition, which appears to be primarily of natural origin, may be the most important input of copper to the surface ocean waters (Maring and Duce, 1989).

Dissolved organic matter and possibly cations in seawater increase the dissolution of aerosol copper. Cu is known to vary considerably between anthropogenic and crustal sources adding another layer of complexity: metals in anthropogenic aerosols have the potential to cause greater toxicity due to their more rapid dissolution and relatively higher total metal content, compared to crustal source material (Sholkovitz et al., 2010).

Lead

Lead is an important heavy metal that is widely distributed throughout the word. It is not essential to metabolism and it is highly toxic for biota, even at very low concentration, since it reduces plant photosynthesis and retards the growth of living organisms (McLaughlin et al., 1999). Natural contribution of lead come from activity of submarine volcanoes and hydrothermal sources

which release fluids enriched with metals due to the contact with the surrounding rocks (Dalla Riva et al., 2003).

In marine environment, Pb is associated with suspended particulate matter, and in this form, it tends to accumulate in sediments (Zabel, 1989). Pb concentration in marine sediments varies from 0.6 mg/kg to 1000 mg/kg (Sadiq, 1992). Pb can be absorbed directly from sea water and sediments, especially from filter feeders and detritivores. Among all the inorganic species, Pb^{2+} is considered the more easily adsorbibile from bodies (Libes, 1992). Some studies have suggested that this element does not undergo biomagnification along the trophic chain. Tests carried out on freshwater and marine organisms showed that the toxicity of methyl and ethyl - lead is about 10-100 times greater than that expected by inorganic forms of Pb (Demayo et al, 1984).

Lead is not required to the physiological cellular metabolism and can therefore only negatively influence the growth at very low concentrations reducing photosynthesis and retarding cell growth (Della Riva et al., 2003). This element can replace other metals in various biological sites by altering the normal metabolic function of enzymes, receptors and other biological components. The bioaccumulation of lead in marine phytoplankton is dominated by surface uptake (Fisher et al., 1987). It includes adsorption, precipitation, absorption, and other physical, chemical and biological processes (Sposito, 1986). Consequently, the concentration of Pb in marine phytoplankton appears to be proportional to the surface area to volume ratios of the cells.

Lead can be taken up by organism both in inorganic form and as organometallic compound from the seawater, the sediment, and through the food chain; the toxic effects on the biota are determined by various detoxification mechanisms that regulate anomalous concentrations of this metal (Bettger and Odell, 1981). It has been demonstrated that lead can be adsorbed by the alga *Dunaliella tertiolecta* and complexed by the exudates excreted by the algae. Variation in factors such as pH, temperature and salinity have additional effects on the adsorption and complexation of lead. Although the Arctic and Antarctic phytoplankton communities assimilate Pb to the same degree, significant differences were observed between the two communities: Arctic communities were tolerant to Pb, while Antarctic one were more sensitive; probably Arctic phytoplankton communities have developed more evolved mechanisms to face the higher recurrent historical exposure to pollutants, both from the surrounding industrialized area and subsequent atmospheric transport and from local intense mining activities (Braune et al., 2005, Duce et al., 1991, Lu et al., 2013, Macdonald et al., 2000, Presley, 1997). Lead increased the average size of the largest Arctic and Antarctic diatoms but decreased that of the smallest and medium sized Antarctic diatoms. Larger sized cells, as those of the Arctic and Southern Oceans, have a lower surface to volume ratio,

resulting in a slower metal uptake, and conferring a higher tolerance to metals (Echeveste et al., 2012).

The particulate lead concentrations along the pack ice core, which are of the same order of magnitude as in the sea-water, indicate that the release of suspended particulate matter (SPM) during ice melting is a significant process by which the metal enters the water column. The mean particulate lead concentrations in the aerosol and marine microlayer were 16.0 μg/g and 18.3 μg/g SPM, respectively (Dalla Riva et al., 2003). These values are comparable with the particulate lead mean concentration in sea-water (10.0-25.8 μg/g SPM) and marine sediments (19.3-29.0 μg/g). Therefore, it can be supposed that particulate lead enters the water column through different paths: release from the pack ice during its melting, input from the continental land through the wet deposition and transport by aerosol and marine microlayer (Dalla Riva et al., 2003).

2. Aim and Scope

Within the framework of the Italian Antarctic Programme the aim of my PhD project is to study the processes that regulate the heavy metal distribution between aerosol, seawater, non-algal marine particulate and phytoplankton in the Antarctic ecosystem, with particular attention paid to the phytoplankton. In fact, while in the case of the total particulate matter analytical data on the metal content are normally available, data for the marine phytoplankton (above all nano and micro phytoplankton) separated from the raw particulate matter are absent. During the XXIX Italian Antarctic Expedition (austral summer 2013-2014) samples of atmospheric aerosol, seawater and phytoplankton were collected from about mid-November 2013 to mid-February 2014. CTD data (in particular fluorescence) were recorded during samplings. During the period of the PhD the following activities were carried out on samples transported to the laboratory, to reach the scope of the thesis. The determination of Cd, Pb and Cu in seawater and phytoplankton samples were carried out by Square Wave Anodic Stripping Voltammetry (SWASV). For aerosol samples, Cd, Pb and Cu in the insoluble and total metal content fractions and Cd in the soluble fraction were determined by Graphite Furnace Atomic Absorption Spectrometry (GFAAS), while Pb and Cu in the soluble fraction was determined by voltammetry, due to the low concentrations and high detection limit of AAS for these metals.

The analytical methodology for metal determination in phytoplankton, after the separation of nano and micro phytoplankton from non-living particulate matter, was set up and optimized.

Here I present and discuss the results of the analyses carried out in terms of (*i*) metal distributions in seawater and phytoplankton along the water column and their evolution during the austral summer;

(*ii*) relationships between all the variables observed in seawater, with particulate reference to the nutrients and metal-nutrients correlations;

(*iii*) metal distributions in the aerosol, and estimates of metal deposition fluxes from the atmosphere, integrated into an overall model for the biogeochemical cycles of metals in the area of Terra Nova Bay.

3. Materials and Methods

3.1. Laboratory and apparatus

Clean room laboratory ISO 14644–1 Class 6 (or US Fed. Std. 209e Class 1000), with areas at ISO Class 5 (or US F. S. 209e Class 100) under laminar flow, was available for decontamination of materials, sample treatment, and sample analysis. The laboratory temperature is set at 20±1 °C during the winter and 23±1 °C during the summer. Clean-room garments, masks, and gloves were worn by the personnel, who strictly followed clean room procedures during all the most critical treatments and sample analysis phases. The voltammetric instrumentation, consisting of a Metrohm (Herisau, Switzerland) 746 VA Trace Analyser and a 747 VA Stand, equipped with a Teflon PFA (perfluoroalkoxycopolymer) cell and a three-electrode system, which includes an epoxy-impregnated graphite (Ultra Trace Graphite) rotating disk working electrode (to be used, after Hg deposition, as a rotating TMFE), an Ag/AgCl, KCl 3 mol/l reference electrode (to which all potentials are referred throughout) and a glassy carbon rod counter electrode, was used for metal determination in sea water and pack ice samples. A microwave (MW) accelerated reaction system MARS 5 (magnetron frequency 2450 MHz) from CEM (Matthews, NC, USA) was used for the sample digestion. One 20-L GO-FLO bottle from General Oceanics (Florida, USA) was used for sea water sample collection.

CTD probe mod. Ocean Seven 316 from Idronaut (Milan, Italy) equipped with a fluorometer from Seapoint Sensors, inc. (Kingston, USA) was used to measure the master variables along the water column. The filtration apparatus was the Sulfoflo (polysulfone) mod. 300–4100 from Nalgene (Rochester, New York) equipped with 0.45-µm pore size membrane filters (cellulose mixed esters ∅ 47 mm, Schleicher &Schuell, Dassel, Germany). A Zeiss Axiovert 25 inverted microscope was used for phytoplankton separation. The laboratory analytical balance mod. XS205 from Mettler Toledo (Greifensee, Switzerland; readability 0.01 mg, repeatability SD=0.015 mg) was used for the marine particulate matter weighings. The UV/Vis spectrophotometer mod. 6705 from Jenway (Staffordshire, UK) was used for nitrate, nitrite, phosphate and sulphate determination, while the photometer NANOCOLOR, mod. 500 D, from VELP Scientifica (UsmateVelate, MB) was used for ammonium and silicate determination in all seawater samples.

A Teflon-coated high-volume PM_{10} sampler from Analytica Strumenti (Air flow HVS-PM_{10}-10EPA/EN, Pesaro, Italy) and the precleaned 8 × 10 in (20.3 × 25.4 cm) cellulose filters (Whatman 41, Cat. No. 1441–866, thickness 220 µm, ashes ≤0.007%, pore size 20–25 µm, basis weight 85

g/m^2) were used for aerosol collection. The atomic absorption spectrophotometer, AAS, mod. GTA 120-2402AA including the Zeeman Effect correction from Agilent Techonologies (Santa Clara, USA) was used for metal determination in aerosol samples.

Plastic containers used for the storage of both digested and not-digested sea water samples were of low-density polyethylene material. Variable-volume micropipettes and neutral tips were from Brand (Wertheim, Germany, Transferpette).

3.2. Reagents and standards

The laboratory detergent solution for decontamination procedures was 1+100 diluted RSB-35 from Baker (Phillipsburg, NJ, USA). Ultrapure water was Milli-Q from Millipore (Bedford,MA, USA). Nitric acid (analytical grade, 65%), hydrochloric acid (analytical grade, 37%) and sulphuric acid (analytical grade, 96%) were from Carlo Erba (Cornaredo, MI). Ultrapure HNO_3 (70%, UpA), ultrapure HCl (34.5%, UpA), ultrapure HF (47–51%, UpA), ultrapure H_2O_2 (30%, UpA) and superpure HCl (34–37%, SpA) were from Romil (Cambridge, UK). Superpure KCl and hexadistilled mercury were from Merck (Darmstadt, Germany; Suprapur). Research grade nitrogen (Sol, Monza, Italy; purity ≥99.999%) and research grade Argon (Air liquid, Milano, Italy; purity ≥99.996%) were used. Standard solutions were from Romil (Cambridge, UK); metal standard solutions were prepared every two weeks by direct dilution of AAS standards using acidified ultrapure water (2 ml ultrapure HCl in 1000 ml final solution).

Potassium nitrate, KNO_3 (purity ≥99.9%); sodium chloride, NaCl (purity ≥99%); citric acid, $C_6H_8O_7$ (purity ≥ 98%) and palladium $Pd(NO_3)_2{\cdot}2H_2O$ (purity ≥99.5%) were from Sigma Aldrich (Saint Louis, Missouri). N-(1-Naphthyl) ethylenediamine dihydrochloride, $C_{10}H_7NHCH_2CH_2NH_2{\cdot}2HCl$ (purity ≥99.9%); sulphanilamide, $C_6H_8N_2O_2S$ (purity ≥99.9%); monopotassium phosphate, KH_2PO_4 (purity ≥99.5%); ascorbic acid, $C_6H_8O_6$ were from Carlo Erba (Cornaredo, MI). Antimony potassium tartrate, $K(SbO)CH_4H_4O_6{\cdot}1/2H_2O$ (purity ≥99.9%); ammonium molybdate tetrahydrate, $(NH_4)_6Mo7O_{24}{\cdot}4H_2O$ (purity ≥99.9%), sodium nitrite, $NaNO_2$ (purity ≥99.9%); sodium sulphate, Na_2SO_4 (purity ≥99.9%); and barium chloride $BaCl_2{\cdot}2H_2O$ (purity ≥99.5%) were from J.T. Baker (Phillipsburg, New Jersey). Nanocolor standard tests AMMONIO (CM 0091805) and SILICA (CM 0091848) were from Macherey-Nagel (Duren, Germany).

Certified reference materials NASS-6 (open ocean seawater) was from National Research Council of Canada (NRCC, Ontanio, Canada), BCR-414 plankton certified reference material was from Joint Research Centre (JRC, Bruxelles, Belgium) and NIST 1648a urban particulate reference material was from National Institute of Standards and Technology (NIST, Gaithersburg, USA).

3.3. Decontamination procedures

All the plastic containers (Kartell, Milan) used for sample collection and treatment were decontaminated according to the following procedures (Truzzi, 2002). Briefly, new containers were washed with detergent solution to eliminate possible organic residuals. After a thorough rinse with tap water, deionised water and Milli-Q water (three times for each type of water), the bottles were immersed in 1:10 diluted HNO_3 solution (analytical grade) and, after two weeks, rinsed with Milli-Q water.

Decontamination procedures continued with immersion in 1:10 diluted superpure HCl for one week and rinsing with Milli-Q water. The latter step with superpure HCl was repeated a second time. Finally the bottles were stored filled with 1:1000 diluted, superpure HCl until use. Similar acid washings were used for sampling equipment and filtration apparatus. Membrane filters for seawater filtration were cleaned by soaking twice in 1:10 diluted superpure HCl for one week and then left in a 1:1000 HCl solution.

Cellulose filters for aerosol sampling were washed and decontaminated carefully with diluted superpure HCl, rinsed with Milli- Q water, dried under Class 100 laminar flow cabinets, and stored in acid-cleaned plastic bags until use.

3.4. Study area

During the XXIX Italian Antarctic Expedition (austral summer 2013-2014) samples of pack ice, seawater and phytoplankton were collected in the Gerlache Inlet area (site B14, bathymetry 300m, coordinates 74.6667 °S-160.1167 °E). Gerlache Inlet is an inlet 4 nautical miles (7 km) wide in the northwest corner of Terra Nova Bay, indenting the Northern Foothills just south of Mount Browning (Fig.2). Terra Nova Bay (TNB) is a wide inlet occupying an area of about 6000 km^2 in the western region of the Ross Sea, along the Victoria Land coasts, near the Italian station “Mario Zucchelli” (MZS). The bay has one of the deepest continental shelf of the Ross Sea, the mean depth is of 450 m, but it is deeper close to the coast and exceeds 1000 m in the central part (Accornero et al., 2003, Cappelletti et al., 2010). The main feature of TNB is a persistent coastal polynya. Katabatic winds which originate over the Antarctic continental plateau and blown offshore form the wind-driven flaw polynya as they shift the newly-formed ice far from the coasts (Bromwich and Kurtz, 1984 da Cappelletti, 2010). This area is characterized by a maximum of both microphytoplankton abundances and biomass in late December, followed by a decrease in January and a secondary peak in February, due to an increasing percentage of nano phytoplankton (Nuccio et al., 1992).

The TNB polynya has been intensely investigated by Italian researchers in recent years, studying the plankton community (Accornero et al., 2003, Arrigo et al., 1999, Fonda Umani et al., 2003/2005, Nuccio et al., 1992, Saggiomo et al., 2002), the physical structure of the water column (Cappelletti et al., 2010), the nutrient and trace element distribution in sea water (Abollino et al., 2001/2004, Biesuz et al., 2006, Catalano et al., 1997, Dalla Riva 2003, Rivaro et al., 2012, Scarponi et al., 1995, Scarponi et al., 2000).

Antarctic atmospheric particulate matter was collected at Faraglione Camp (74.7161 °S – 164.1150 °E), about 3 km southern from the "Mario Zucchelli" Italian Station (MZS). The sampling site is a promontory and the collection place is located at an elevation of 57 m above sea level (a.s.l.) and at ~250 m far from the sea. Fig. 2 shows a map of the area near MZS, where Faraglione Camp is located, and the wind rose with the prevailing wind direction highlighted.

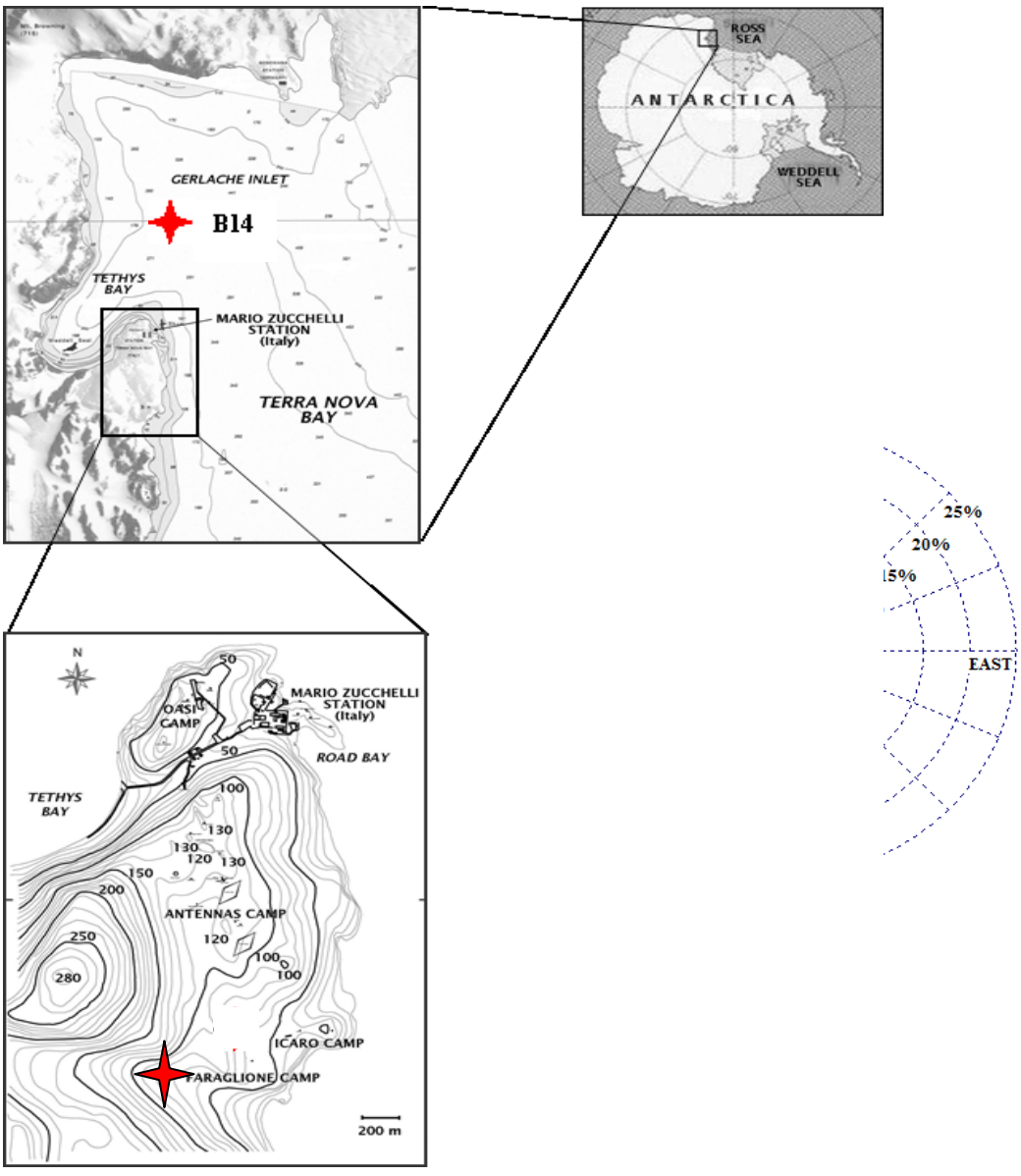

Fig. 2. Map of Terra Nova Bay area (Victoria Land, Antarctica) showing the location of the main Italian Station (MZS), the aerosol sampling site Faraglione Camp, the seawater sampling site Gerlache Inlet area, and the wind rose with the prevailing wind direction for the 2013-2014 Antarctic Campaign.

3.5. Field sampling and sample treatments

3.5.1. Seawater and phytoplankton

Coastal seawater samples were collected by 20-L GO-FLO bottles at six different depths every ten days from November, the 28th 2013 to February, the 2nd2014. Due to technical problems, only one sampling was carried out in absence of ice at the end of the Antarctic summer (on February 2nd), while the other samplings were carried out in presence of the pack ice. Typically, some depths were maintained fixed (superficial, –10 m, –100m, –200m), while other depths were varied depending on the CTD profiles, i.e. maximum of fluorescence depth, temperature pycnocline and dissolved oxygen curve.

Seawater samples were divided in aliquots subjected to different treatments for the determination of the principal metal fractions. The first aliquot was acidified (raw sample) with ultrapure HCl (2+1000, pH ~2) for the determination of the total metal concentration (M_{tot}). An aliquot (raw sample) was not acidified and subjected to a procedure previously set-up by our group (Truzzi et al., 2015) for the phytoplankton separation from the inorganic particulate in order to determine the metal fraction associated to the organic particulate matter (M_{phyto}).

The physical separation of phytoplankton by the non-living particulate referred to the Uthermol method (Uthermol, 1958). After homogenization, variable volumes of subsamples (from 20 to 100 ml, depending on chlorophyll-a values) were settled in a Uthermol chamber and observed using a Zeiss 25 inverted microscope. Phytoplanktonic cells were sucked with a Pasteur connected to the cell isolator. The Pasteur was spun by hand so that the diameter of capillary was of the same order of magnitude as the microalgal cells.

A third aliquot was filtrated through 0.45 μm pore size membrane filter and then acidified with ultrapure HCl (2+1000 at pH ~2) for the determination of the dissolved metal content (M_{diss}). Before analysis, all acidified seawater and phytoplankton samples were subjected to microwave digestion in order to destroy organic matter, to leach bound metals, and to avoid possible adverse effect on the voltammetric determination (Kolb 1992 da Annibaldi 2011, Truzzi, 2015). In the present work, total particulate concentrations of metals ($M_{totpart}$) were obtained by difference between the total and the dissolved concentrations, whereas the metal concentrations in the inorganic particulate fraction (M_{inpart}) were obtained by difference between total particulate and phytoplankton concentrations.

3.5.2. Atmospheric aerosol

Six samples of atmospheric particulate matter were collected every 10 days from December the 1st 2013 to February the 2nd 2014 using a Tish high-volume sampler (aerodynamic size≤10 μm, PM10). An half of each filter was reserved for our work and put into decontaminated LDPE bottles and stored frozen (−20 °C) until analysis. Five blank filters were also collected in the field (called "field blanks") approximately every ten days; these were not exposed to air flux, but were simply installed onto the switched-off samplers for few tens of minutes and then treated at the same filters. 1/8 of the original filter was subjected to sequential extraction with 50 ml of ultrapure H_2O, for two days in order to obtain the water-soluble fraction of the studied metals. The extract was microwave digested with 2:1000 HNO_3 Upa and 1:1000 H_2O_2 Upa. The filter containing the residue after the extraction procedure was then totally solubilised and mineralized using a MW procedure previously set up (Illuminati et al., 2015) with 5ml of HNO_3 Upa, 1 ml of H_2O_2 Upa and 1 ml of HF Upa, in order to obtain the insoluble fraction. After digestion, the solutions were diluted to 10 ml using ultrapure water and subjected to metal determination. To test the measurement additivity of the two-aliquot fractionation with respect to the total content, a further 1/8 of the original filter was directly MW digested using the same procedure of the insoluble fraction, to obtain the total metal content. The results were then compared with the total content computed from the sum of the soluble and insoluble fractions.

3.6. Metal determination

Metals (Cd, Pb and Cu) in seawater and phytoplankton, were determined simultaneously, by using the Square Wave Anodic Stripping Voltammetry (SWASV) in the background-subtraction mode, according to procedures set-up and optimized in our previous works (Illuminati et al., 2013, Truzzi et al., 2002, 2008, 2015). For aerosol samples, Cd, Pb and Cu in the insoluble and total metal content fractions and Cd in the soluble fraction were determined by Graphite Furnace Atomic Absorption Spectrometry (GF-AAS), while Pb and Cu in the soluble fraction was determined by voltammetry, due to the low concentrations and the high detection limit of AAS for these metals.

3.6.1. Metals in seawater and phytoplankton

Preparation of the mercury film electrode. The thin mercury film electrode was prepared by electrochemical deposition each day according to a procedure reported in Annibaldi et al., 2007, Truzzi et al., 2008 and Illuminati et al., 2013. Briefly, the graphite electrode surface was polished (rotation 1000 rpm; for ~30s) using wet alumina powder (0.015 μm, if necessary preceded by 0.3 μm) cleaned with 1+200 diluted ultrapure HCl and rinsed with ultrapure water. The mercury film was then prepared in a 25-ml outgassed solution (10 min flux of N_2) of 6×10^{-5}mol/l $Hg(NO_3)_2$ and

12 mmol/l KCl as support electrolyte. The 2.5×10^{-2} mol/l $Hg(NO_3)_2$ solution was obtained by oxidation of the superpure hexadistilled mercury with ultrapure nitric acid.

With electrode rotation at 3000 rpm, three sets of fast cyclic triangular wave potential scans were applied from−1000 mV to 0 mV at a rate of 1 V/s and from 0 mV to −1000 mV at 10 V/s, one set of 100 cycles and two sets of 10 cycles, alternating with short depositions at −1300 mV for 60 s and followed by square wave scans (initial potential −1100 mV, SW amplitude 25 mV, frequency 100 Hz, step height 8 mV, step time 150 ms, measurement time 3 ms, total no. of SW cycles in each step 4, final potential −20 mV). Then, the electrochemical deposition of the mercury film was carried out at a potential of−1000 mV for 20 min (rotation3000 rpm). Film cleaning followed at −150 mV for 5 min (3000 rpm) and finally a square-wave voltammetric (SWV) scan was carried outfrom−900 mV to−150 mV to check the mercury film performance (instrumental parameters as above in the electrode pre-treatment). If the voltammogramm obtained did not show any irregular peack or recognized metal (Cd, Pb, Cu) peaks and if the background current at the curve minimum was sufficiently low (2-3 μA), then the sample was analysed; otherwise the Hg film was wiped out and the Hg film preparation procedure was repeated.

Voltammetric analysis. Cd, Pb and Cu were simultaneously determined using the following procedure. A 10-ml sample digested solution was poured into a Teflon voltammetric vessel placed in an outgassing post outside the electrochemical stand. The sample was then outgassed with nitrogen flushed for 10-15 min after which it was rapidly transferred with its vessel under the head of the electrochemical cell, where the mercury film electrode was already prepared and tested (as explained above). After a further 30-s purging with N_2, metal deposition was carried out with electrode rotation at 3000 rpm, and with N_2 continuously flowing over the solution. For all the samples, the metal depositions were carried out at a potential of –1100 mV (electrode rotation of 3000 rpm) with times varying as a function of metal concentrations. For seawater and phytoplankton samples, deposition time varied from 5 to 30 min. In cases of very different concentrations between the three metals (especially with very low values of Cd and Pb in comparison with the high concentration of Cu), copper was measured in separate analysis using reduced deposition time (from 5 min to 7 min). Concerning the total marine particulate matter, deposition times of 5-45 min were used (in case of different concentrations, Pb and Cu were determined in separate analysis with reduced deposition times, i.e. from 5 to 7 min).

The electrode rotation was then stopped, and after a 30-s quiescent time, the anodic stripping voltammetric scan was carried out from –1100 mV to a final of –50 mV for seawater and phytoplankton; and +70 mV for the marine particulate samples. The following instrumental

parameters were applied to all samples: frequency 100 Hz; square-wave amplitude 25 mV; potential step height 8 mV; step time 150 ms; current sampling time 3 ms. At the end of the scan, the electrochemical cleaning of the mercury film was carried out with the potential held at –150 mV for 3 min for seawater and phytoplankton, and at +20 mV for 3 min in particulate matter samples. The background voltammogram to be subtracted from the analytical voltammograms was obtained before sample analysis by applying an equilibration potential equal to the deposition potential (–1100 mV) for an equilibration time of 7.5 s in all cases, except when Cd was involved (t_{equil} =120 s). This background voltammogram was then subtracted from the sample voltammogram and from all the subsequent analytical voltammograms (background subtraction mode) in order to achieve a significant improvement of the detection capability. To verify the repeatability, two/three replicates were carried out with the sample in the cell, after that the quantification was obtained using the multiple standard addition procedure.

3.6.2. Metals in the aerosol

Metals in the Antarctic atmospheric particulate matter were determined by graphite furnace atomic absorption spectrometer equipped with the Zeeman background correction. The hollow cathode multi element lamps were operated at 5mA with a 0.5 nm slit and wavelengths of 228.8 nm ad 283.3 nm for Cd and Pb, respectively; while for Cu the hollow cathode lamp operated at 10 mA with a slit of 0.5 nm and a wavelength of 324.8 nm. All the measurements were performed directly in the digested solutions. For Cd and Pb analysis a chemical modifier was used. The chemical modifier was a palladium solution prepared by 0.120 g of $C_6H_8O_7$, 200 µl of UpA HNO_3, 200 µl of $Pd(NO_3)_2{\cdot}2H_2O$ in 6ml of ultrapure H_2O.

The multiple standard addition procedure was used to quantify Pb content in aerosol, while the calibration procedure was used for Cd and Cu quantification. To test repeatability, at least three replicates were performed in the sample and after each addition.

Pb and Cu in the soluble fraction of the aerosol were determined by SWASV with the same procedure of seawater samples. The following instrumental parameters were used: deposition potential −1100 mV; deposition time 10 min for Pb and 30s for Cu, voltammetric scan from −1100 mV, to +120 mV; cleaning potentials +20 mV, cleaning time 3min; equilibration potential −1100 mV; equilibration time 120 s; frequency 150 Hz; square-wave amplitude 20 mV; potential step height 8 mV; step time 100 ms; current sampling time 2 ms.

3.7. Laboratory blanks and accuracy

Repeated SWASV measurements of the laboratory blank were carried out during the period of work, with deposition times of 20 min. Results showed that generally no voltammetric signals are observed for Cd and Cu, indicating metal contents below the detection limit of the technique for 20 min deposition time, i.e. about 1-3 pmol/l, with the exception of Pb for which an instrumental blank signal of 10 pmol/l (Annibaldi et al., 2007, Truzzi et al., 2002) was observed.

Phytoplankton separation from inorganic particulate was carried out under microscope, sucking with a Pasteur pipette and using plastic containers. Considering that all these manipulations expose samples to possible contamination, a further blank (derived from the sum of plastic containers blank and phytoplankton microwave vessel blank) was subtracted to the metal concentrations measured in the algal particulate. Results of the different blanks analysed are reported in Table 1 separated for each metal and each sample.

To ascertain accuracy and to assure comparability of data produced during metal determinations, analytical quality control of Cd, Pb and Cu measurements were carried out by analysing the NASS-6 certified reference material (NRCC, 2010) for seawater samples, the BCR-414 certified reference material (Europea Commission, 2007) for phytoplankton samples and the NIST 1648a urban particulate reference material (NIST, 2012) for aerosol samples. These materials were subjected to the same treatments of the samples. The results of the systematic measurements (n = 5-7) carried out on reference materials during the entire period of work are showed in Table 2. As it can be noted, concentrations of Cd, Pb and Cu measured in the reference materials were in good agreement with certified reference values within the experimental errors, showing a good accuracy of all measurements.

Tab. 1. Cd, Pb and Cu concentrations in the blank solutions of the plastic containers for separated phytoplankton samples and of the microwave vessels. Data reported as mean ± SD[a] of at least three measurements

Sampling date	Depth, m	Metal concentrations, ng/l		
		Cd	Pb	Cu
28/11/2013	3	bdl	37±2	1216.4±3
	8	73±18	102±4	2127.4±3
	18	bdl	32±2	289.4±21
	40	bdl	bdl	bdl
	80	21±1	32±1	72±0.0
	200	bdl	bdl	bdl
07/12/2013	1	bdl	20±1	138±3
	10	bdl	33±2	214±4
	30	9±2	64±7	276±4
	50	bdl	35±1	295±4
	100	3±0	34±2	211±4
	200	9±1	45±2	224±3
17/12/2013	1	bdl	31±3	374±32
	10	bdl	bdl	bdl
	30	bdl	42±3	359±8
	60	bdl	20±1	138±3
	100	5±0	71±15	385±17
	200	0.0±0.0	80±3	584±21
02/02/2014	1	12±1.5	78±2	334±13
	10	15±1	32±2	288±4
	20	7±0	31±2	260±3
	40	3±1	42±2	218±24
	60	15±1	144±2	188±3
	80	24±1	26±2	409±32
	100	6±0.0	38±2	321±12
	200	10±2	36±1	217±3.
	300	bdl	bdl	bdl

[a]±SD computed as the square root of the sum of variances
bdl= below the detection limit

Tab. 2. Accuracy tests on the NASS-6 certified reference material for open sea waters, on the BCR-414 certified reference material for plankton and NIST-1648 certified reference material for atmospheric particulate matter.

	Metal concentrations								
	NASS-6, ng/l			BCR-414, µg/g			NIST-1648a, mg/kg		
	Cd	Pb	Cu	Cd	Pb	Cu	Cd	Pb*	Cu
Experimental values	30±4	6.0±0.4	270±46	0.39±0.02	3.81±0.15	28.3±0.6	79.0±7.0	0.678±0.032	619±37
Certified values	31.1±2[a]	6±2[a]	248±25[a]	0.383±0.014[b]	3.97±0.19[b]	29.5±1.3[b]	73.7±2.3[c]	0.655±0.033[c]	610±70[c]
Δ%	+4	+0	−9	+1.8	−4.3	−4.0	+7.2	+3.5	+1.5

*values reported as percentage, %
[a] ±expanded uncertainties
[b] ±half-widht of the 95% confidence intervals
[c] ±expanded uncertainties

3.8. Ancillary measurements

3.8.1. CTD data processing

During the 2013-2014 Antarctic campaign, continuous water column profiles (vertical resolution of 0.5 m), were sampled for the master hydrographic variables (i.e. temperature, salinity, conductivity, dissolved oxygen, oxygen saturation, pH, redox potential) using a CTD probe fitted with a fluorimeter for the chlorophyll-a vertical profiles. The salinity is expressed according to the UNESCO practical salinity scale, PSS 1978 (UNESCO, 1981/331). Temperature and salinity data obtained from the CTD measurements were used to calculate the density (ρ) and the water column stability. The latter is proportional to the Brunt-Värsälä buoyancy frequency $N^2(z)$, which represents the strength of density stratification and it is defined by the equation

$$N^2(z) = -\frac{g}{\rho(z)}\frac{\Delta\rho(z)}{\Delta z}$$

where g is the gravitational acceleration, ρ is the mean density averaged over Δz depth interval, (Agustì and Duarte, 1998, Garcia et al., 2008, Fofonoff and Millward, 1983). The depth at which the Brunt-Värsälä buoyancy frequency was estimated to be maximal represents the Upper Mixed Layer (UML), which also corresponds approximately to the middle of the pycnocline. The value of $N^2(z)$ was also taken as a stability index of the water column (i.e. what it is commonly called pycnocline strength). The depth at the base of the pycnocline corresponds to the top of the winter

water and it is considered to be unaffected by the summer dilution or phytoplankton assimilation (Fabiano et al., 1993).

3.8.2. Nutrient determination

For each sampling, several discrete samples were also collected at different depths for the determination of dissolved inorganic nutrients (nitrate–NO_3^-; nitrite–NO_2^-; ammonium–NH_4^+, phosphate–PO_4^{3-} and silicate–$Si(OH)_4$. Nutrient analysis utilized modifications of the procedure developed by Strickland and Parsons (1972) and by Thomas and Chamberlin (1974). N-Ammonium was determined by a nanocolor method, based on the Berthelot reaction, in which ammonia reacted first with hypochlorite, and then with a phenolic compound, to give the blue-green colored indophenol complex which is measured at ~625 nm. Sodium nitroprusside was used to enhance the sensitivity of the method.

Nitrite was measured by reacting the sample under acid conditions with sulphanilamide to form a diazo compound that then couples with N-(1-Naphthyl)-ethilendiamine to form a reddish purple azo dye that is measured at 540 nm.

Nitrate was determined in the sample under acid conditions (by adding 1 mol/l HCl) at 220 nm.

Orthophosphate determination was carried out by a spectrophotometer method in which a blue compound is formed by the reaction of phosphate and molybdate in presence of antimony followed by reduction with ascorbic acid. The blue compound is detectable at 704 nm.

The colorimetric method for the determination of soluble orthosilicates is based on the reaction of a silicomolybdate in acid solution to molybdenum blue which is detectable at 802 nm.

Dissolved inorganic nitrogen (DIN) was calculated as the sum of the NO_3^-, NO_2^- and NH_4^+ concentrations.

3.8.3. Meteorological parameters and air mass origin

Meteorological parameters (air temperature, relative humidity, ambient pressure, wind speed and direction) were continuously registered at time intervals of 1h by the Automatic Weather Station (ASW) sited close to the sampling sites of both aerosol and seawater.

In order to characterize the transport pathways of air masses before they arrive at the study site, 7-day backward trajectories were computed using the Hybrid Single Particle Lagrangian Integrated Trajectories (HYSPLIT) model assessed via NOAA Air Resources Laboratory READY (Real-time Environmental Applications and Display sYstem) site http://www.arl.noaa.gov/ready/hysplit4.html, (Draxler and Rolph, 2015) and the NCEP/NCAR Global Reanalysis Data. The back trajectories were calculated for three arrival heights: 100 m, 500 m and 1000 m a.g.l. (above the ground level).

Generally, these trajectories changed altitudes as a function of the transit time and the heights here considered are only those at which they arrived at the study site. The height of 100 m was chosen between the sampling height (~60 m above the sea level, a.s.l.) and the upper limits of the Antarctic marine boundary layer, typically of 400 m (Argentini et al., 2005), which is much shallower than the typical mid-latitude or tropical convective boundary layer, as a result of the persistent stability of the overlaying atmosphere limiting the boundary layer development (King and Turner, 1997). The choice of 7 days was made due to the longer lifetime expected for aerosols in this region (Shaw, 1988) with respect to mid-latitudes.

WARNING: *Data and information on local meteorology were obtained from Operational Meterological Infrastructure of ENEA-UTA (www.enea.uta.it) through the "Meteo-Climatological Observatory" of PNRA (www.climanantartide.it).*

4. Results

4.1. Environment

4.1.1. Meteorological parameters

Daily means of the different weather parameters are reported in Fig.3. Measured temperatures were typical of summer season at Terra Nova Bay (Grigioni et al., 1992), varying between −17 °C and +5.4 °C, with an average value of about −3 °C (Fig. 3a). An increasing trend in daily mean temperature was observed during the summer, reaching values that oscillated around +5 °C at the beginning of January. After this period, the temperature slightly decreased, remaining however to values that are typical of the summer season.

No snowfall occurred during the studied period, this was confirmed by the atmospheric pressure (P) and relatively humidity (RH) values.

Relative humidity (RH) averaged for the entire studied period around 46%, showing the dryness of the continent. Even if it greatly oscillated from very low values (~18%) to maximum of 80%, RH remained practically constant during the entire sampling period (Fig. 3b).

The mean daily pressure at Faraglione Camp was 970 hPa. Atmospheric pressure was low (~950 hPa) at the beginning of the summer season (November 2013), while it increased at December to ~977 hPa and remained constant until the end of the season (Fig. 3c).

The wind speed (Fig. 3d) was generally high, ranging from ~2 knots to ~39 knots. Several katabatic-wind events occurred, especially in the first half of the summer season. In these events the wind speed reached values of ~40 knot (~20 m/s). The wind rose reported in Fig.1 shows that the prevailing wind direction over Faraglione Camp was West. The katabatic winds in Terra Nova Bay have been the subject of numerous observational studies, they are strongly modulated by the presence of deep glacial valleys, draining dense air from Plateau and driving it towards the coast (Davolio and Buzzi, 2002). The 7-day back trajectories ending over Faraglione Camp on December the 1st 2013, December the 22th 2013 and January the 3rd 2014 (Fig.4) seemed to confirm that the air masses were mainly originated in the inner part of the Antarctic continent and arrived at Faraglione Camp running along the coast.

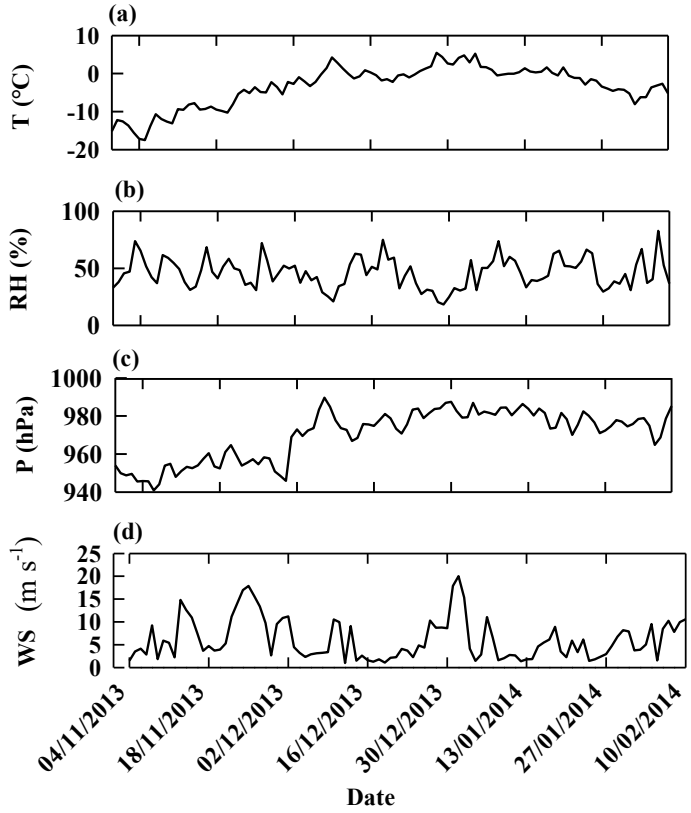

Fig. 3. Meteorological parameter variations at Faraglione Camp during the sampling period. The panels **(a)**, **(b)**, **(c)** and **(d)** show the day to day variation of air temperature (°C), relative humidity (%), pressure (hPa) and wind speed (m s^{-1}), respectively.

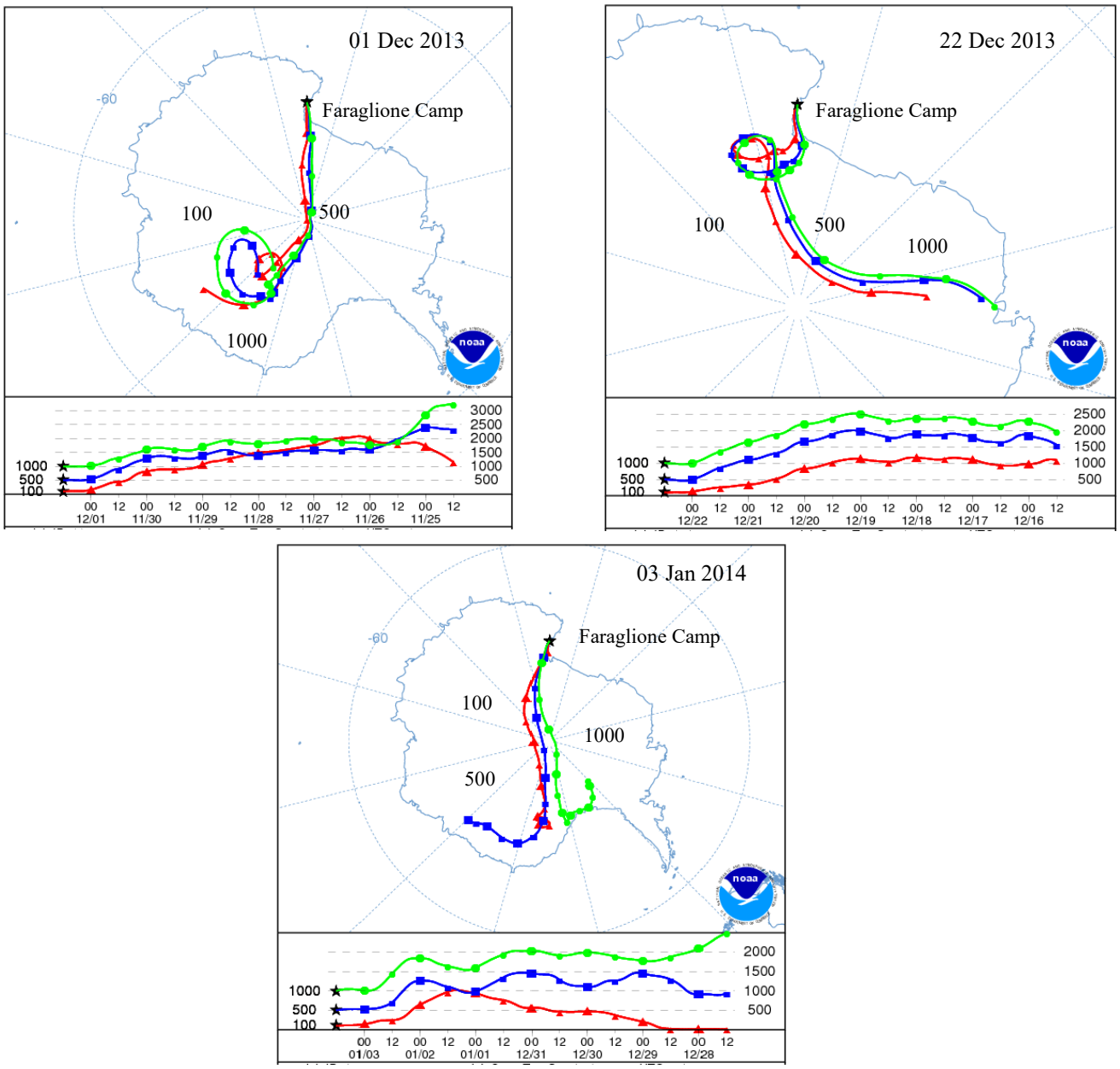

Fig. 4. Seven days back-trajectories on 01 December 2013 (beginning of the sampling period), 22 December 2013 and 03 January 2014 over Faraglione Camp, Antarctica. (Top) Geographical location of the air parcel. (Bottom) Altitude variation of air parcel with time. Height is in meter above the ground level.

4.1.2. Hydrography of the study area

Vertical profiles of the principal hydrographic variables (temperature, salinity, conductivity, dissolved oxygen, redox potential and pH) obtained in the Gerlache Inlet Area during the sampling period (austral summer 2013-2014) are showed in Figures 5-12. Note that from time to time values corresponding to the first few meters are anomalous since they refer to water present in the hole made in pack ice.

In the austral spring 2013, the pack ice was 2.5 m thick and it started to melt from mid-December, with the Gerlache Inlet area completely free from ice from the end of December. As reported above, unfortunately only one sampling was carried out after the pack ice melting, due to technical problems.

Temperature and salinity varied greatly from –1.95 °C to +1.36 °C and from 19.69 psu to 35.14 psu, respectively (Figures 5-6). Density anomaly (Fig. 7) computed from temperature and salinity data varied from 15.76 kg/m^3 to 28.30 kg/m^3. Temperature varied within a narrow range (~30% variability), thus density variations were essentially due to salinity variations. At the beginning of the sampling period the pack ice covered the most part of Terra Nova Bay. In this period, no stratification of the water column was observed (density values almost constant), with temperature gradually decreasing (from –1.66 °C to –1.85 °C), and salinity increasing, varying little and very gradually with depth (from 34.50 to 34.74 psu). Wide ice-free areas started to appear from mid-December, with the subsequent increasing of the solar radiation incidence in the surface waters. As a result, surface and sub-surface waters were warmer (from –1.7 °C to –1.4 °C) and less salty (from 34.65 psu to 32.92 psu) with the appearance of weak thermocline and halocline. The water column was still homogeneous, the density gradient decreased for the dilution effect following the pack ice melting (Fig 6.). At the end of the campaign (February the 2nd, 2014) all the pack ice was fully melted. In this period a steep and deep (~60 m) thermocline was observed, which was associated with an equivalent salinity steep gradient. As a result, the water column was stratified, the picnoclyne being as strong as $N^2(z) = 63.6 \times 10^{-5} s^{-1}$.

Dissolved oxygen (Fig. 8) showed concentrations in the range 10.3-16.6 mg/l with percentages (Fig. 9) generally over saturation levels (100%) within the euphotic zone (the first 50-m layers). The vertical profiles of O_2 showed the typical bell-shaped trend with depth, with the highest values corresponding to the DCM. In the superficial layer O_2 concentration remained constant during the summer, however in February, along the seawater column, it decreased to values below the saturation level, however never reaching hypoxia levels ($<$50%).

The redox potential (Fig. 10) showed values that ranged from ~290 mV to ~400 mV. Eh decreased from November to mid-December, while it greatly increased in February, reaching the

highest values for the season (~400 mV). The redox potential remained almost constant along the seawater column for all the samplings. pH (Fig. 11) ranged from 7.3 to 8.5, and showed a temporal trend similar to that observed for dissolved oxygen. For all the samplings, pH remained almost constant the way down to the bottom.

Chlorophyll-*a* (Chl-*a*) concentrations measured in situ by the CTD probe ranged from ~0.08 µg/l to ~27 µg/l (Fig. 12). A clearly defined Deep Chlorophyll Maximum (DCM) was observed throughout the sampling period. At the end of November, the Chl-*a* concentration was low at the DCM (~7 µg/l) and the Chl-*a* peak was very shallow (~10-20 m depth). During summer, it increased and deepened, reaching the highest concentrations on mid-December (26.7 µg/l) at the depth of 40 m. On early February, the Chl-*a* decreased to values similar to those observed in November and with the same broader shape of the DCM. In the deepest layer (200 m depth) of the water column, Chl-*a* showed values close to zero throughout the sampling period.

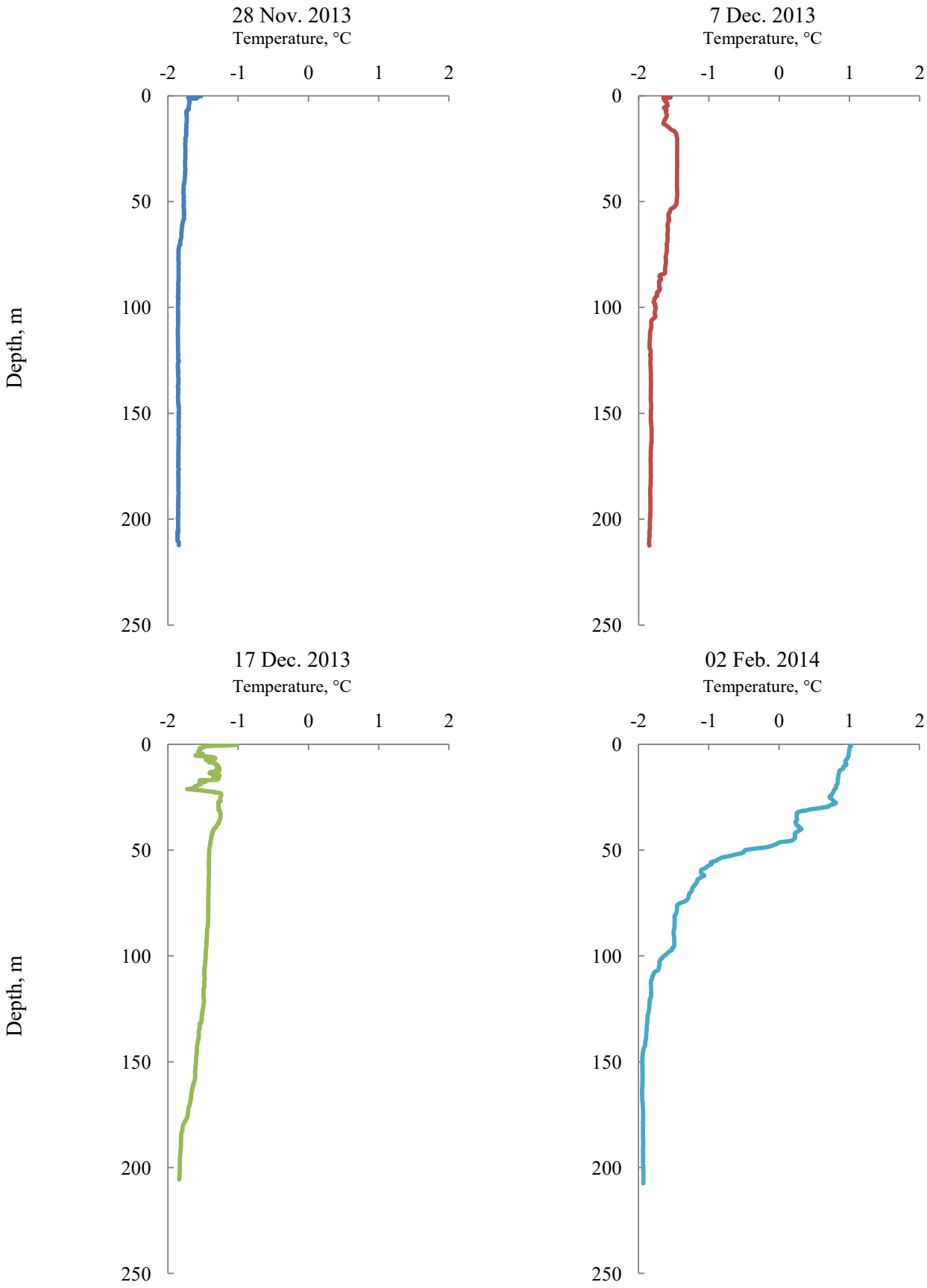

Fig. 5. Vertical profiles of temperature trend recorded on November the 28th 2013, December the 7th and 17th 2013 and February the 2nd, 2014.

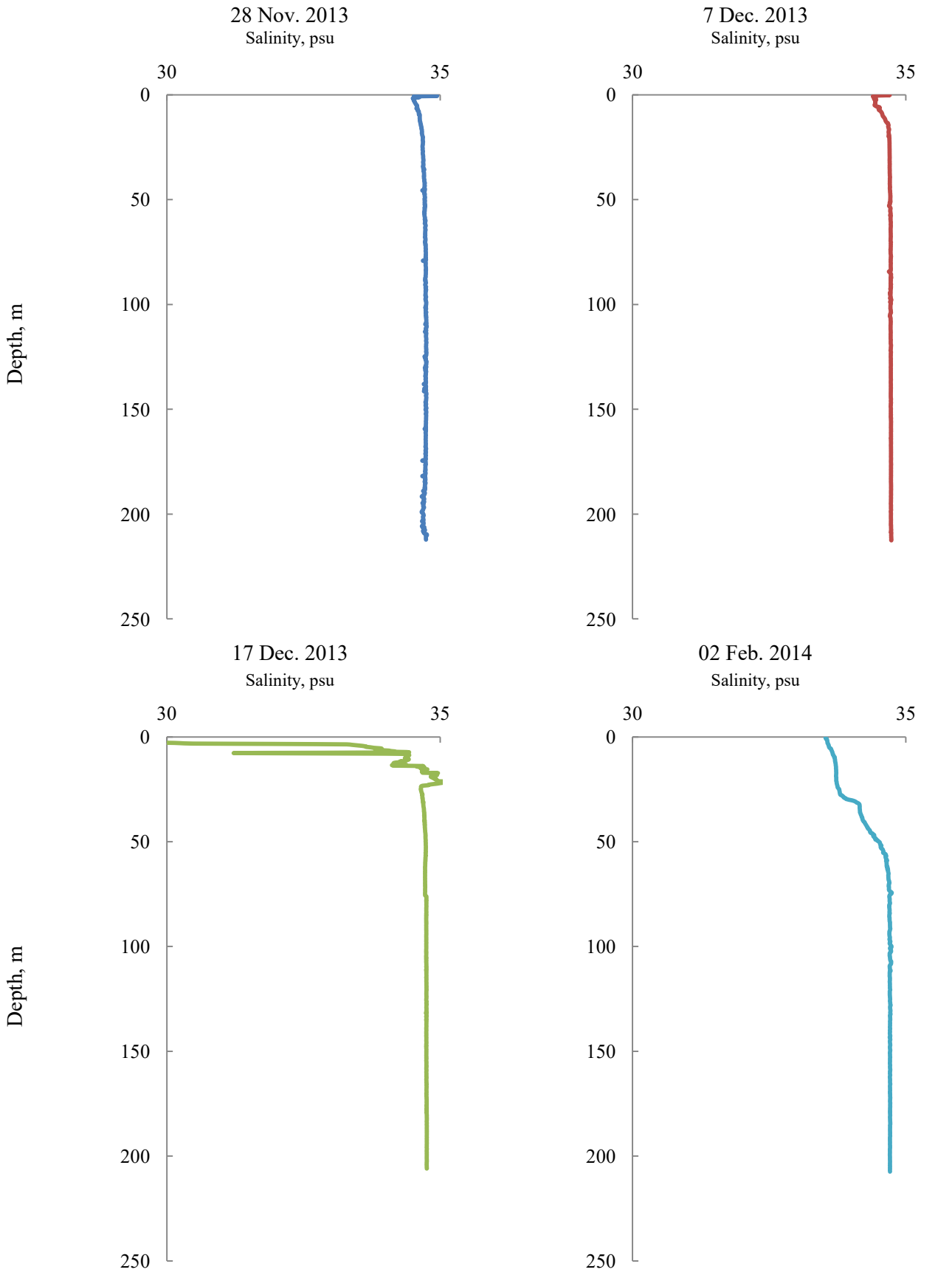

Fig. 6. Vertical profiles of salinity trend recorded on November the 28th 2013, December the 7th and 17th 2013 and February the 2nd, 2014.

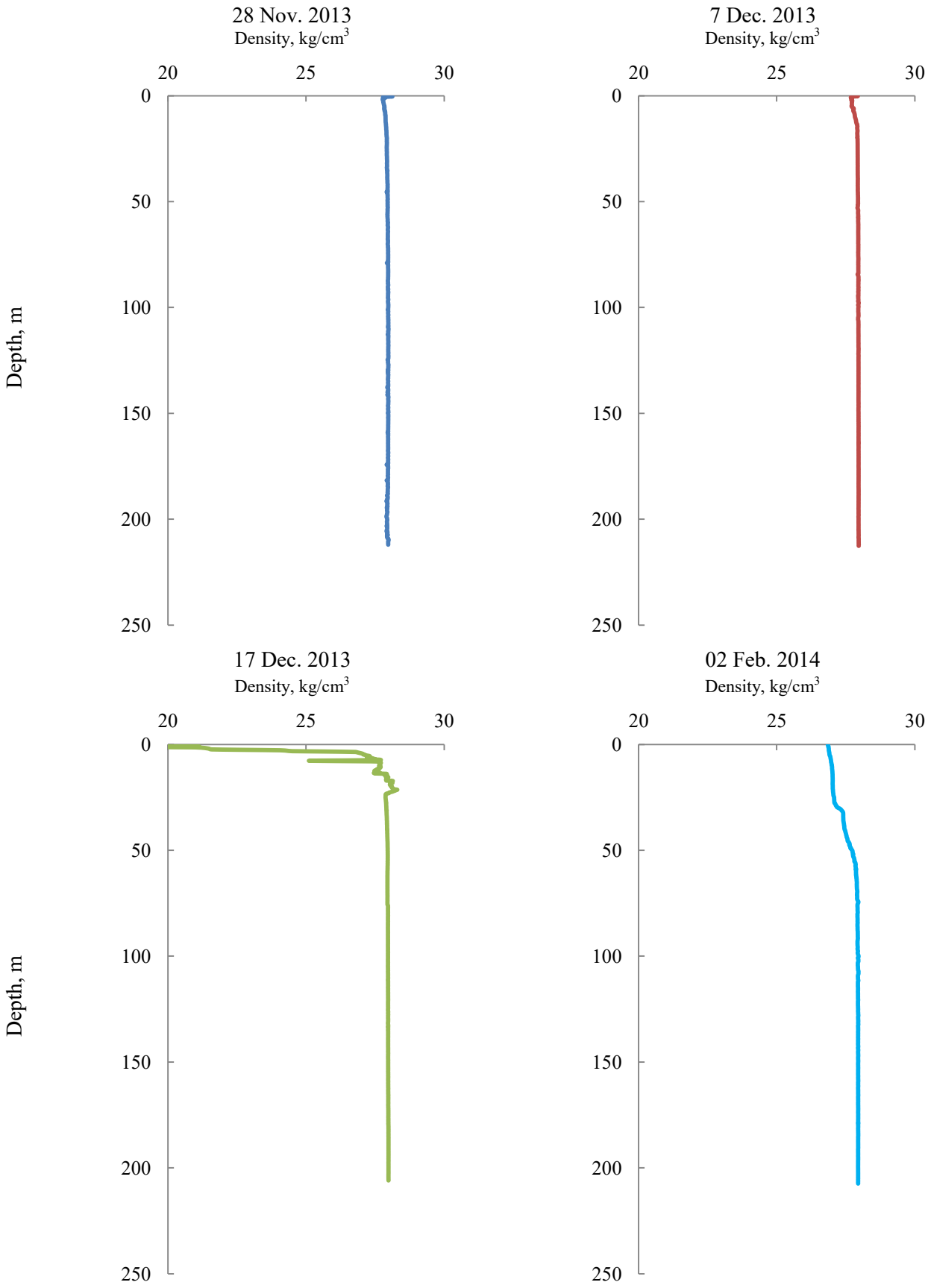

Fig. 7. Vertical profiles of density anomaly trend recorded on November the 28th 2013, December the 7th and 17th 2013 and February the 2nd, 2014.

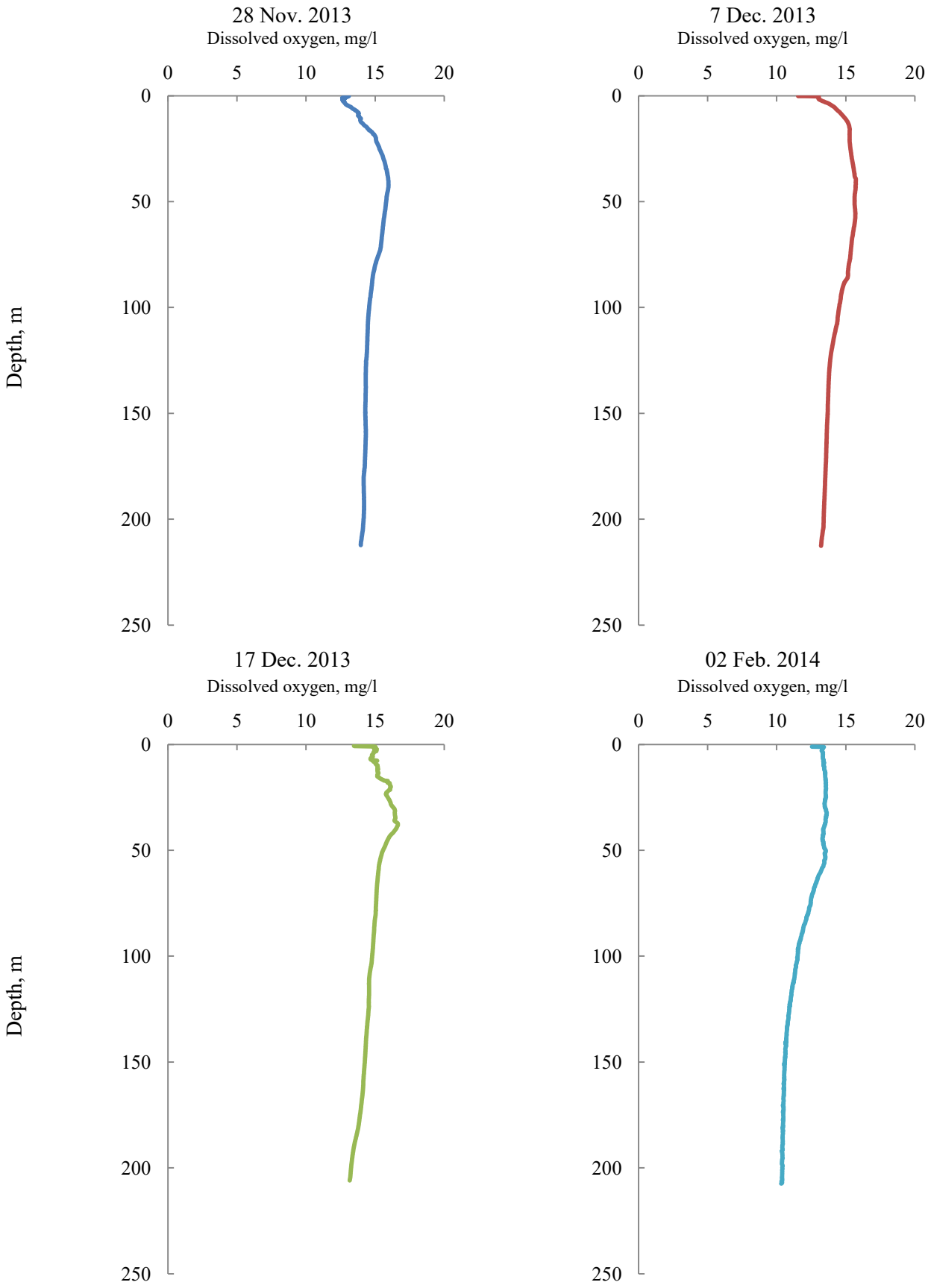

Fig. 8. Vertical profiles of dissolved oxygen trend recorded on November the 28th 2013, December the 7th and 17th 2013 and February the 2nd, 2014.

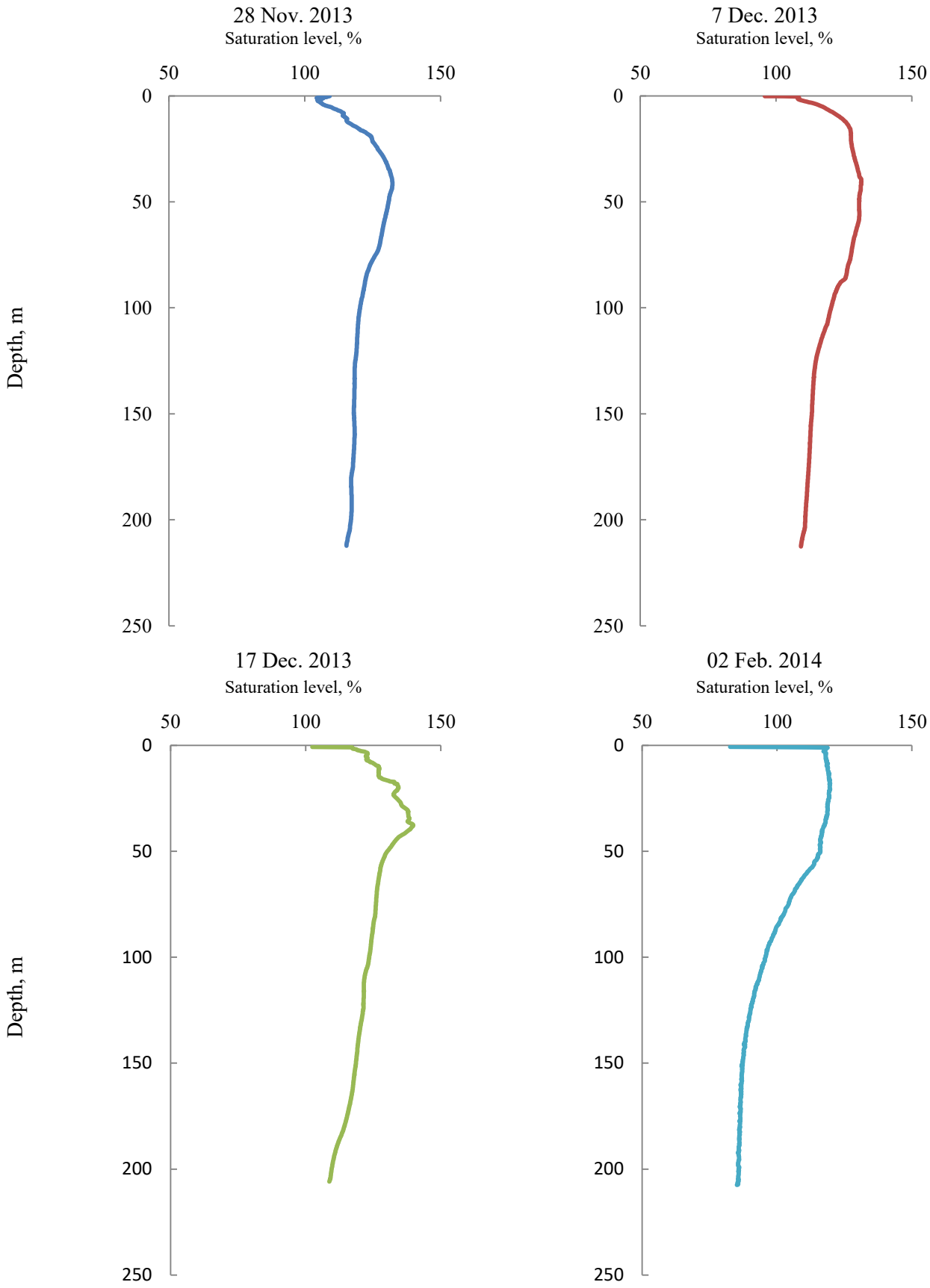

Fig. 9. Vertical profiles of oxygen saturation trend recorded on November the 28th 2013, December the 7th and 17th 2013 and February the 2nd, 2014.

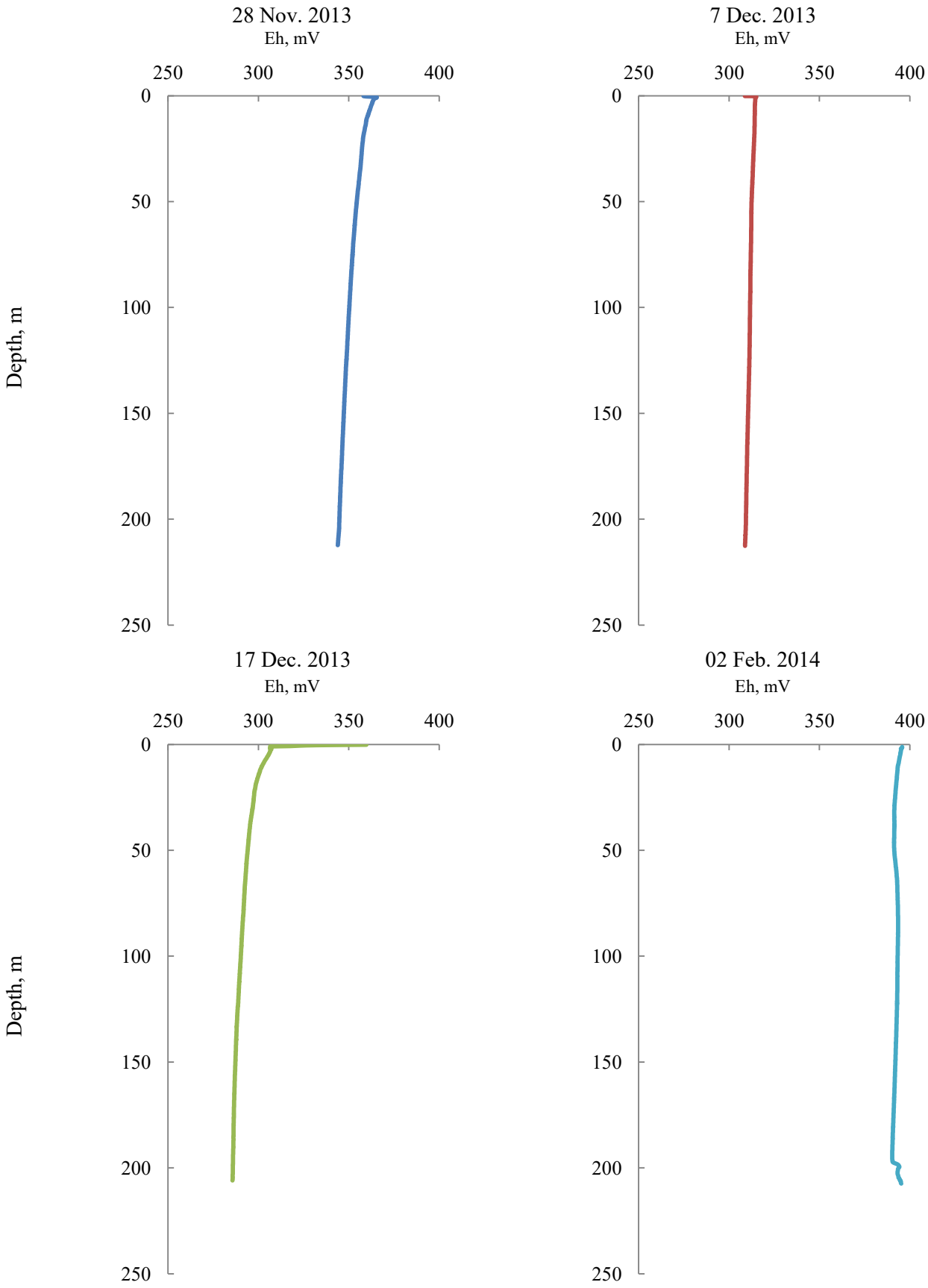

Fig. 10. Vertical profiles of redox potential (Eh) trend recorded on November the 28th 2013, December the 7th and 17th 2013 and February the 2nd, 2014.

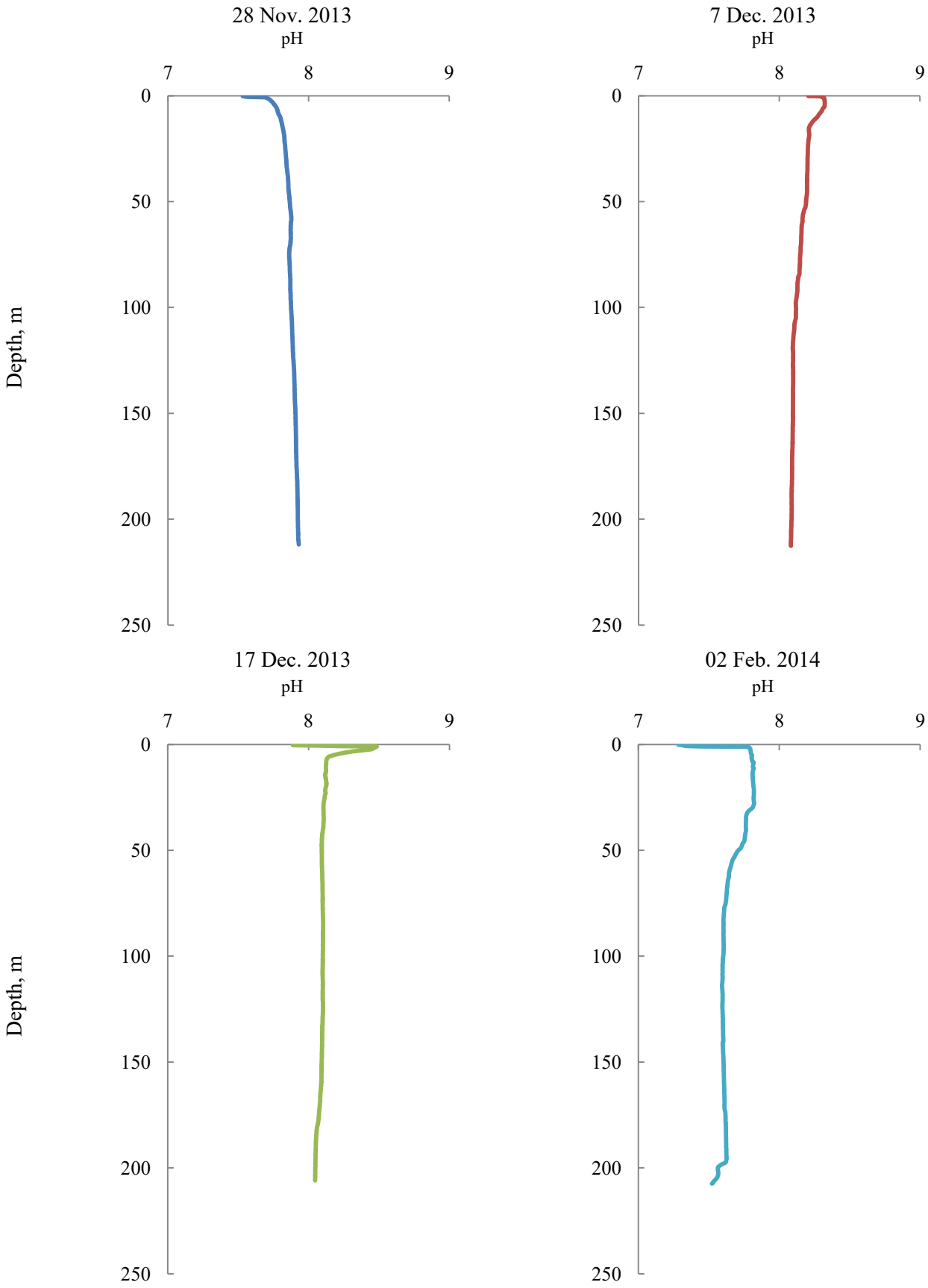

Fig. 11. Vertical profiles of pH trend recorded on November the 28th 2013, December the 7th and 17th 2013 and February the 2nd, 2014.

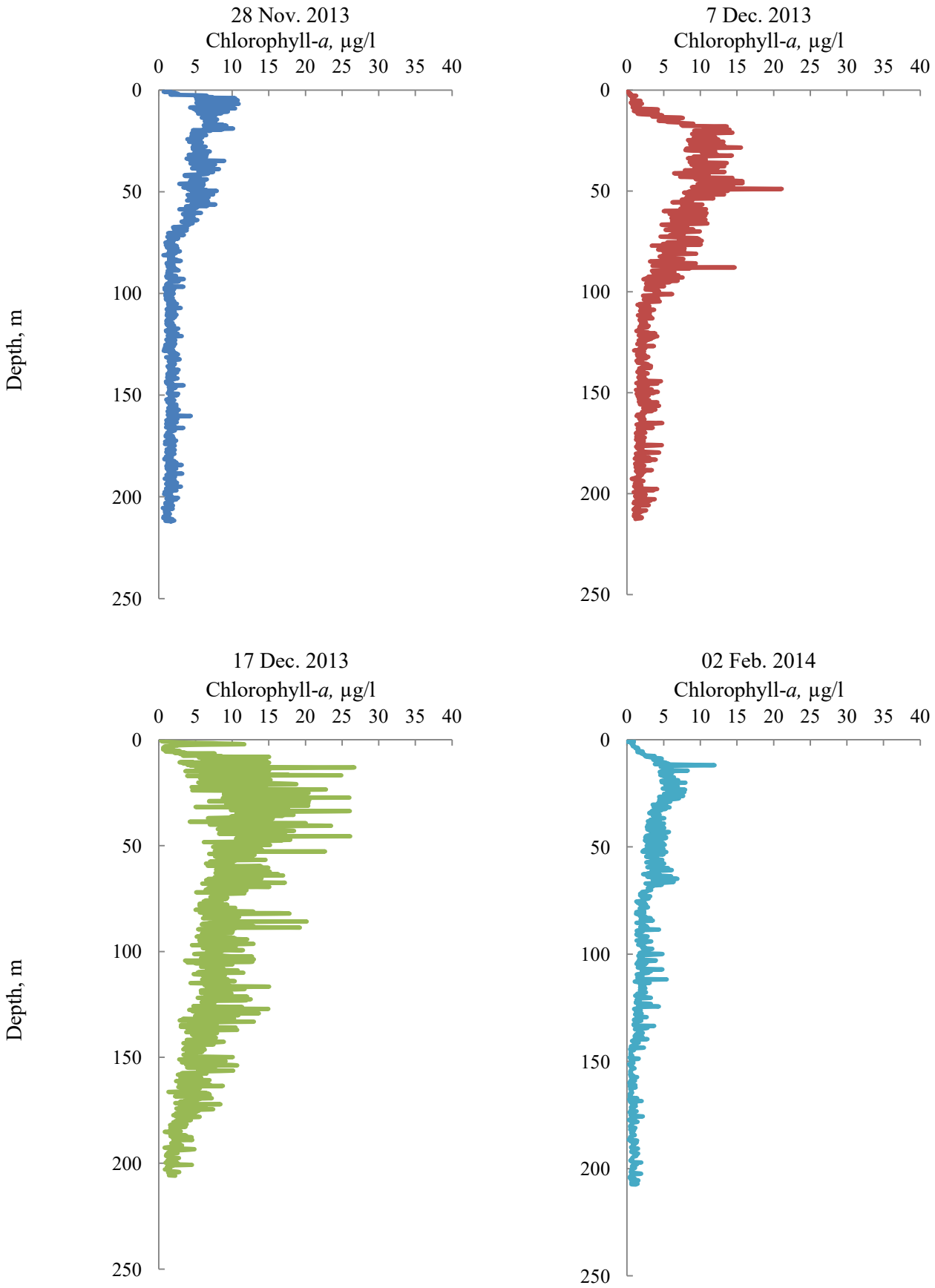

Fig. 12. Vertical profiles of chlorophyll-*a* trend recorded on November the 28th 2013, December the 7th and 17th 2013 and February the 2nd, 2014.

4.1.3 Nutrients

Dissolved nutrients concentrations in seawater during the 2013-2014 Antarctic Campaign are reported in Table 3, their vertical profiles are reported in Figures 13.

Data showed that nutrient concentrations were generally high to sustain high biomass stock and they were never fully depleted.

During the 2013-2014 Antarctic campaign PO_4^{3-} concentrations varied from ~0.17 µM to ~1.45 µM (mean ± SD of 0.74 ± 0.33 µM), NH_4^+ from ~9 µM to ~33 µM (mean ± SD of 18 ± 6 µM), NO_3^- from ~16 to ~80 µM (mean ± SD of 48.2 ±16.1 µM), NO_2^- from ~0.1 to ~0.5 µM (mean ± SD of 0.3 ± 0.1 µM), $S_i(OH)_4$ from ~4 µM to ~98 µM (mean ± SD of 50 ± 25 µM). DIN concentrations (calculated as the sum of NO_3^-, NO_2^- and NH_4^+) varied from to ~39.6 µM to ~89.5 µM (mean ± SD 66.3 ± 16.4 µM), it was represented for the most part by nitrates (30-90% of the sum). A small fraction (ranging from 11% to 67%) of the DIN was represented by ammonium, while nitrites represented generally a low quote (0.1-0.8% of the total).

To study relationships between all the variables (hydrologic, nutrients, metals) the correlation matrix (and the corresponding p values) was computed. The full correlation matrix obtained using all the data (samplings C1, C2, C3, and C4) is reported in Table A1 of the Appendix. Cases with $p<0.05$ are in bold face while cases with $0.05 \leq p<0.1$ are underlined. Correlations matrices obtained excluding the first sampling (Tab. A2), the first two (Tab. A3) and the first three (Tab. A4) are reported too.

Considering nutrients and all the samplings (Tab. A1) it can be seen that, excluding the obvious correlation between nitrate and DIN ($r=0.93$ $p<0.05$), all the others are not significant (except DIN *vs* silicates $r=0.41$, $p=0.04$, and NO_3^- *vs* silicate $r=0.35$, $p=0.08$). However, if we excluded the first two profiles (Tab. A3, samplings C3, C4) it can be seen that significant relationships ($p<0.05$) are obtained for the couples NO_3^- *vs* PO_4^{3-} ($r=0.65$, $p=0.01$), NH_4^+ *vs* DIN ($r=0.60$, $p=0.02$) and DIN *vs* PO_4^{3-} ($r= 0.63$, $p=0.01$). Moreover, if we consider the significant level $\alpha=0.1$ ($p<0.1$), other two couples can be added: silicate *vs* NO_3^- ($r=0.49$, $p=0.07$) and silicates vs DIN ($r=0.53$, $p=0.05$).

No significant relationships are observed between Chl-*a* and nutrients from all the data, nor higher correlations are obtained if we exclude the first two profiles (Tab A3 in the Appendix).

The nitrate *vs* phosphate and silicate *vs* nitrate relationships (obtained by regression analysis) are plotted in Fig. 14 considering all the data obtained for all the samplings. No significant correlations were found between nitrate and phosphate: $NO_3^- = 11.6\ PO_4^{3-} + 39.7$ ($r=0.23$, $p=0.23$) and between silicate and nitrate: $Si(OH)_4 = 0.44\ NO_3^- + 37$ ($r=0.35$, $p=0.08$).

The silicate:nitrate ratio was ~1 from November to mid-December in the superficial layer and at the DCM, therefore $Si(OH)_4$ resulted available in seawater. A slight decrease was observed on February.

Tab.3. Nutrients [NH_4^+, NO_2^-, NO_3^-, DIN, PO_4^{3-}, $Si(OH)_4$] concentrations in seawater samples during the austral Summer 2013-2014. Data reported as mean ± SD of at least three measurements.

Sampling date	Depth, m	Nutrients concentration, μM						
		NH_4^+	NO_2^-	NO_3^-	DIN[a]	PO_4^{3-}	$Si(OH)_4$	$Si(OH)_4$:NO_3^-
28/11/2013	3	12±3	0.36±0.05	53.4±0.7	66±3	0.46±0.08	74±4	1.39
	8	25±3	0.24±0.02	50.9±0.5	76±3	0.17±0.03	67±1	1.32
	18	25±3	0.22±0.00	49.5±0.7	75±3	0.62±0.05	98±5	1.97
	40	17±1	0.32±0.01	52.9±0.5	70±1	1.03±0.05	59±2	1.12
	80	19±3	0.38±0.02	63.1±0.7	82±3	0.52±0.17	72±1	1.13
	200	9±2	0.35±0.05	65.7±0.2	75±2	0.38±0.05	46±3	0.70
07/12/2013	1	16±4	0.36±0.05	23.9±0.5	40±4	1.03±0.03	40±3	1.69
	10	19±3	0.24±0.02	26.5±0.5	46±3	1.45±0.08	54±1	2.03
	30	33±1	0.22±0.00	15.6±0.7	48±2	0.37±0.08	43±1	2.73
	50	25±4	0.32±0.01	31.6±0.2	57±4	0.30±0.03	41±4	1.29
	100	17±2	0.38±0.02	33.7±0.9	51±2	0.43±0.05	78±2	2.31
	200	13±3	0.35±0.05	38.1±0.2	51±3	0.88±0.06	75±3	1.98
17/12/2013	1	32±2	0.36±0.01	61.2±0.7	94±2	0.95±0.04	80±2	1.31
	10	15±2	0.18±0.02	42.2±0.5	58±2	0.69±0.05	57±3	1.34
	30	17±5	0.29±0.01	56.6±0.2	74±5	1.17±0.08	45±1	0.79
	60	14±3	0.28±0.00	35.6±0.5	50±3	0.90±0.08	66±3	1.84
	100	21±3	0.26±0.00	79.4±1.1	100±3	0.98±0.10	42±2	0.53
	200	22±1	0.46±0.01	66.1±1.1	88±1	1.25±0.06	81±1	1.23
02/02/2014	1	11±1	0.32±0.00	37.9±0.7	49±1	0.41±0.02	9±2	0.24
	10	22±4	0.32±0.00	35.6±0.3	58±4	0.34±0.08	26±2	0.74
	20	14±3	0.32±0.00	25.4±0.2	40±3	0.31±0.02	37±1	1.44
	40	13±3	0.38±0.00	52.4±0.2	66±3	0.89±0.04	36±3	0.68
	60	13±3	0.17±0.00	55.3±0.2	68±3	0.94±0.05	67±2	1.21
	80	16±2	0.18±0.00	55.3±1.3	71±3	0.95±0.07	73±2	1.32
	100	16±2	0.21±0.00	58.7±0.9	75±2	0.72±0.12	64±1	1.09
	200	15±3	0.24±0.00	74.5±0.7	90±3	0.70±0.05	74±4	0.99
	300	12±2	0.30±0.00	60.0±0.9	72±2	1.02±0.07	<2	-

[a] ±SD computed as the square root of the sum of variances

a)

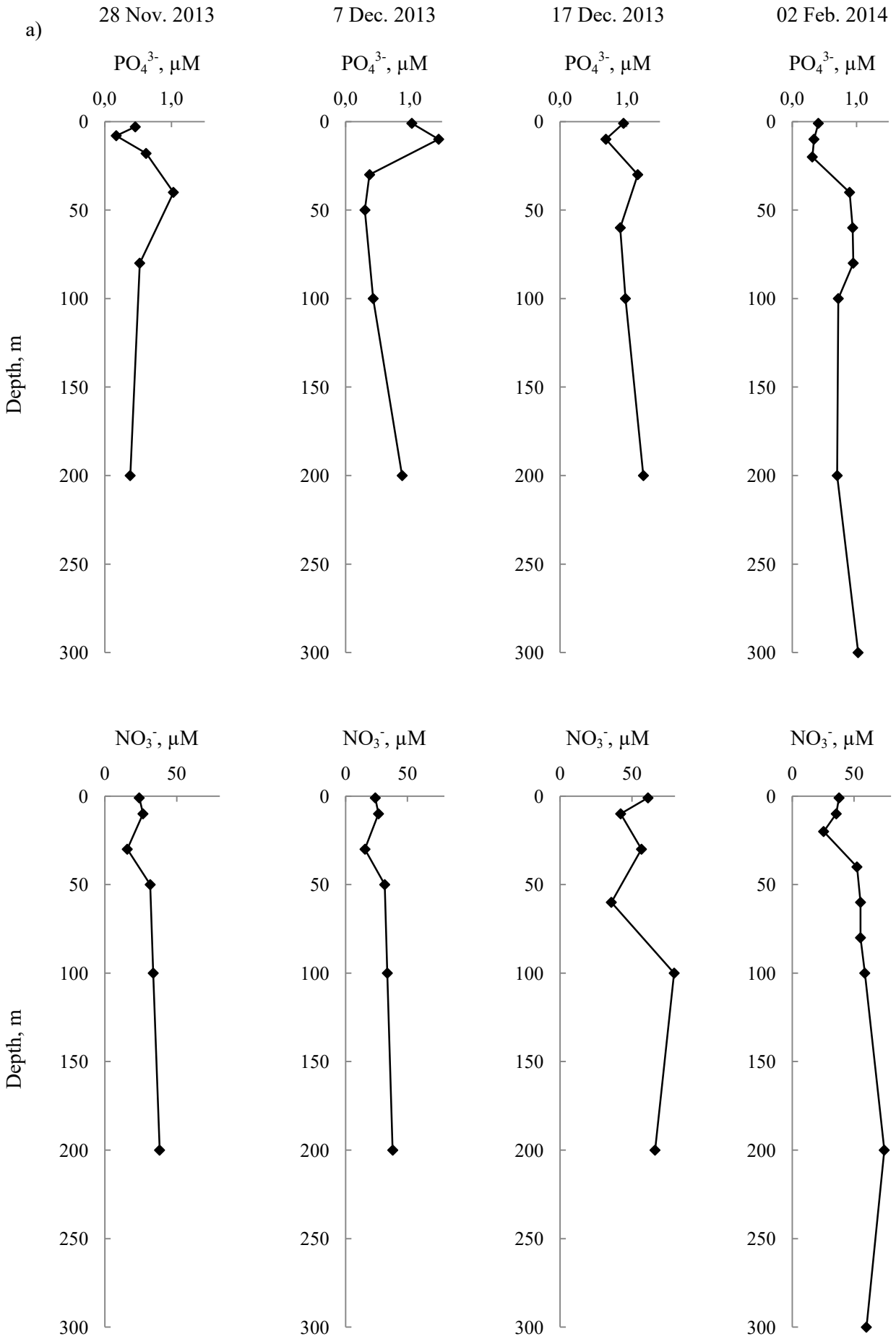
28 Nov. 2013
7 Dec. 2013
17 Dec. 2013
02 Feb. 2014
PO_4^{3-}, µM
0,0
1,0
NO_3^-, µM
0
50
Depth, m
0
50
100
150
200
250
300

b)

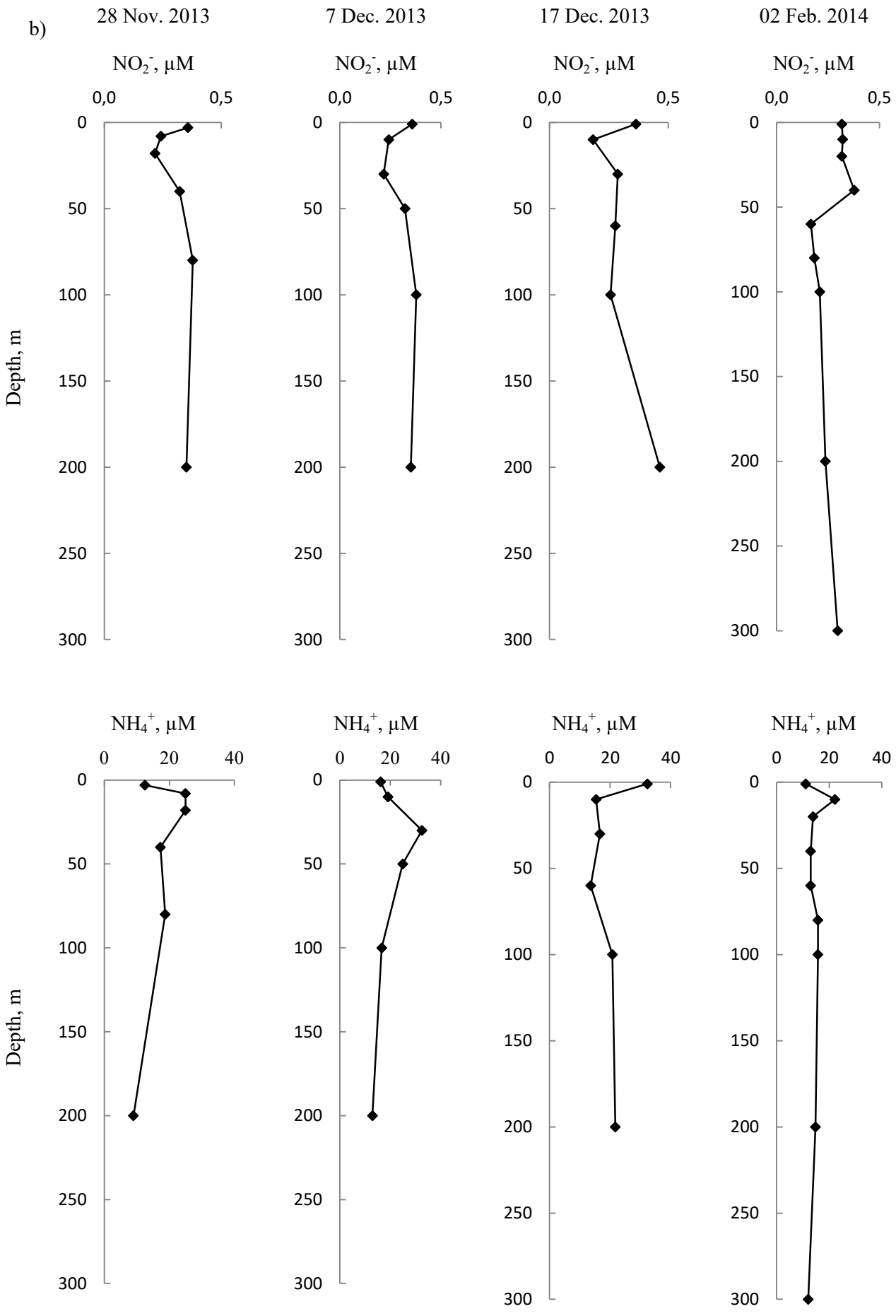
28 Nov. 2013
7 Dec. 2013
17 Dec. 2013
02 Feb. 2014
NO_2^-, µM
0,0
0,5
NH_4^+, µM
0
20
40
Depth, m
0
50
100
150
200
250
300

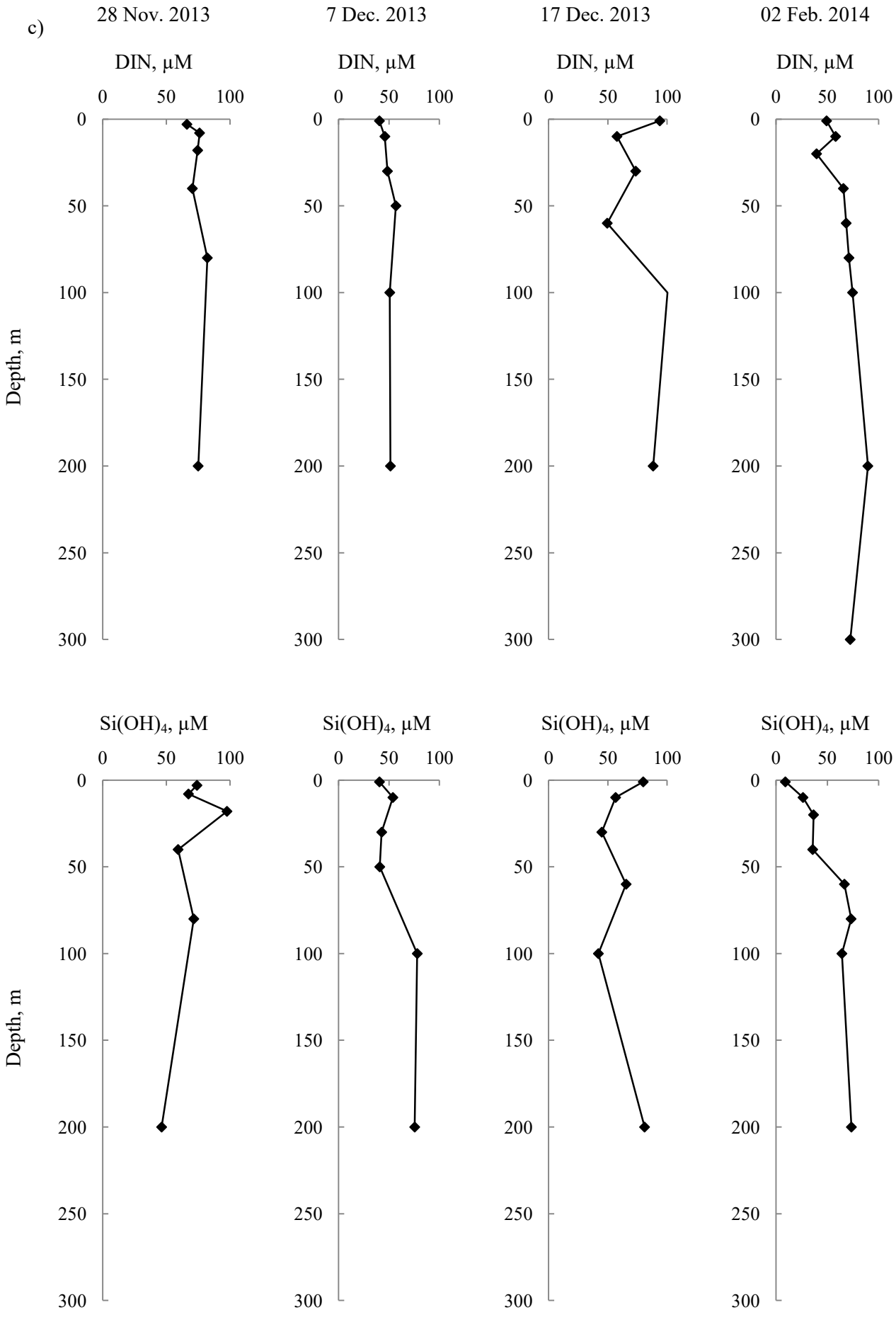

Fig.13. a-c Vertical profiles of nutrients recorded on November the 28th 2013, December the 7th and 17th 2013 and February the 2nd, 2014.

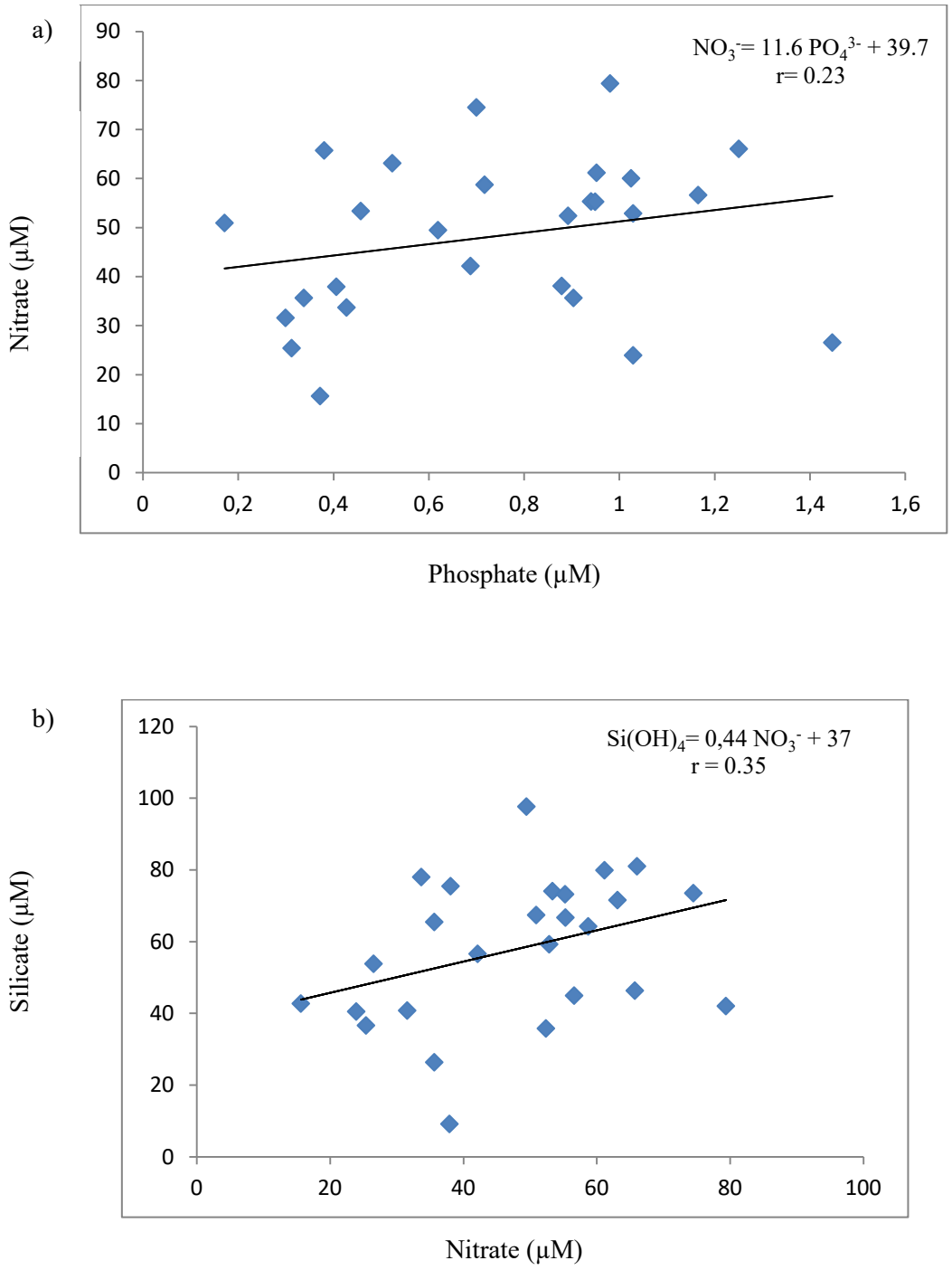

Fig. 14. Plots of nitrate concentration versus phosphate (a) and of silicate versus nitrate (b) concentration in the analysed samples.

4.2 Metal distribution in seawater and phytoplankton

Results regarding the total concentrations of metals in seawater and their distribution between dissolved and particulate fractions, and among the latter the distributions between algal and inorganic phases, are reported in Tables 4, 5 and 6. Vertical profiles of the studied metals are reported in Figures 15-17, and total, dissolved, total particulate, non-living particulate and phytoplankton particulate concentrations measured during the cruise are given for each element.

For the relationships between metals, metal fractions and between metals and hydrologic variables and nutrients refer to the same correlation matrices quoted above for nutrients (see Tables A1-A4 in Appendix).

4.2.1 Cadmium

The total concentration of Cd (Cd_{tot}) ranged from ~20 ng/l to ~99 ng/l, with a mean ± SD of 67 ± 19 ng/l. Cd_{tot} was quite constant at the beginning of summer, showing a slightly increase on mid-December. Cd_{tot} did not vary substantially during the austral summer with values around 70 ng/l, however a slightly decrease at the end of the season was observed, with values passing from ~77 ng/l on November to ~58 ng/l on February. Along the water column, Cd_{tot} showed a maximum in correspondence of the DCM, remaining approximately constant until 200 m, then on February slightly increased at the bottom.

Dissolved cadmium (Cd_{diss}) represented a remarkable fraction (60-100%) of the total with values ranging from ~14 ng/l to ~84 ng/l (mean ±SD of 59 ± 19 ng/l). During summer and along the water column Cd_{diss} followed a trend similar to that of Cd_{tot}. The production of Cd_{diss} (i.e the percentage of Cd_{diss} *vs* Cd_{tot}) remained almost constant at the beginning and at the end of the season. In correspondence of the DCM the percentage of Cd_{diss} *vs* Cd_{tot} decreased from ~90% at the beginning of the summer to ~60% at mid-December and on February, this mean that a remarkable amount of Cd (~40%) at this depth was associated to the particulate fraction.

Total Cd particulate was generally low, ranging from values close to zero to 50 ng/l.

Cd associated to the particulate matter is represented for the almost totality by phytoplankton (median =1.66 ng/l (min 0.35-max 4.35)).

In general, Cd_{phyto} remained practically constant during summer, although at the surface an increase (from ~2 ng/l to ~4 ng/l) was observed at mid-December, maintaining then the same values also in February. A maximum of $Cd_{phyto,}$ strictly following the Chl-*a* maximum, was observed along the water column, afterwards Cd_{phyto} decreased to very low values. In the deepest layers and at the bottom, Cd_{phyto} was practically close to zero.

The percentage of Cd_{phyto} *vs* $Cd_{totpart}$ in correspondence of DCM strongly decreased from 100% on November to ~40% on mid-December and ~10% on February. In deep waters and at the bottom, with the exception of the two samplings in December, $Cd_{totpart}$ was represented for 90-100% by the non-living fraction of the metal.

Cd stochiometry, expressed as Cd_{phyto}:Chl-*a* (Echeveste et al., 2014), ranged from ~0 ng/µg to ~12 ng/µg. In November and the beginning of December Cd:Chl-*a* ratio showed values close to zero along the entire seawater column. On mid-December, an increase in the superficial layer and at the DCM was observed, this can be due to an increase of phytoplanktonic cells that uptakes Cd. Two anomalous peaks were observed at the beginning of February: one in the superficial layer and one in correspondence of the DCM.

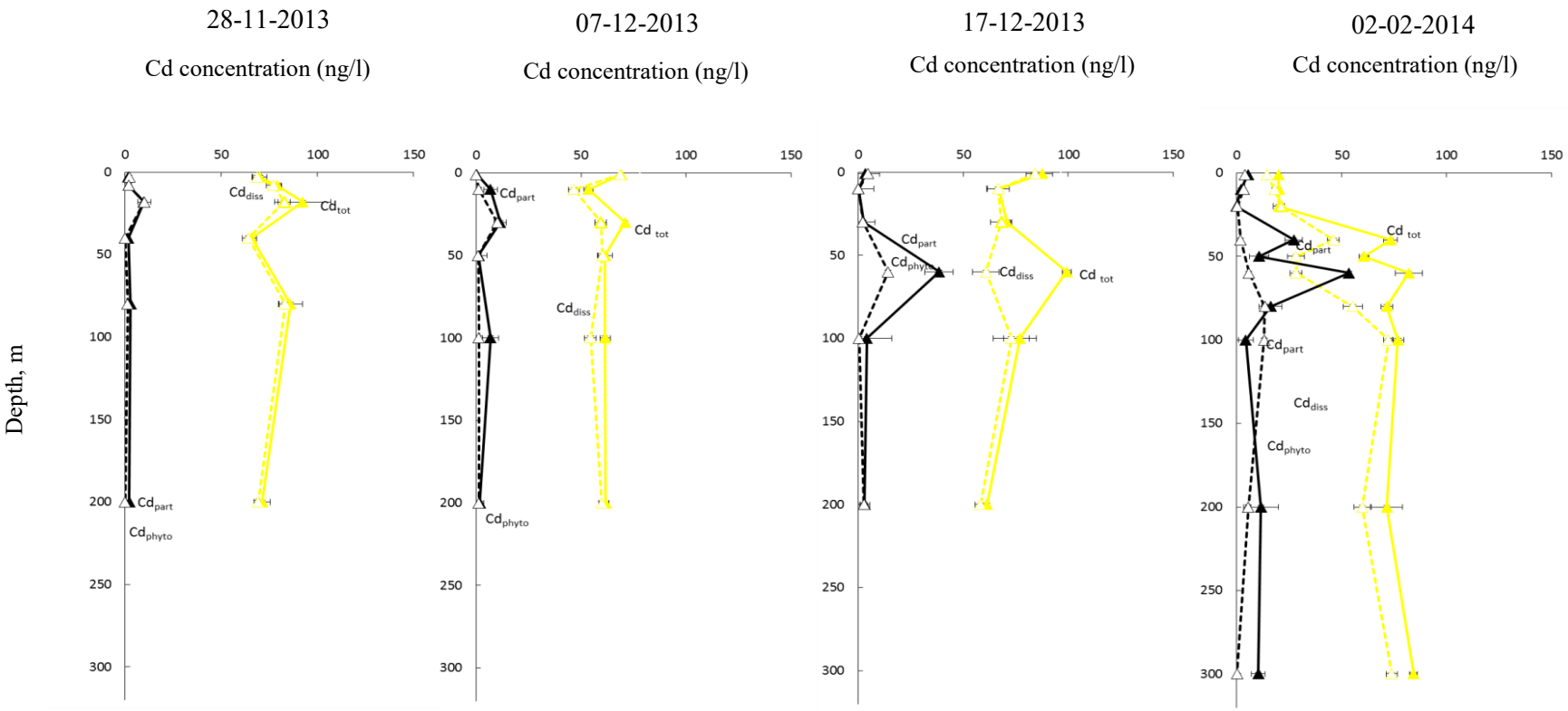

Fig. 15. Cd distribution along the water column and during the season.

4.2.2 Copper

Total Cu concentration (Cu_{tot}) ranged from ~130 ng/l to ~470 ng/l with a mean ± SD of 233±78 ng/l. During the season, Cu_{tot} showed a maximum (~335 ng/l) on mid-December, decreasing on February about 25% (values ~180 ng/l) respect to November values (~240 ng/l).

Dissolved Cu concentration (Cu_{diss}) ranged from 86 ng/l to 244 ng/l with a mean ± SD of 173 ± 39 ng/l, representing a remarkable fraction (from ~40% to ~100%) of Cu_{tot}.

Cu_{diss} slightly decreased during summer with values on February ~38% lower than November, this decrease was more marked at the surface than the deepest layers along the water column.

The percentage of Cu_{diss} *vs* Cu_{tot} decreased on mid-December, passing from ~90% on November to ~55%; as a result in this period, when pack ice started to melt, a consistent amount of Cu was associated to the total particulate fraction.

Total Cu particulate ($Cu_{totpart}$) varied from values below the detection limit to ~295 ng/l, ranging from ~2% to ~60% of the total concentration.

Levels of copper associated to phytoplankton (Cu_{phyto}) ranged from values below the detection limit to ~104 ng/l with a median of 20.3 ng/l (min 5.1-max 50.7), reaching ~40% of the total concentration and 100% of the total particulate fraction. Generally, throughout the season Cu associated to phytoplankton strongly increased from November (~14 ng/l) to early February (30 ng/l).

Except for the sampling of November, where Cu_{phyto} decreased with depth, during summer a maximum of this fraction was observed at the DCM. The amount of this Cu_{phyto} seemed to decrease and deepened during the season, strictly following the Chl-*a* trend along the water column. In the vicinity of the bottom, Cu_{phyto} showed values below the detection limit, except on December the 17^{th}, where Cu_{phyto} showed concentrations similar to that noted at the DCM depth.

Cu_{phyto} increased throughout the season from 6 to ~20 ng/l. Cu_{phyto} *vs* $Cu_{totpart}$ increased with depth, with the highest values at the DCM, except on mid-December when Cu_{phyto} was 95% of the total particulate down the bottom.

Cu stochiometry, expressed as Cu:Chl-*a* ranged from ~0 ng/µg to ~48 ng/µg. Cu:Chl-*a* ratio did not showed great differences between November and the beginning of December with an approximately constant trend along the seawater column. On mid-December, an increase in the superficial layer, probably connected to the pack ice melting, was observed. On February, this peak still persisted and seemed to extended until 100m layer.

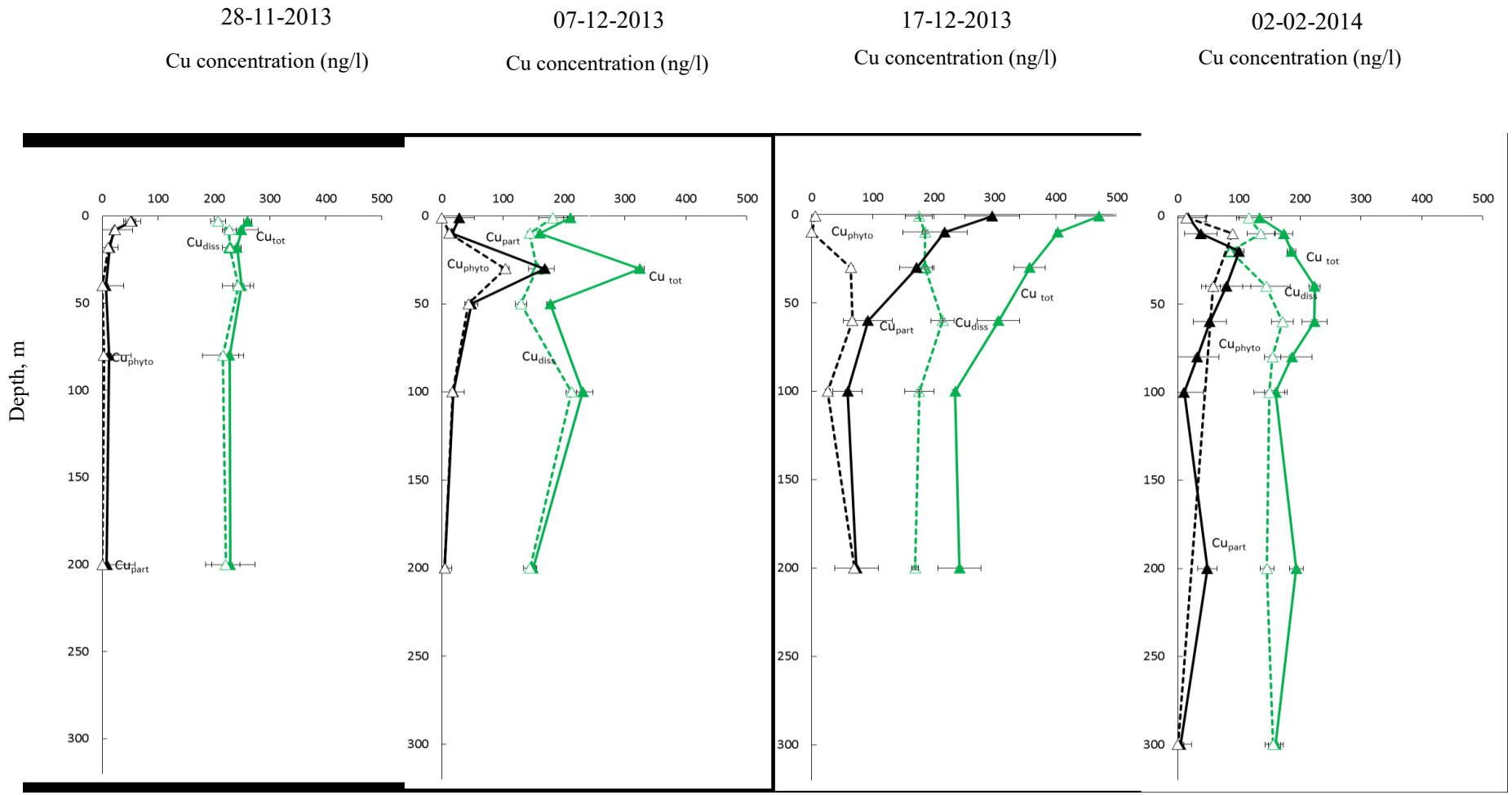

Fig. 16. Cu distribution along the water column and during the season.

4.2.3 Lead

The surface and sub-surface values of Pb_{tot} content measured on November 2013 were very high, probably due to contamination problems during the sample treatment.

Total Pb concentration (Pb_{tot}) was very variable ranging from ~30 ng/l to ~271 ng/l, with a mean ±SD of 106 ± 66 ng/l. Keeping out the values of November, Pb_{tot} at the surface remained almost constant at the beginning of the sampling period, while on February, when the pack ice was completely melt, it decreased by about 60%.

Along the water column, Pb_{tot} showed a maximum at the DCM for the samplings from December to the end of the season.

Dissolved Pb concentration (Pb_{diss}) ranged from ~24 ng/l to ~101 ng/l with a mean ±SD of 50 ± 24 ng/l representing a very variable fraction (from ~15% to ~90%) of the total Pb content. Pb_{diss} showed a maximum on mid-December, then on early February it returned to values similar to those of November.

Along the seawater column Pb_{diss} was characterized by a broad seek within the UML, then it decreased to values that in some cases were similar to the surface and constant down to the bottom.

Pb_{diss} *vs* Pb_{tot} greatly increased during the summer from ~ 25% to ~ 60%. Along the water column Pb_{diss} *vs* Pb_{tot} showed high values in correspondence of the superficial layer and lower values at deepest layers.

Pb associated to particulate matter ($Pb_{totpart}$) varied from ~6 ng/l to ~230 ng/l, ranging from 10% to 85% of the total concentration. Throughout the season, it strongly decreased from ~100 ng/l on November to ~20 ng/l on February. It followed an opposite trend respect $Pb_{diss,}$ with remarkable values in the deepest layer.

Pb quota in the phytoplankton (Pb_{phyto}) ranged from values close to the detection limit and ~128 ng/l with a median of 29.0 ng/l (min 1.2 - max 22.7), reaching ~56% of the total content and 100% of the total particulate fraction. Pb_{phyto} showed two surface maxima during summer; the first at the beginning of the collection campaign, and the second at mid-December.

As well as the other metals, Pb_{phyto} vertical profile showed a maximum at the DCM, following strictly the Chl-*a* trend along the water column. At the deepest layers, Pb_{phyto} decreased to values close to zero except on December the 17th, where Pb_{phyto} showed values about 50 ng/l.

Pb_{phyto} *vs* Pb_{tot} in correspondence of the DCM showed a maximum during December samplings (~70%), then on February it returned to percentages similar to those noted in November (40%).

In the case of Pb, the amount of metal associated to the inorganic particulate was remarkable (from 0 ng/l to 135 ng/l), especially in November, where it accounted for 80-100% of the $Pb_{totpart.}$ It generally decreased during the summer passing from ~80 ng/l. to 20 ng/l. Along the water column

Pb inorganic particulate was high in the proximity of surface/sub-surface layers, then it showed a maximum at the depth below the Chl-*a* maximum and generally increased at the bottom or at its proximity.

Pb stoichiometry, expressed as Pb:Chl-*a* ranged from ~0 ng/µg to ~67 ng/µg. In the superficial layer, it showed low values during the entire season (on February there was probably an anomalous value). On mid-December and in February an increase of this ratio was observed at the DCM, indicating a probably high adsorption on external phytoplankton surface.

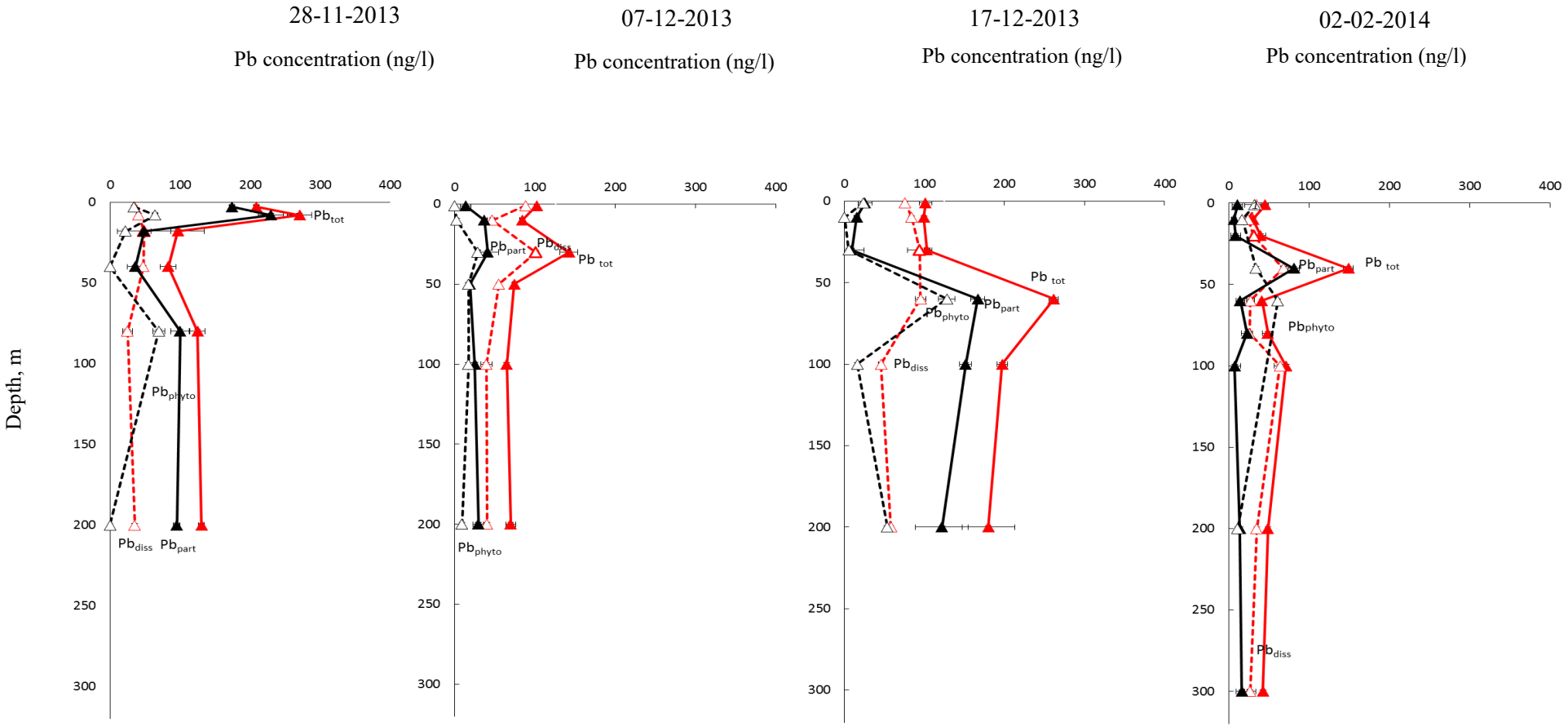

Fig. 17. Pb distribution along the water column and during the season.

Tab. 4. Cadmium distribution of total concentration between dissolved, total particulate, phytoplankton and inorganic particulate fractions measured during the austral summer 2013-2014. Cd_{phyto}:Chl-*a* ratio is also reported. Data reported as mean ± SD of at least three measurements.

		Cd concentration, ng/l					
Sampling date	Depth (m)	Total	Dissolved (% *vs* total)	Total particulate (% *vs* total)	Phytoplankton Particulate (% *vs* Tot part, % *vs* Tot)	Inorganic particulate (% *vs* Tot part)	Cd_{phyto}:Chl-*a* ratio ng/µg
28/11/2013	3	70.1±3.7	68.5±2.6 (97.7%)	1.6±4.5 (2.3%)	2.2±0.3 (100%) (3.1%)	0.0±4.5 (0%)	2.06
	8	79.0±2.4	77.1±3.7 (97.6%)	1.9±4.4 (2.4%)	1.9±0.2 (100%)(2.4%)	0.0±5.3 (0%)	0.29
	18	92.3±14.5	82.6±3.1 (89.5%)	9.7±14.8 (10.5%)	9.9±3.3 (100%) (10.7%)	0.0±15.2 (0%)	1.32
	40	65.7±2.6	64.0±3.0 (97.5%)	1.7±4.0 (2.5%)	0 (0%) (0%)	1.7±4.0 (100%)	bdl
	80	85.9±6.1	83.1±3.1 (96.7%)	2.8±6.9 (3.3%)	1.3±0.1 (46.9) (1.5%)	1.5±6.9 (53.1%)	0.73
	200	71.2±4.3	69.0±1.0 (97.0%)	2.2±4.4 (3.0%)	0 (0%) (0%)	2.2±4.4 (100%)	bdl
07/12/2013	1	69.2±0.7	68.7±0.2 (99.3%)	0.5±0.7 (0.7%)	0 (0%) (0%)	0.5±0.7 (100%)	bdl
	10	53.5±2.0	46.6±2.5 (87.0%)	6.9±3.2 (13.0%)	1.3±0.1 (19.4%) (2.5%)	5.6±3.2 (80.6%)	0.56
	30	70.9±0.6	59.4±2.9 (83.7%)	11.5±2.9 (16.3%)	10.1±0.3 (87.6%) (14.2%)	1.4±2.9 (12.4%)	1.26
	50	61.4±3.4	60.2±1.9 (98.0%)	1.2±3.9 (2.0%)	1.1±0.1 (88.2%) (1.8%)	0.1±3.9 (11.7%)	0.08
	100	61.4±2.5	54.5±2.8 (88.7)	6.9±3.7 (11.3%)	1.4±0.1 (20.4%) (2.3%)	5.5±3.7 (79.6%)	0.35
	200	61.7±1.5	59.9±1.3 (97.0%)	1.9±2.0 (3.0%)	1.4±0.3 (76%) (2.3%)	0.4±2.0 (23.9%)	1.11

Tab. 4. (continued)

Sampling date	Depth (m)	Total	Dissolved (% *vs* total)	Total particulate (% *vs* total)	Phytoplankton Particulate (% *vs* Tot part, % *vs* Tot)	Inorganic particulate (% *vs* Tot part)	Cd_{phyto}:Chl-*a* ratio ng/µg
17/12/2013	1	87.5±5.1	84.1±4.2 (96.1%)	3.4±6.6 (3.9%)	4.5±0.4 (100%) (5.1%)	0.0±6.6 (0%)	12.91
	10	66.7±5.1	66.6±5.4 (100%)	0.0±7.4 (0%)	0 (0%) (0%)	0.0±7.4 (100%)	bdl
	30	70.8±1.8	68.2±5.1 (96.4%)	2.6±5.4 (3.6%)	2.2±0.2 (87.4%) (3.2%)	0.3±5.4 (12.6%)	0.19
	60	99.2±2.2	60.7±6.3 (61.2%)	38.5±6.7 (38.8%)	14.1±0.7 (36.7%) (14.2%)	24.3±6.8 (63.2%)	1.52
	100	76.9±7.8	72.8±8.7 (94.7%)	4.1±1.7 (5.3%)	0.3±0.0 (8.3%) (0.4%)	3.8±11.7 (91.7%)	0.04
	200	61.2±0.5	58.2±2.5 (95.0%)	3.0±2.6 (5.0%)	2.7±0.3 (87.1%) (4.3%)	0.4±2.6 (12.8%)	1.50
02/02/2014	1	20.0±1.2	14.6±0.7 (72.9%)	5.4±1.4 (27.1%)	3.9±0.2 (73.3%) (20%)	1.4±1.4 (26.7)	5.22
	10	20.2±0.7	18.1±1.2 (89.7%)	2.1±1.4 (10.3%)	3.3±0.7 (100%) (16.3%)	0.0±1.5 (0%)	0.84
	20	20.2±2.6	21.1±0.6 (104.8%)	0 (0%)	0.4±0.0 (0%) (2%)	0.0±2.6 (0%)	0.08
	40	73.3±3.1	46.1±2.7 (62.9%)	27.2±4.1 (37.1)	1.9±0.0 (7%) (2.6%)	25.3±4.1 (93.0%)	0.48
	60	82.0±6.4	28.4±2.7 (34.6%)	53.6±6.9 (65.4%)	13.5±1.4 (25.2%) (16.5%)	40.1±7.1 (74.8%)	3.28
	80	71.6±2.8	55.3±4.6 (77.3%)	16.3±5.4 (22.7%)	13.2±1.0 (81.1%) (18.4%)	3.1±5.5 (18.9%)	6.20
	100	76.8±2.8	72.4±2.2 (94.2%)	4.5±3.6 (5.8%)	5.6±1.3 (100%) (7.3%)	0.0±3.8 (0%)	1.98
	200	71.5±7.4	59.9±3.8 (83.7%)	11.7±8.3 (16.3%)	0.2±0.5 (1.7%) (0.3%)	11.5±8.3 (98.3%)	0.22
	300	84.2±1.8	73.8±2.6 (87.7%)	10.4±3.2 (12.3%)	0	10.4±3.2 (100%)	bdl

bdl= below detection limit

Tab. 5. Copper distribution of total concentration between dissolved, total particulate, phytoplankton and inorganic particulate fractions measured during the austral summer 2013-2014. Cu_{phyto}:Chl-*a* ratio is also reported. Data reported as mean ± SD of at least three measurements.

Sampling date	Depth (m)	Cu concentration, ng/l					
		Total	Dissolved (% *vs* total)	Total particulate (% *vs* total)	Phytoplankton Particulate (% *vs* Tot part, % *vs* Tot)	Inorganic particulate (% *vs* Tot part)	Cu_{phyto}:Chl-*a* ratio ng/µg
28/11/2013	3	260.3±7.1	207.3±13.3 (79.7%)	53.0±15.1 (20.3%)	50.8±8.7 (95.8%) (19.5%)	2.2±17.4 (4.2%)	48.00
	8	248.7±30.2	227.2±12.7 (91.3%)	21.6±32.7 (8.7%)	23.0±1.1 (100%) (9.3%)	0±32.7 (0%)	3.50
	18	240.8±8.2	228.0±12.7 (101.1%)	12.8±15.1 (0%)	10.7±0.4 (0%) (4.4%)	2.2±15.1 (100%)	1.43
	40	249.0±14.7	243.0±28.3 (97.6%)	6.0±31.9 (2.4%)	0 (0%) (0%)	6.0±31.9 (100%)	bdl
	80	227.7±16.0	215.8±37.1 (94.8%)	11.8±40.4 (5.2%)	2.8±0.2 (23.7%) (1.2%)	9.0±40.4 (76.3%)	1.55
	200	228.9±44.4	221.1±25.3 (96.6%)	7.8±51.1 (3.4%)	0 (0%) (0%)	7.8±51.1 (100%)	bdl
07/12/2013	1	211.3±5.6	182.6±23.9 (86.4%)	28.7±24.6 (13.6%)	0 (0%) (0%)	28.7±24.6 (100%)	bdl
	10	160.5±1.0	143.8±2.4 (89.6%)	16.7±2.6 (10.4%)	12.2±1.2 (72.7%) (7.6%)	4.6±2.9 (27.3%)	5.04
	30	324.7±7.3	156.0±14.0 (48.1)	168.7±15.8 (51.9%)	103.9±6.9 (61.6%) (32.0%)	64.8±17.2 (38.4)	12.94
	50	177.6±5.5	129.5±9.1 (72.9%)	48.1±10.7 (27.1%)	43.5±1.7 (90.5%)(24.5%)	4.6±10.8 (9.5%)	3.27
	100	230.8±16.8	212.4±8.4 (92.0%)	18.4±18.8 (8.0%)	17.4±1.6 (94.9%) (7.5%)	0.9±18.8 (5.1)	4.33
	200	149.5±4.2	144.7±11.1 (96.8%)	4.8±11.8 (3.2%)	4.6±0.2 (96.8%) (3.1%)	0.2±6.7 (3.2)	3.61

Tab. 5. (continued)

Sampling date	Depth (m)	Total	Dissolved (% *vs* total)	Total particulate (% *vs* total)	Phytoplankton Particulate (% *vs* Tot part, % *vs* Tot)	Inorganic particulate (% *vs* Tot part)	Cu_{phyto}:Chl-*a* ratio ng/µg
17/12/2013	1	470.7±39.3	175.4±21.7 (37.3%)	295.3±44.9 (62.7%)	5.5±0.2 (1.9%) (1.2%)	289.8±44.9 (98.1)	15.81
	10	403.5±4.6	185.8±36.6 (46.1%)	217.7±36.9 (53.9%)	0 (0%) (0%)	217.7±36.9 (100%)	bdl
	30	357.4±25.4	185.3±11.5 (51.8%)	172.1±27.9 (48.2%)	64.0±2.5 (37.2%) (17.9%)	108.1±28.0 (62.8%)	5.29
	60	306.2±34.8	214.4±19.2 (70.0%)	91.8±39.8 (30.0%)	66.5±2.1 (72.4%) (21.7%)	25.3±39.8 (27.6%)	7.14
	100	234.7±1.9	176.2±24.1 (75.1%)	58.5±24.1 (24.9%)	26.1±3.2 (44.6%) (11.1%)	32.4±24.3 (55.4%)	2.80
	200	242.3±35.3	169.2±5.9 (69.8%)	73.1±35.8 (30.2%)	69.5±1.6 (95.0%) (28.7%)	3.6±35.8 (5.0%)	39.24
02/02/2014	1	133.5±20.0	116.0±20.3 (86.9%)	17.5±28.5 (13.1%)	14.3±2.1 (81.7%) (10.7%)	3.2±28.6 (18.3%)	18.76
	10	173.6±14.6	136.2±22.4 (78.5%)	37.4±26.8 (21.5%)	17.6±0.7 (47.0%) (10.1%)	19.8±26.8 (53.0%)	4.47
	20	186.5±7.2	86.0±1.1 (46.1%)	100.5±7.3 (53.9%)	73.0±11.4 (72.6%) (39.1%)	27.5±13.5 (27.4%)	14.26
	40	224.0±9.4	144.9±39.1 (64.7%)	79.2±40.3 (35.3%)	67.2±9.5 (84.9%) (30.0%)	12.0±41.4 (15.1%)	17.08
	60	223.8±20.2	171.4±18.1 (76.6%)	52.4±27.2 (23.4%)	50.7±4.6 (96.8%) (22.7%)	1.7±27.5 (3.2%)	12.31
	80	186.8±33.4	155.3±13.4 (83.1%)	31.5±36.0 (16.9%)	32.9±6.5 (100%) (17.6%)	0±46.9 (0%)	15.44
	100	160.1±18.5	149.8±25.1 (93.6%)	10.3±31.2 (6.4%)	13.4±1.6 (100%) (8.4%)	0±31.3 (0%)	4.70
	200	193.9±11.4	146.0±11.1 (75.3%)	48.0±15.9 (24.7%)	6.7±1.86 (0%) (0%)	0±48.1 (100%)	7.44
	300	160.2±12.5	156.3±12.8 (97.6%)	3.9±17.9 (2.4%)	0 (0%) (0%)	3.9±17.9 (100%)	18.76

bdl= below detection limit

Tab. 6. Lead distribution of total concentration between dissolved, total particulate, phytoplankton and inorganic particulate fractions measured during the austral summer 2013-2014. Pb_{phyto}:Chl-*a* ratio is also reported. Data reported as mean ± SD of at least three measurements.

Sampling date	Depth (m)	Pb concentration, ng/l					
		Total	Dissolved (% *vs* total)	Total particulate (% *vs* total)	Phytoplankton Particulate (% *vs* Tot part, % *vs* Tot)	Inorganic particulate (% *vs* Tot part)	Pb_{phyto}:Chl-*a* ratio ng/µg
28/11/2013	3	209.0±4.0	34.8±1.32 (16.7%)	174.2±4.2 (83.3%)	34.4±0.6 (19.7%) (16.4%)	139.8±4.2 (80.3%)	32.48
	8	270.8±17.5	40.9±3.01 (15.1%)	229.9±17.8 (84.9%)	64.4±3.8 (28.0%) (23.8%)	165.5±18.2 (72.0%)	9.78
	18	97.0±38.1	48.4±0.8 (50.0%)	48.6±38.1 (50.1%)	21.9±1.5 (45.1%) (22.6%)	26.7±38.1 (55%)	2.94
	40	83.4±11.3	47.4±1.6 (56.8%)	36.0±11.4 (43.2%)	0 (0%) (0%)	36.0±11.4 (100%)	bdl
	80	124.9±11.2	24.7±7.0 (19.8%)	100.1±13.2 (80.2%)	69.8±8.2 (69.7%) (55.9%)	30.4±15.6 (30.3%)	38.55
	200	130.6±4.4	35.1±1.8 (26.9%)	95.5±4.8 (73.1%)	0 (0%) (0%)	95.5±4.8 (100%)	bdl
07/12/2013	1	102.2±3.0	88.5±5.9 (86.6%)	13.7±6.7 (13.4%)	0 (0%) (0%)	13.7±6.7 (100%)	bdl
	10	84.2±3.3	47.0±2.0 (55.8%)	37.3±3.9 (44.2%)	2.6±0.1 (7.0%) (3.1%)	34.7±3.9 (93%)	1.08
	30	142.2±11.4	101.0±7.3 (71.0%)	41.2±13.5 (29.0%)	29.0±2.8 (70.4%) (20.4%)	12.2±13.8 (29.6%)	3.61
	50	74.5±2.2	55.2±0.5 (74.2%)	19.2±2.3 (25.8%)	17.2±0.8 (89.5%) (23.1%)	2.0±2.4 (10.5%)	1.29
	100	64.8±108	39.5±1.7 (60.9%)	25.3±2.5 (39.1%)	17.4±0.9 (68.5%) (26.8%)	8.0±2.7 (31.5%)	4.32
	200	69.8±6.0	40.3±3.2 (57.7%)	29.5±6.8 (42.3%)	9.2±0.9 (31.2%) (13.2%)	20.3±6.9 (68.8%)	7.16

Tab. 6. (continued)

Sampling date	Depth (m)	Total	Dissolved (% *vs* total)	Total particulate (% *vs* total)	Phytoplankton Particulate (% *vs* Tot part, % *vs* Tot)	Inorganic particulate (% *vs* Tot part)	Pb_{phyto}:Chl-*a* ratio ng/µg
17/12/2013	1	101.4±7.7	75.8±3.3 (74.7%)	25.6±8.4 (25.3%)	23.4±2.8 (91.4%) (23.1%)	2.2±8.8 (8.6%)	67.60
	10	99.3±2.7	83.8±2.4 (84.4%)	15.5±3.7 (15.6%)	0 (0%) (0%)	15.5±3.7 (100%)	bdl
	30	103.1±3.5	93.9±15.1 (91.1%)	9.2±15.5 (8.9%)	5.5±0.4 (59.9%) (5.3%)	3.7±15.5 (40.1%)	0.45
	60	261.5±5.8	95.0±6.6 (36.3%)	166.5±8.8 (63.7%)	127.9±10.1 (76.8%) (48.9%)	38.6±13.4 (23.2%)	13.74
	100	197.2±6.9	45.8±2.9 (23.2%)	151.4±7.4 (76.8%)	16.3±0.2 (10.8%) (8.3%)	135.1±7.4 (89.2%)	1.75
	200	179.8±32.8	58.0±0.5 (32.2%)	121.9±32.8 (67.8%)	53.5±1.4 (43.9%) (29.7%)	68.4±32.8 (56.1%)	30.20
02/02/2014	1	45.6±4.0	34.8±5.2 (76.3%)	10.8±6.6 (23.7%)	10.0±12.4 (100%) (100%)	0.81±14.0 (100%)	13.16
	10	30.3±1.6	24.0±2.5 (79.1%)	6.3±3.0 (20.9%)	4.7±0.1 (73.9%) (15.5%)	1.7±3.0 (26.1%)	1.19
	20	39.7±6.0	31.1±0.6 (78.5%)	8.5±6.1 (21.5%)	0 (0%) (0%)	8.5±6.1 (100%)	bdl
	40	149.1±6.3	68.2±3.6 (45.7%)	80.9±7.3 (54.3%)	40.0±1.6 (49.4%) (26.8%)	41.0±7.4 (50.6%)	bdl
	60	41.4±0.7	27.0±5.0 (65.2%)	14.4±5.0 (34.8%)	16.1±1.5 (100%) (38.9%)	0.0±5.3 (0%)	9.39
	80	48.7±6.6	25.8±2.0 (53.0%)	22.9±6.9 (47.0%)	20±6.4 (100%) (65.9%)	2.9±9.4 (0%)	1.88
	100	71.4±1.5	63.9±7.2 (89.5%)	7.5±7.4 (10.5%)	5.3±0.5 (71.4%) (7.5%)	2.1±7.4 (28.6%)	2.63
	200	48.8±0.9	34.8±1.7 (71.3%)	14.0±1.9 (28.7%)	2.4±0.1 (16.9%) (4.9%)	11.6±1.9 (83.1)	13.16
	300	42.6±2.0	26.4±7.0 (62.0%)	16.2±7.2 (38.0%)	0 (0%) (0%)	16.2±7.2 (100%)	1.19

bdl= below detection limit

4.3 Metal distribution in atmospheric aerosol

Concerning metal content of the aerosol samples collected during the 2013-2014 Antarctic summer campaign, expressed as atmospheric concentrations, results obtained from the chemical fractionation are reported in Table 7, after blank subtraction. Temporal evolutions of the soluble and insoluble fractions of the particulate metal concentrations in the aerosol are reported in Figures 18-20.

As regards the additivity test, the results (reported in Table 8) showed that the total contents obtained by summing the water soluble plus insoluble fractions of metals are in good agreement with those obtained by direct digestion of the sample as it is. This agreement suggests that the sequential extraction of sample filters and the digestion of the residue were done quantitatively, and subsequent analyses performed accurately.

4.3.1 Cadmium

The total (soluble fraction plus insoluble fraction) atmospheric concentration of Cd ranged from 0.4 pg/m^3 to 0.6 pg/m^3 (mean ±SD of 0.9 ± 0.6 pg/m^3). It showed a bell-shaped trend with an increase at the end of December/beginning of January (2.0 ± 0.2 pg/m^3).

The Cd soluble fraction, mainly due to marine aerosol, ranged from 0.3 pg/m^3 to 1.6 pg/m^3 (representing from 60% to 96% of the total content), showing a bell-shaped trend during the season. At the beginning of the season low concentration (~0.60 pg/m^3) was observed, probably due to the presence of the pack ice and therefore to a reduced formation of marine aerosol. Then at the end of December /beginning of January an increase was observed, with the content reaching a maximum of 1.62 pg/m^3.

The Cd insoluble fraction ranged from 0.03 pg/m^3 to 0.4 pg/m^3 (mean ±SD of 0.18±0.14 pg/m^3) with a slightly decrease at the end of the season. The high values showed for the insoluble fraction of the last sampling (from 23/01/2013 to 02/02/2014) respect to the total content, probably was due to contamination problems and it was not considered in the mean calculation.

4.3.2 Copper

The total (soluble fraction plus insoluble fraction) atmospheric concentrations of Cu ranged from 30 pg/m^3 to 56 pg/m^3 (mean ± SD of 42 ± 9 pg/m^3). Cu concentration showed an increase in the middle of the campaign with values of 47 ± 8 pg/m^3. The Cu soluble fraction ranged from 16 pg/m^3 ± 32 pg/m^3 (mean ± SD of 23 ± 7 pg/m^3) showing an increase in correspondence of the period of pack ice melting. It represented from 38% to 72% of the total content. The Cu insoluble fraction

ranged from 10 pg/m^3 to 26 pg/m^3 (mean ±SD of 19 ±6 pg/m^3). It represented from 28% to 62% of the total content showing an approximately constant trend during summer.

4.3.3 Lead

The total (soluble fraction plus insoluble fraction) atmospheric concentration of Pb ranged from 10 pg/m^3 to 22 pg/m^3 (mean ± SD of 16 ± 4 pg/m^3). At the beginning of the season, Pb total concentration showed an increase, then a constant trend during the season was maintained. The soluble fraction ranged from 2.2 pg/m^3 to 3.3 pg/m^3 (mean ± SD of 3 ± 0.4 pg/m^3). It represented from 14% to 30% of the total content and not showed a well-defined trend during the season. The insoluble fraction ranged from 7 pg/m^3 to 19 pg/m^3 (mean ± SD of 13 ± 4 pg/m^3) and represented the highest amount (until 85%) of the total content. As the soluble fraction, did not show a well-defined trend with fluctuating values during all the season.

Tab. 7. Chemical fractionation of Cd, Pb and Cu in Antarctic aerosol expressed as atmospheric concentration (Faraglione Camp, near to Mario Zucchelli Station, Victoria Land, East Antarctica).

Sample Ref. no.	Exposure period, dd/mm/yy	Air volume (±RSD%), m^3	Atmospheric concentration Cd (±SD), pg/m^3 [percentage]			Atmospheric concentration Pb (±SD), pg/m^3 [percentage]			Atmospheric concentration Cu (±SD), pg/m^3 [percentage]		
			Soluble	Insoluble	Total	Soluble	Insoluble	Total	Soluble	Insoluble	Total
1	01/12/13-12/12/13	18400±10%	0.7±0.1 [96%]	0.03±0.01 [4%]	0.7±0.1	2.2±0.3 [16%]	11.7±1.2 [84%]	13.9±1.2	19.6±2.2 [66%]	10.3±1.1 [34%]	29.8±2.4
2	12/12/13-22/12/13	16310±10%	0.6±0.1 [60%]	0.4±0.0 [40%]	0.9±0.1	3.3±0.3 [16%]	17.6±1.8 [84%]	20.9±1.8	15.6±2.1 [38%]	25.7±2.6 [62%]	41.3±3.3
3	22/12/13-03/01/14-	19577±10%	1.6±0.2 [82%]	0.3±0.0 [18%]	2.0±0.2	3.3±0.3 [22%]	11.8±1.2 [78%]	15.1±1.3	30.4±3.6 [54%]	25.8±2.6 [46%]	56.3±4.4
4	03/01/14-13/01/14	16397±10%	0.3±0.1 [68%]	0.1±0.0 [32%]	0.4±0.1	3.2±0.4 [15%]	18.4±1.9 [85%]	21.6±1.9	32.5±3.6 [73%]	12.3±1.3 [27%]	44.8±3.9
5	13/01/14-23/01/14	16341±10%	0.5±0.1 [83%]	0.1±0.0 [16%]	0.6±0.1	2.8±0.3 [19%]	12.2±1.2 [81%]	15±1.3	18.5±2.1 [49%]	19.6±2.1 [51%]	38.2±3.0
6	23/01/14-02/02/14	16270±10%	0.5±0.1 [82%]	2.7±0.3(*) [*]	3.2±0.3	3.1±0.3 [31%]	6.9±0.7 [69%]	10±0.8	21.4±2.4 [52%]	19.4±2.0 [48%]	40.8±3.1
Average (outliers axcluded *)			0.7±0.5 [78%±12%]	0.2±0.1 [22%±13%]	0.9±0.6	3±0.4 [20%±6%]	13.1±4.3 [80%±6%]	16±4.4	23.0±6.9 [55%±12%]	45±612 [44%±22%]	42±9

(*) Outliers due to possible contamination

Tab. 8. Additivity test carried out on all the samples. Comparison between results of sequential extractions and direct total digestion. Data after blank subtraction.

Sample Ref. no.	Atmospheric concentration Cd (±SD), pg/m^3			Atmospheric concentration Pb (±SD), pg/m^3			Atmospheric concentration Cu (±SD), pg/m^3		
	Total computed	Total measured	Recovery %	Total computed	Total measured	Recovery %	Total computed	Total measured	Recovery %
1	0.7±0.1	0.7 ±0.1	100	13.9±1.20	8.4 ±0.8	100	29.8±2.4	27.6±2.7	100
2	0.9±0.1	0.9 ±0.0	100	20.9±1.8	21.0 ±2.1	99	41.3±3.3	47.5±4.8	87
3	2.0±0.2	4.9± 0.5	40	15.1±1.3	14.2± 1.4	100	56.3±4.4	56.7±5.7	99
4	0.4±0.1	0.4± 0.0	100	21.6±1.9	22.3 ±2.2	96	44.8±3.9	43.2±4.3	100
5	0.6±0.1	0.6± 0.06	100	15±1.3	15.1± 1.5	99	38.2±3.0	27.5±2.7	100
6	3.2±0.3*	0.6 ±0.0	*	10±0.8	10.1±1.0	98	40.8±3.1	40.4±4.0	100

(*) Outliers due to possible contamination

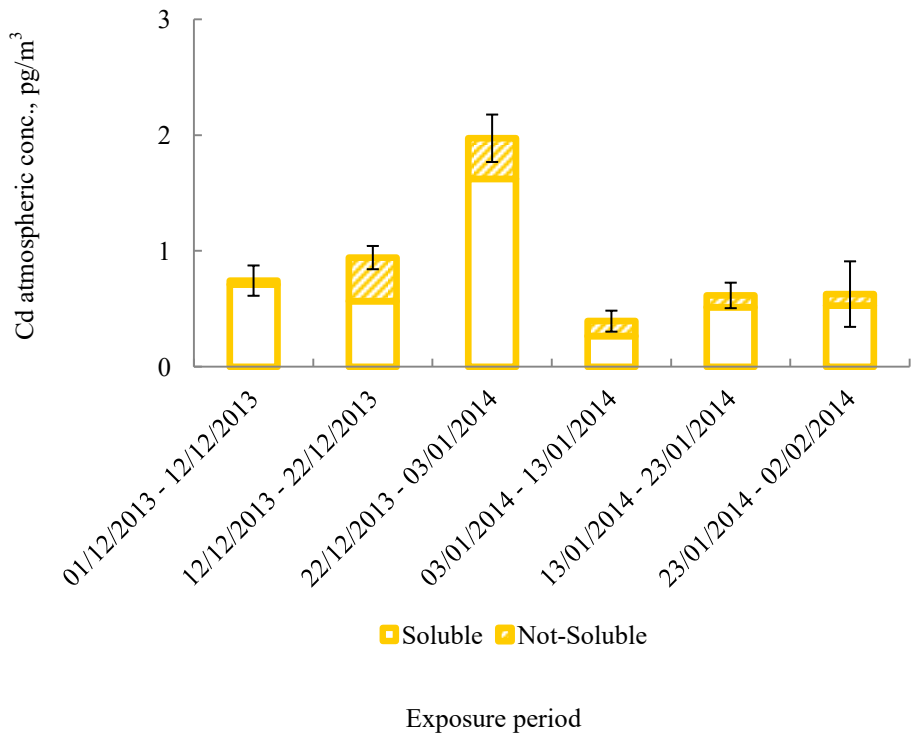

Fig. 18. Temporal evolutions of the soluble and insoluble fractions of the particulate Cd concentrations in the aerosol collected during the 2013-2014 Antarctic summer campaign at Faraglione Camp.

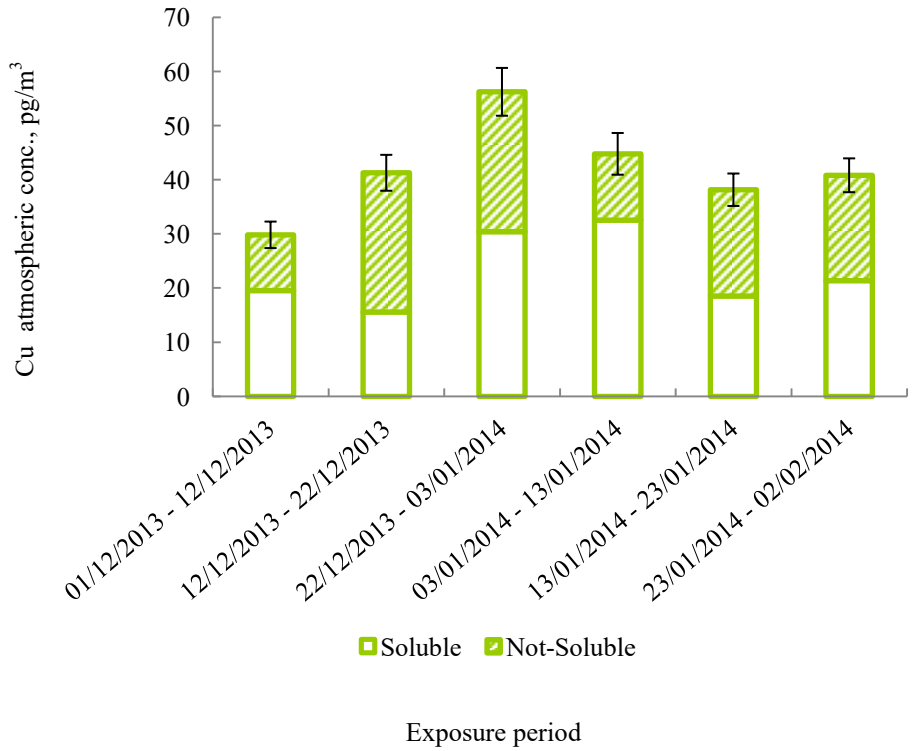

Fig. 19. Temporal evolutions of the soluble and insoluble fractions of the particulate Cu concentration in the aerosol collected during the 2013-2014 Antarctic summer campaign at Faraglione Camp.

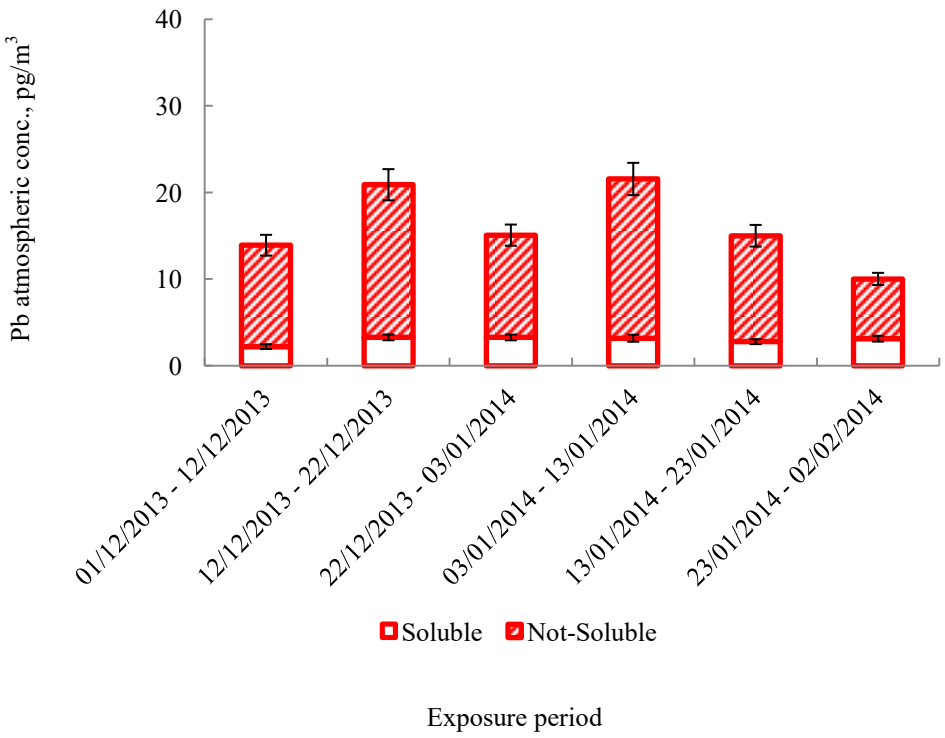

Fig. 20. Temporal evolutions of the soluble and insoluble fractions of the particulate Pb concentration in the aerosol collected during the 2013-2014 Antarctic summer campaign at Faraglione Camp.

5. Discussion

5.1 Environment

The TNB polynya has been intensely investigated by Italian researchers in recent years, studying the physical structure of the water column (Cappelletti et al., 2010), the plankton community (Accornero et al., 2003, Arrigo et al., 2004, Fonda et al., 2003, 2005; Nuccio et al., 2000, Saggiomo et al., 2002), the nutrient and trace element distribution in sea water (Abollino et al., 2001, 2004, Biesuz et al., 2006, Dalla Riva 2003, Rivaro et al., 2012, Scarponi et al., 2000).

In the studied campaign, the water column showed a quite stability during the season. In the first part of the campaign pack ice covered the most part of Terra Nova Bay and no stratification of the water column was observed, although at mid-December a weak pycnocline started to appear. On February, all the pack ice was fully melted, a steep and deep thermocline appeared, and it was associated to a steep salinity gradient.

Salinity values are typical of the Ross Sea area (Corami et al., 2005); they were approximately constant throughout the season, the surface decrease on February probably resulted from the dilution effect derived from the melting of pack ice.

Generally, seawater was well oxygenated, as high redox potential values (from ~300 mV to ~400 mV) indicated. Oxygen supersaturation (~140%) and high values of dissolved oxygen (~15 mg/l) were observed in correspondence of the chlorophyll-*a* peak of December the 17th. This could indicate the dominance of the primary production of phytoplankton cells. At the end of summer season both values decreased (oxygen saturation ~100%, or dissolved oxygen ~12 mg/l) in relation to a reduction of primary production as low Chl-*a* values indicated.

pH around 8 was indicative of high-salinity waters. Highest values of pH (showed on December samplings) coincided with oxygen super saturation and with high values of Chl-*a*, indicating high phytoplankton activity which leaded to pH increase. Lower pH (~7.6) observed on February was associated to lower values of saturation percentage and oxygen concentration, consequently to a decreasing of phytoplankton activity.

Nutrient concentrations in seawater were generally high to sustain high biomass stock and they were never fully depleted. Data here obtained were in good agreement with literature values found in the polynya close to our site (Rivaro et al., 2011, 2012), except for NH_4^+ which was almost ten times higher, while only slightly higher values were observed for the other nitrogen compounds (NO_3^-, NO_2^-). The higher values of these compound with to respect literature probably reflect the closeness to the Station MZS in our case and then to anthropogenic inputs.

It is well known that anthropogenic activities have enhanced N supply especially to coastal and waters. High rates of anthropogenic atmospheric N deposition to the North Atlantic have been reported in earlier studies (Duce et al., 1991). These studies indicate that anthropogenic sources dominate the current dissolved inorganic nitrogen (DIN) inputs, whereas natural sources dominate the dissolved organic nitrogen (DON).

It was observed above (from the correlation matrices reported in Tables A1 to A3) that higher associations between nutrients can be observed if we exclude the first two samplings of the season. In this respect, it can be argued that, in Antarctica, the strength of the relationships between nutrients increase during the summer when interaction with the phytoplankton become important and typical "nutrient" distributions develop along the water column.

The Nitrate *vs* Phosphate uptake ratio (the molar incremental ratio of 11.6 from all the data) (Fig. 13) was lower than the value predicted by Redfield for a typical plankton community (N:P =16; Redfield et al., 1963), however our value is in close agreement with other studies carried out in the area (11 from Soggiomo et al., 2002, and 7.8 from Rivaro et al., 2011). A higher uptake ratio of ~21 is obtained if we excluded the first profile (28/11/13) from the analysis (see Appendix Tab A2).

This results can be due to the slightly higher nitrate values with respect to the literature (Rivaro et al., 2011, 2012) associated probably to anthropogenic activities close to MZS station, that enhanced N supply as reported for coastal areas and also for open oceans (Naqui et al., 2000, Nevison et al., 2004).

The silicate to nitrate uptake ratio (0.44 molar ratio from all the data) (Fig. 14) observed in our study was much lower than values around 2.3 found either close to our site (Rivaro et al., 2011), or in Southern Ocean (Takeda, 1998), or offshore the Ross Sea (Fitzwater et al., 2000). This result probably reflects the higher nitrate values as referred above. Higher uptake ratios are obtained if we exclude the first two profiles from the analysis, or if we use only the last profile, i.e. 0.69 and 1.2 molar ratio, respectively (see Appendix). However, the silicate to nitrate uptake ratio is a function not only of the algal assemblage composition, but also of the physiology of the micronutrient uptake. Diatoms have an absolute requirement for silicic acid, while other algal groups, such as *Phaeocystis sp.,* do not remove silicic acid at all. Therefore, the specific composition of the algal assemblage determines the Si:N uptake ratio, and then this ratio is controlled by the different micronutrient requirements too (Boyle et al., 2001, Smith et al., 2003), which can be different in different sites or in different periods for the same site.

Typically, the summer evolution of phytoplankton assemblages at TNB showed the main peak between December and January, followed by a decrease in January and a second peak in February (Arrigo and Van Dujken 2004, Nuccio et al., 2000). During the 2013/2014 field campaign, the pack

ice started to break in mid-December. However due to technical problems, it was not possible to collect samples for one month and half. The first sampling before the end of the Antarctic expedition was that of February. Therefore, it was not possible to study the central part of the austral summer and, in particular, the metal distribution during the effective bloom of phytoplankton. In fact, according to literature (Fonda Umani et al., 2005, Nuccio et al., 2000, Saggiomo et al., 2002), the Chl-*a* concentrations observed at mid-December seemed to confirm the incoming bloom event. Contrary to previous surveys, during our field campaign, the late phytoplankton bloom, typical of the end of summer, was not observed.

During this campaign, a Deep Chlorophyll Maximum (DCM) was observed throughout the sampling period. One of the most common features of the vertical distribution of plankton, is the presence of a DCM (Cullen 1982). The existence of a DCM may be explained by light availability and a high nutrient concentration in deep waters (Longhurst and Harrison, 1989). There is evidence that in some circumstances photo acclimation (i.e. the change of the chlorophyll content per cell) could also explain the formation of DCM (Falkowski et al., 1998, Fennel and Boss, 2003), and it can happen that it not coincides with maxima o cell abundance, biomass or primary production (Perez et al., 2006, Zubkov at al., 2000). One main peak of chlorophyll was observed in the profiles, which extended from ~10 m to ~50 m during the period. This was due to phytoplanktonic cells, which lived under light limitation, and produced high amount of chlorophyll.

The TNB polynya (close to our site) is an important element of the regional climate since strong air–sea coupling events occurs over the open water, especially in winter, as cold, dry, continental air flows over the relative warm open water. Many studies of atmospheric aerosol in both coastal and continental areas of Antarctica were carried out (Annibaldi 2011, 2013, Dick 1991, Toscano et al., 2005). The Italian Research Programme in Antarctica had paid particular attention to the study of atmospheric aerosol since the 1990-1991 Antarctic campaign, showing that the atmospheric contribution of Cd, Pb and Cu in the snow in the neighbourhood of the Italian Antarctic station "Mario Zucchelli" was higher than in the other sites in Antarctica (Annibaldi et al., 2013), therefore a remarkable contribution also for the seawater is presumable.

Concerning meteorological parameters, the studied campaign showed temperature typical of summer season at Terra Nova Bay (average value of −3 °C) (Grigioni et al., 1992) with an increase during the summer.

No snowfall occurred during the sampling period: relative humidity and atmospheric pressure were generally low (~46% and ~950 hPa respectively).

Winds mainly come from West and their speeds were generally high. Several katabatic wind events occur (~40 knots) at the beginning and at the half of the sampling campaign.

In the 2013-2014 Antarctic campaign the back trajectories confirmed that air masses coming from the inner part of Antarctica. Moreover, the air masses from December the 22th to January the 3rd, correlated with pack ice melting, seemed to running along the coast so inputs to and from the seawater, and from Erebus Mount, near located, were hypothesized.

5.2 Metal distribution in seawater and phytoplankton

Metal distribution in the coastal waters of TNB were mainly affected by the dynamic of the pack -ice melting and the phytoplankton activity.

In particular, surface and subsurface layers are strongly influenced by these two phenomena. Concerning the surface seawater layer, it was found that metal concentrations are mainly affected by the dynamic of the pack ice melting, in fact this process influences both the input of metals from melt waters and the covering of the seawater surface, allowing atmospheric dust input only when all ice has been melt or removed. The release of particulate matter (SPM) during ice melting is a significant process by which the metal enters the water column. Moreover, sea ice is one the major factors controlling phytoplankton primary production (Smetacek et al., 1992). During the early spring, productivity is limited by irradiance, due to wind mixing, unfavourable solar angle and substantial amount of ice cover (Smith et al., 2000). Later in spring, the phytoplankton bloom appears to begin when vertical stability is imparted by sea ice melting coincident with greater daily insolation (Smith et al., 2000). The release of micronutrients (e.g. iron) during the sea ice melting is another process which may influence the seasonal cycle of phytoplankton productivity and growth (Fitzwater et al., 2000, Sedwick & DiTullio, 1997).

The three metals here investigated have different biogeochemical characteristics in the ocean. They have been classified (Donat and Bruland, 1995) as recycled (Cd), scavenged (Pb) and both recycled and scavenged (Cu) metals.

5.2.1 Distribution of Cadmium

During the austral summer 2013-2014, cadmium was mainly present in its dissolved form (~90% of the total). Results here obtained for all the Cd fractions studied are in good agreement with values found by several authors in the same site (Capodaglio et al., 1998, Frache et al., 2001, Scarponi et al., 1995, Scarponi et al., 1997, Scarponi et al., 2000), in the Ross Sea (Corami et al., 2000, Fitzwater at al., 2000) and in the Weddel Sea (Nolting and de Baarm 1994, Westerlund and Ohman, 1991).

Cd associated to the algal particulate fraction was very low, with surface values of 3-4 ng/l both in presence and in absence of the pack ice. This fraction tended to increase both in absolute and in relative terms in the correspondence of the Chl-*a* maximum, as a consequence of the increasing densities of phytoplanktonic cell.

In correspondence of the DCM the percentage of Cd_{diss} *vs* Cd_{tot} decreased from ~90% at the beginning of the summer to ~ 60% at mid-December until the end of the season: a decrease of dissolved Cd and a simultaneous increase of particulate Cd (in particular of the algal phase) was observed.

It is well known that Cd concentrations in the Polar Regions are subject to two main phenomena. The first is related to the seasonal evolution of phytoplankton which uptakes Cd. For its physical and chemical similarity with other Group 2B metals, such as Zn, Cd acts as a micronutrient and may substitute Zn in metal-enzyme complexes (Morel and Price, 2003), promoting the growth of Zn-limited phytoplankton. The second process is related to the pack ice melting. In fact, from the literature (Grotti 2005, Lannuzel 2011) it is known that Cd concentration in the pack ice is higher than that of the underlying seawater and it is mainly present in its dissolved form. On December, the 17th, in correspondence of the pack ice melting, an increase of Cd total concentration (from ~60 ng/l to ~80 ng/l) was observed with the prevalence of Cd dissolved fraction.

At the same time the reduction of dissolved Cd and the Cd-algal particulate production was a consequence of the uptake of Cd by phytoplankton which moved this metal from the dissolved to the particulate phase. On February, Cd dissolved concentration strongly decreased in the superficial layer (with a maximum at ~60 m) assuming a nutrient-like profile, this is due to the biological activity of phytoplankton. This behaviour was highlighted from highly significant ($p<0.01$) Cd/PO_4^{3-} correlations (Figures 21 and 22) in this sampling period.

This observation agrees with previous surveys (Capodaglio et al., 1998, Scarponi et al., 1997, Finale PhD thesis) where a nutrient-like profile for Cd was showed along the water column. In fact at the deepest layers, Cd was released following the sedimentation of dead phytoplankton cells (Bruland, 1983).

More generally, it can be observed from the correlation matrices (see Appendix) that high correlations are observed between all the Cd fractions (except particulate) with nutrients NO_3^-, PO_4^{3-} and $Si(OH)_4$ (but not with Chl-*a*); and that correlations increase when we exclude the first profiles progressively. In particular, r passes from 0.4-0.6 (p 0.0004-0.02) with all the profiles, to 0.74-0.94 (p 0.0006-0.03) when we consider only the last sampling. We interpret this fact (as done before for nutrients) as a natural consequence of the fact that in Antarctica the “nutrient” profile develops only gradually during the Summer.

The distribution of Cd_{phyto}:Chl-*a* stoichiometry seemed to follow the seasonal variation of pack ice, with low values in November and mid-December and an increase during mid-December in the superficial layer and at the DCM. As reported in the literature (Sunda and Huntsman, 1998, Sunda and Huntsman, 2000) a complex set of variables (bioavailability, phytoplankton species, light regime, concentrations of major nutrients and other trace metals) controlled Cd content in phytoplankton, from our data we hypothesized that an increase of phytoplankton cells that required Cd was observed during the phytoplankton bloom.

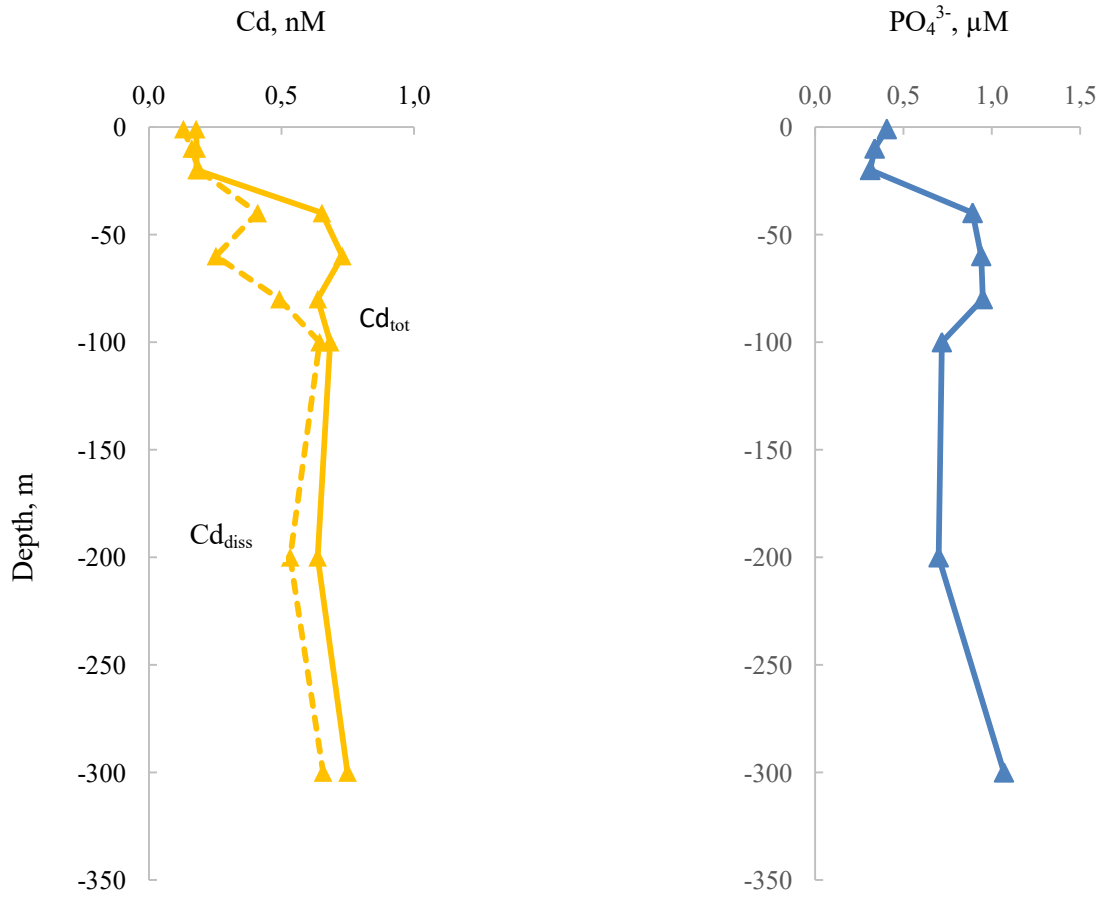

Fig. 21. Cadmium and phosphate distributions along the water column in the 02/02/2014 sampling.

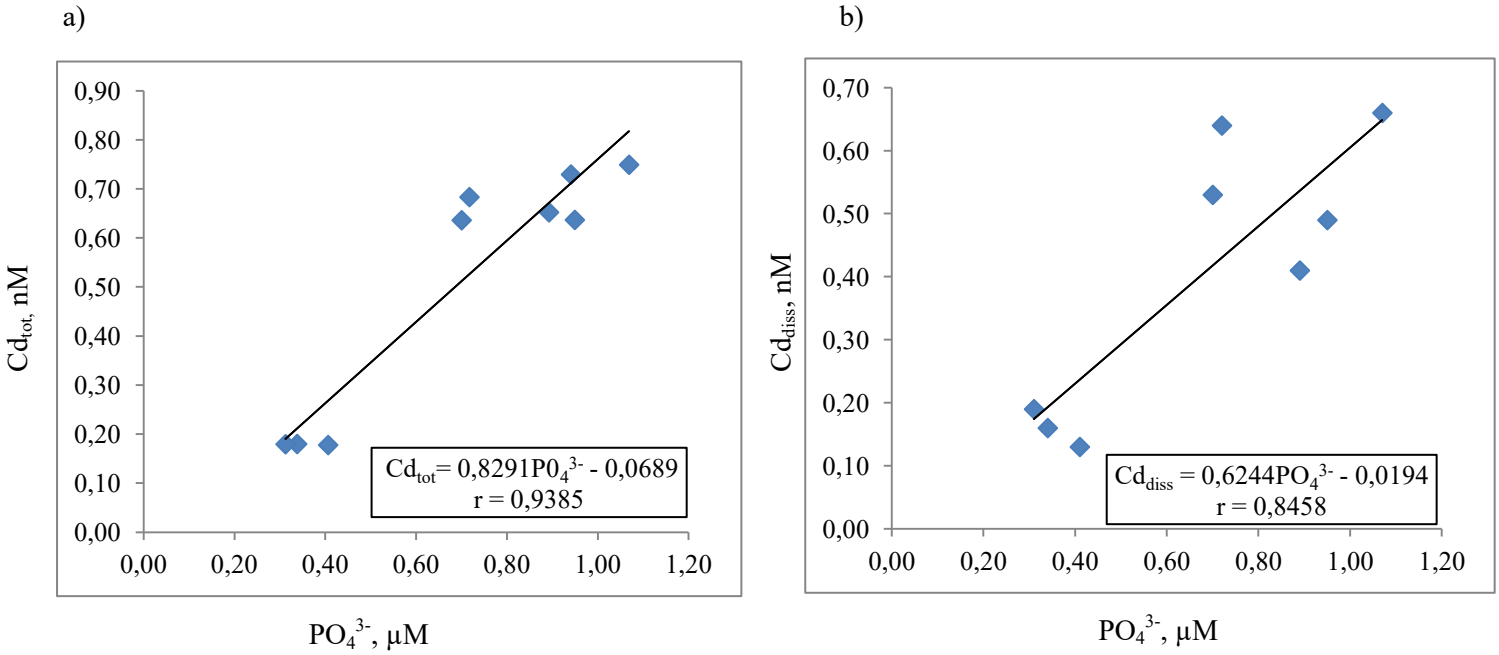

Fig. 22. Plot of cadmium total concentration (a) and cadmium dissolved concentration (b) versus phosphate in the 02/02/2014 sampling.

5.2.2 Distribution of copper

Copper showed a high vertical and seasonal variability of the distribution between dissolved and particulate phases. A general increase of the total content of this metal can be observed on mid-December while on February values slightly lower than the beginning of the summer were recorded. At the beginning of the summer, Cu was mainly present in its dissolved from (~90% of the total) with values that remained practically constant during summer, except a slight decrease on February. Total and dissolved Cu concentration are similar to those measured by other authors in the same area (Capodaglio et al., 1994, Capodaglio et al., 1998, Corami et al., 2005, Frache et al., 1997, Frache et al., 2001, Grotti et al., 2001) and in other Antarctic coastal areas (Fitzwater et al., 2000, Westerlund and Ohman., 1991). Therefore, the increase in Cu total content on mid-December was related to a correspondent increase of the Cu particulate fraction (~50% of the total). The latter was mainly constituted, especially at the surface, by the non-living particulate fraction, which then decreased during the season in favour of the algal phase, accounting in February for the 80% of the total particulate.

From literature, it is known that the sea-ice melting provided a local input of Cu (Rivaro et al., 2011), as reported by different authors for the same area (Frache et al., 1997, Frache et al., 2001, Grotti et al., 2005, Lannuzel et al., 2011), surface maxima of total particulate Cu can be ascribed to the direct release from the ice. Along the water column, Cu distribution was strongly affected by both pack ice melting and phytoplankton activity. In fact, while in November Cu showed a quite homogeneous vertical profile, with the dominance of the dissolved fraction, in December, when the pack ice started to melt, a marked increase was observed in the superficial layer mainly connected with the particulate fraction and probably due to the pack ice melting. Then, when Chl-*a* started to increase (as a result of phytoplankton growth), the vertical profile showed a strong superficial decrease, typical of the nutrient behaviour. Infact Cu, as an essential micronutrient (La Fontaine et al., 2002, Maldonado et al., 2006, Peers et al., 2005) plays a critical role in the physiology of phytoplankton, due to its utilization in certain enzymes (Raven et al., 1999 and Mercant et al., 2006). For this reason, Cu distribution in seawater was characterized by a surface/sub-surface depletion and regeneration in deepest layers where organic detritus of biogenic origin coming from the surface mineralizes. However, if we consider the complete Cu vertical profile, we do not observe a maximum in deep layers but a substantial constancy. This aspect together with the absence of general correlations between copper fractions and nutrients (see e.g. Figures 23 and 24 referred to the last sampling) highlighted that Cu profile cannot be completely considered nutrient-type, but hybrid as reported in literature (Bruland, 1983, Bruland, 2003, Capodaglio et al., 1998, Donat and Bruland, 1995).

Indeed, if we consider the complete set of correlation matrices reported in the Appendix, we can observe some sparce correlations of Cu fractions with NH_4^+, $Si(OH)_4$, NO_3^- and PO_4^{3-} which again increase (as in nutrients and in Cd/nutrients correlations) when we exclude the first profiles progressively. In particular, at the end of the season, we have significant correlations only of Cu_{diss} with NO_3^- (r 0.75, p 0.03), DIN (r 0.78, p 0.02), PO_4^{3-} (r 0.83, p 0.01) and a little lower with $Si(OH)_4$ (r 0.64, p 0.098). This fact strengthens our opinion that in Antarctica the effect of phytoplankton interaction with nutrients and metals develops gradually during the summer, to reach at the end typical profiles and relationships.

It is interesting to note that during the pack ice melting (sampling 17/12/2013), even if Cu associate to particulate matter is high, the phytoplankton quote is almost negligible. This confirms the importance of carrying out the physical separation of the particulate between the non-living and the phytoplanktonic fractions.

The Cu_{phyto}:Chl-*a* ratio did not show great differences between November and the beginning of December with low values along the entire column. An increase of the ratio was observed in the superficial layer in correspondence of pack ice melting and still remained on February.

Cu is a bioactive metal that facilitates many biogeochemical significant processes such as nitrous oxide reduction (Stiefel, 2007), photosynthesis (Peers and Price, 2006), and aerobic ammonia oxidation (Walker et al., 2010). In natural waters, copper is typically complexed by two classes of ligands; the first is strong and of organic origin, while the second class of ligand is generally weak and probably made of refractory organic matter. In the coastal area of TNB, dissolved copper speciation is strongly affected by the concentration of the first ligand, which was generally low and varied greatly during season and with depth. In particular, this ligand increased after the pack ice melting and at the DCM (Capodaglio et al., 1994). We could hypothesize that the first class of ligands, comprising dead phytoplankton cells or organic exudates released during the pack ice melting or resulted from the phytoplankton bloom of mid-December, complexed copper in this period. Alternatively, we can hypothesize that phytoplankton itself produced copper complexing ligands to detoxify this metal in the environment, as suggested by Donat et al. (2008).

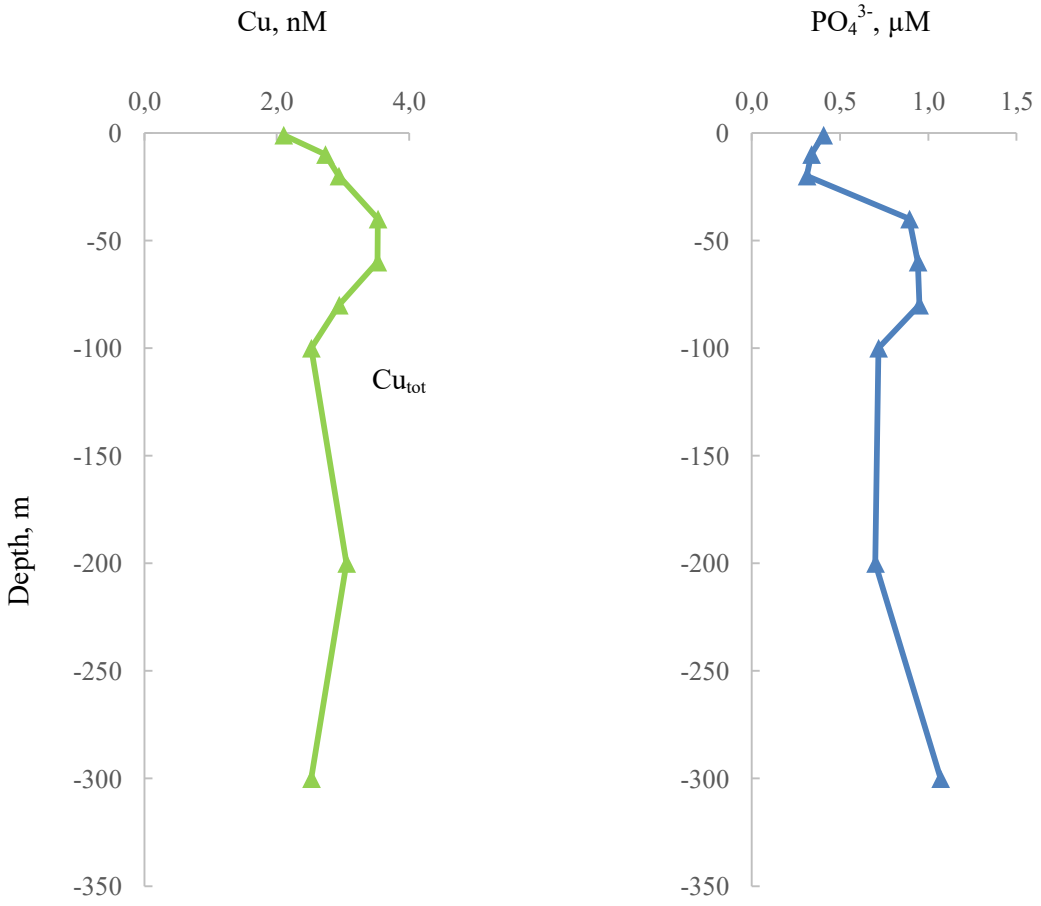

Fig. 23. Copper total and phosphate distributions along the water column in the 02/02/2014 sampling.

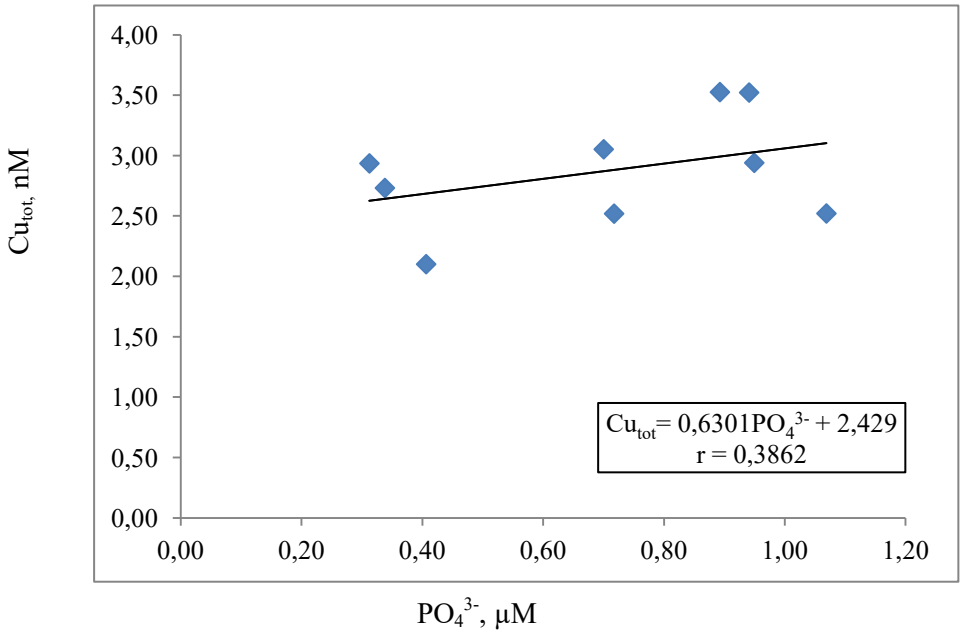

Fig. 24. Plot of copper total concentration versus phosphate in the 02/02/2014 sampling.

5.2.3 Distribution of lead

Partioning of lead between dissolved and particulate phases was completely different from that of Cd and Cu. Total and dissolved Pb concentrations were higher than values reported in the literature for the same area in the past (Capodaglio et al., 1998, Corami et al., 2005, Dalla Riva et al., 2003, Frache et al., 2001, Scarponi et al., 1997, Scarponi et al., 2000). In some cases, a contamination of the sample can be hypothesized. However, these high concentrations are probably related to recent anthropogenic activities in the TNB area, following the building of a new South-Korean research station (opening ceremony on February 2014), which is very close to the sampling site, together with the increased traffic from and to the Italian station "Mario Zucchelli".

A maximum of Pb total concentration at mid-December was observed, with a strong decrease at the end of summer. At the same time, dissolved Pb showed an increasing trend up to mid-December and a decrease on February to values similar to those of November. Total particulate Pb showed two maxima: at the end of November and during mid-December, showing a different speciation between phytoplankonic and inorganic fraction during the season. In fact, at the beginning of the summer Pb total particulate was dominated by the non-living fraction, while at the end of the season, when pack ice was completely melted, the algal phase became more important.

This changing in the speciation of particulate Pb can be related to both the presence of pack ice (Capodaglio et al., 1998, Frache et al., 2001) which could release in seawater particles of different sources origin (i.e. crustal, atmospheric, biogenic) and to phytoplankton. From literature, we can observe that Pb concentration in the pack ice is only slightly increased with respect to the underlying seawater and that the dissolved/particulate distribution between ice and seawater is similar (Grotti et al., 2005). Therefore, the pack ice melting didn't cause a significant increase of Pb in seawater in fact this concentration remained almost constant from November to December the 17^{th} in the superficial layer.

Lead is considered a toxic non-essential element with no known physiological requirements (Maeda and Sakugaki, 1990, Sunda et al., 1989); nevertheless, it has been demonstrated that lead can be adsorbed to algal surfaces or complexed by exudates excreted by the algae (Santana-Casiano et al., 1995). On February, after the phytoplankton bloom, Pb concentration decreased probably for this biological uptake: in fact lead can be adsorbed on the phytoplankton external surfaces.

At the end of the campaign Pb was strongly reduced throughout the entire seawater column showing an almost constant vertical profile and a tendency to decrease with depth as a scavenging-type element (Bruland 1983, Donat and Bruland, 1995).

Pb_{phyto}:Chl-*a* ratio showed, except anomalous data, lower values with respect to Cd and Cu, due to its not nutrient behaviour. On mid-December and on February it showed a peak in

correspondence of the DCM. The increase of Pb_{phyto}:Chl-*a* ratio at the DCM was probably due to an increase in the number of algal cells that adsorbed the metal on their external surfaces that were released during the pack ice melting.

In accordance with this view, practically no correlations are present between Pb fractions and nutrients (see Appendix).

5.3 Correlation between metals

Consider again the data in the Appendix. In this discussion, we exclude the, partially obvious, correlations between the different fractions of the same metals.

Then, considering the relationships between different metals and metal fractions, we observe generally high positive correlations if we consider all the sampling profiles (Tab. A1) for Cd vs Pb, Cd vs Cu, and Pb vs Cu. This fact indicates that the overall variations of all three metals during the season are quite similar. However, the correlations drastically reduce when we progressively exclude the first samplings (Tables A2, A3, A4), until practically no significant correlations are observed (at all) when we consider only one profile, the last (see Tab. A4). This result expresses clearly the fact that along the water column different profiles are showed for different metals (as deeply discussed above).

5.4 Metal distribution in aerosol and relationships with seawater

The total metal content of atmospheric aerosol during the austral summer 2013-2014 showed an increase from the beginning of the season reaching a maximum around the half of December, then it decreased until the end of the summer. The increasing period corresponded to the start of pack ice melting, with a consequently increase of the marine aerosol formation, and to increase in activity at the station.

The soluble fraction was predominant for Cd (60-95% of the total) and Cu (37-72% of the total), while for Pb this fraction was low (14-30% of the total) and the insoluble fraction prevailed.

Data here obtained are in good agreement with values found by several authors in the same site (Bazzano et al., 2015, Capodaglio et al., 1998, Grotti et al., 2005), and the distribution between soluble/insoluble fractions was in agreement with our previous work (Annibaldi et al., 2007).

Data obtained in this work were used to evaluate heavy metal fluxes in the marine environment. For this purpose, the following assumptions were used:

- The atmospheric concentration of aerosol at Terra Nova Bay is not changed during the last 10-15 years (0.92 ± 0.32 μg/m^3, 0.73 ± 0.27 μg/m^3) (Annibaldi et al., 2007, Illuminati et al., 2016); in this elaboration, the aerosol atmospheric concentration was considered to be ~0.8 μg/m^3.

- The Antarctic aerosol depositional flux in the South Pacific Ocean has been estimated 0.35 $g/m^2/y$ (Duce et al., 1991) (see also Huneeus et al., 2011, Schulz et al., 2012), in this work the same value was considered for Terra Nova Bay.

Using these assumptions and the average atmospheric concentrations of metals found in this work (i.e. Cd 1.3 ± 1.0 pg/m^3, Cu 41.9 ± 8.7 pg/m^3, Pb 16.6 ± 4.4 pg/m^3), atmospheric metal deposition fluxes were estimated as follows: Cd ~57, Cu ~1800 and Pb ~700 $pg/cm^2/y$. These values can be compared with literature data, derived from analyses of snow, aerosol and marine ice (compared to seawater) in other Antarctic sites (Boutron et al., 1979, Chance et al., 2015, Hong 2002, Grotti et al., 2005, Lannuzel at al., 2001) (Tab. 9).

Tab. 9. Metal atmospheric deposition fluxes and comparison with other coastal and inland Antarctic sites.

	Metal atmospheric fluxes pg/cm^2/y			
Site	Cd	Cu	Pb	Rif.
Antarctic campaign (2013-2014)	57	1800	700	This work
South-east Atlantic (2004-2012)[a]	4-40	139-1390	68-680	Chance 2015
King George Is. (2000)[b], coast	20.0	3320	696	Hong 2002
Dolleman Is. (1984-85)[b], coast	3.12	156	156	from Hong 2002
Coats Land (1985-86)[b], inland 180 km	0.56	19.6	30.8	from Hong 2002
D55 Adelie Land (1970)[b], inland 200 km	2.48	42.4	43.2	from Hong 2002
Dome C[b], plateau	23	120	120	Boutron 1979
Terra Nova Bay[c], coast	~7000	~20000	~9700	Grotti 2005
East Antarctic[c], coast	60-730	900-15000	-	Lannuzel 2011

[a] from atmospheric concentration and deposition velocity
[b] from snow
[c] from fast/pack ice

The comparison showed that fluxes found in this work, although referred only to the summer period, are comparable with literature values of coastal sites and broadly explain concentrations found in the pack ice, in excess with respect seawater. In fact, we could consider that, during the Antarctic winter, depositional fluxes could be lower than our depositional fluxes calculated during the summer and in presence of activity near the Italian station. From our data, we expect excess of concentrations in the pack ice with respect to seawater of about Cd 0.19 ng/l, Cu 6.0 ng/l, Pb 2.3 ng/l. This excess could explain at least the increase of metal concentrations in the pack ice with respect to the underlying seawater as found in the literature (Grotti et al., 2005, Lannunzel et al., 2011).

From our data, it can be computed also the influence of aerosol accumulation on marine ice during its melting on the seawater metal concentrations. Considering the effect on a thickness of 0.1 m surface seawater, the concentration increase during the pack ice ice melting can be estimated as Cd 6 ng/l, Cu 180 ng/l and Pb 70 ng/l.

These evaluations are rather in accordance with the increase of the metal concentration in the superficial layer consequently the pack ice melting: Cd (Δ ~10 ng/l), Cu (Δ ~200 ng/l), Pb (Δ close to 0 ng/l).

Finally, for each metal it was possible to calculate the marine aerosol flux, considering that the atmospheric concentration of marine aerosol (dimensional fractions higher than ~1.5μm) could be estimated as ~0.2 μg/m^3 (25% of the total amount), (Illuminati, 2016). The results allowed to estimate that the marine spray contribution to the aerosol flux were Cd 14, Cu 175, Pb 450 pg/cm^2/y.

In conclusion, the biogeochemical cycles of metals in the marine coastal area of Terra Nova Bay have been investigated considering, the distribution between abiotic and biotic matrices of the marine environment, the possible role of atmospheric aerosol deposition, and the effect of the pack ice melting (using data from the literature in the latter case). A synthesis of data obtained and computed, within the biogeochemical cycles of metals at TNB is depicted in Figures 24-26.

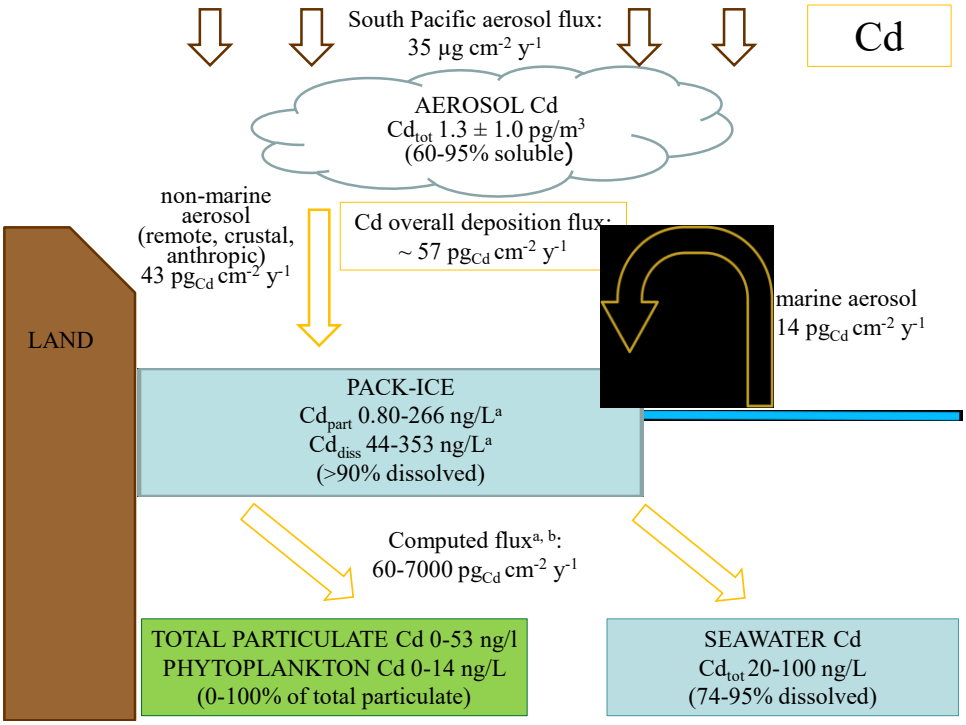

Fig. 25. Proposed model for biogeochemical cycle of Cd in a costal marine area in Terra Nova Bay (Ross Sea, Antarctica). Data from Grotti [(a)] and Lannuzel [(b)].

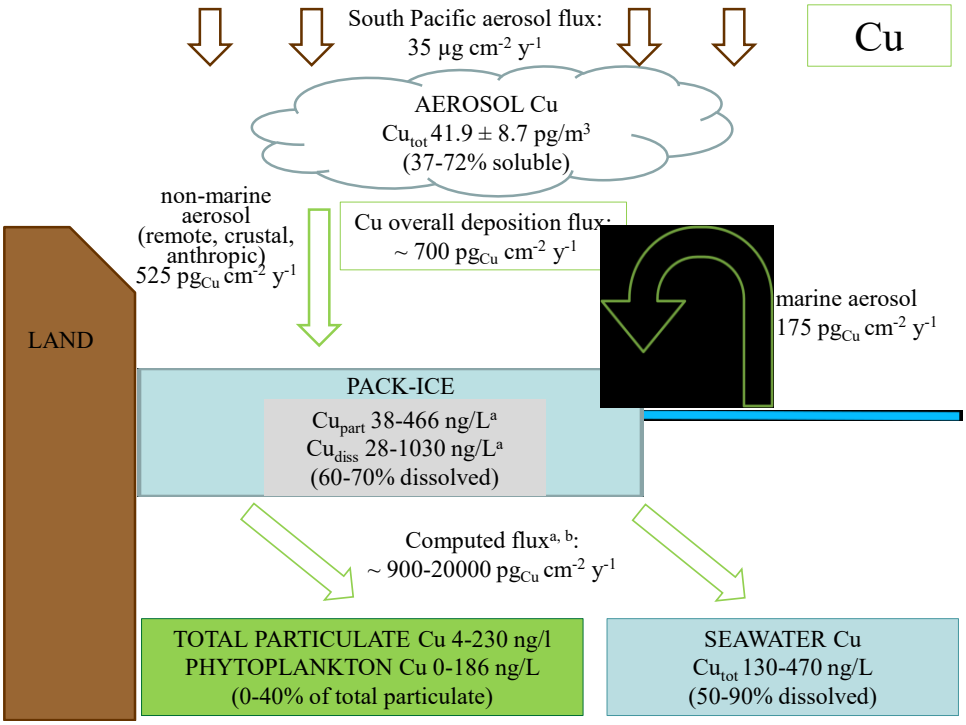

Fig. 26. Proposed model for biogeochemical cycle of Cu in a costal marine area in Terra Nova Bay (Ross Sea, Antarctica). Data from Grotti [(a)] and Lannuzel [(b)].

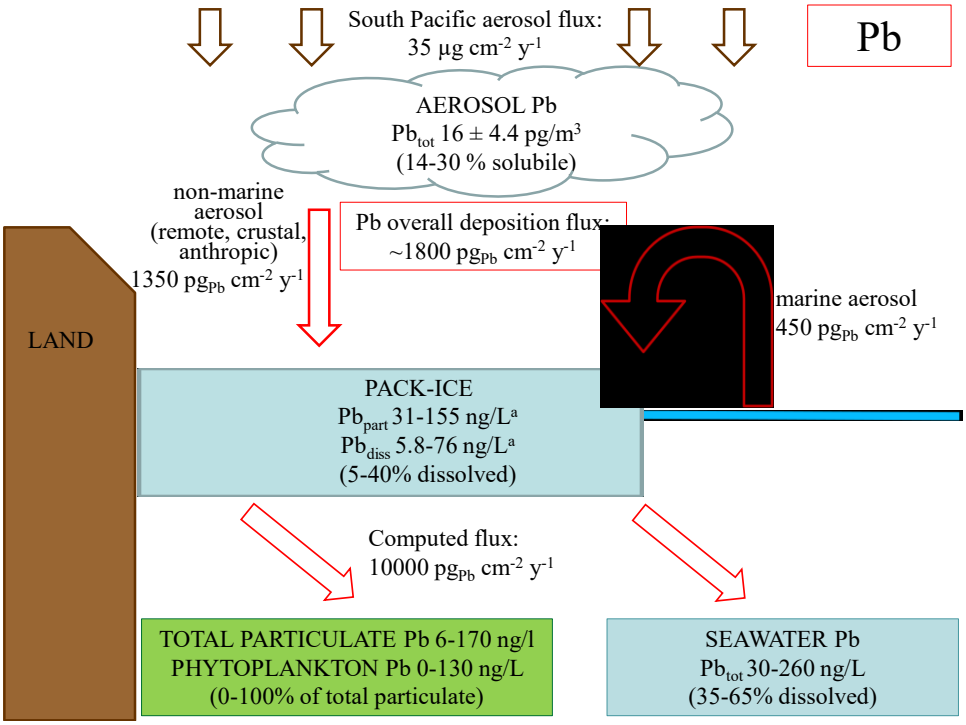

Fig. 27. Proposed model for biogeochemical cycle of Pb in a costal marine area in Terra Nova Bay (Ross Sea, Antarctica). Data from Grotti [(a)].

6. Conclusions

The marine distribution of Cd, Pb and Cu in dissolved, inorganic and algal particulate in the marine environment of Terra Nova Bay (Ross Sea, Antarctica) was investigated from November 2013 to February 2014 with the aim to clarify the role of phytoplankton in the heavy metal distribution in seawater. Cd, Pb and Cu in aerosol samples was also investigated to understand if heavy metals distribution in seawater could be influenced by this matrix.

The separation of the algal fraction from the particulate phase permitted us to obtain first direct measurements of metal contents in the micro and nano-phytoplankton separated from the particulate matter at Terra Nova Bay and let us to better understand heavy metal distributions between algal and non-algal fractions along the water column.

Our data highlighted the significant influence of the phytoplankton on the distribution of metals in seawater, especially Cd and Cu, showing a determinant role in their biogeochemical cycles.

Metal distributions in TNB area were mainly affected by the phytoplankton activity, the dynamic of the pack ice melting and to some extent to aerosol input.

In general metals associated to the algal particulate varied with depth and during the season: the highest values were measured at the surface and in presence of the phytoplankton bloom.

Cadmium was dominated by dissolved species and its distribution was mainly controlled by nutrient-like biogeochemical cycling, with a surface phytoplankton uptake of dissolved Cd and a recycling along the water column.

Also, copper was mainly dominated by dissolved species with a nutrient-like vertical profile in presence of the phytoplankton and in surface, while it assumes and almost scavenging profile on deep waters (the so-called hybrid-behaviour).

Lead (for which we suspect sample contamination in a few cases) features the typical distribution of a scavenged element, at least the end of the season, with particulate fraction generally prevailing. Its distribution was affected by several factors, the phytoplankton influences its behaviour only partially.

Aerosol atmospheric flux (~25% of marine aerosol) seemed to increase slightly metal concentrations in seawater (mainly in their dissolved form for Cd and Cu and in particulate fraction for Pb). However, since atmospheric aerosol is collected on pack ice during all the winter season, its contribution is particularly important in summer because of melting of marine ice.

The separation of the algal fraction from the particulate phase let us to better understand heavy metal distributions between dissolved and particulate fractions along the seawater column, highlighting important exchanges with phytoplankton cells. However, further studies with pack ice

analysis would be required to provide a better comprehension of the metal behaviours along the water column during the season, especially following the process of ice melting.

In any case, our data highlighted the significant influence of the phytoplankton on the distribution of Cd, Pb and Cu in seawater, showing a determinant role in their biogeochemical cycles (Figures 24-26).

7. References

1. Abollino, O., Aceto, M., La Gioia, C., Sarzanini, C., Mentasti, E. Spatial and season variations of major, minor and trace elements in Antarctic seawater. Chemometric investigation of variable and site correlations. *Advanced Environment Research,* **6** (2001) 29-43.
2. Abollino, O., Aceto, M., Buoso S., Gasparon, M., Green, W. J., Malandrino, M., Mentasti, E. Distribution of major, minor and trace elements in lake environments of Antarctica. *Antarctic Science*, **16** (2004) 277-291.
3. Accornero, A., Manno, C., Esposito, F., Gambi, M.C. The vertical flux of particulate matter in the polynya of Terra Nova Bay. *Antarctic Science,* **15** (2003) 175-188.
4. Agusti, S., Duarte, C.M., Phytoplankton chlorophyll a distribution and water column stability in the central Atlantic Ocean. *Oceanologica Acta,* **22** (1999) 193-203.
5. Annett, A. L., S. Lapi, T. J. Ruth, and M. T. Maldonado. The effects of Cu and Fe availability on the growth and Cu:C ratios of marine diatoms. *Limnology and Oceanography*, **53** (2008) 2451–2461.
6. Annibaldi, A., Truzzi, C., Illuminati, S., Bassotti, E., Scarponi, G. Determination of water-soluble and insoluble (dilute-HCl-extractable) fractions of Cd, Pb and Cu in Antarctic aerosol by square wave anodic stripping voltammetry. Distribution and summer seasonal evolution at Terra Nova Bay (Victoria Land). *Analitical Bioanalitical Chemistry,* **387** (2007) 977-998.
7. Annibaldi, A., Truzzi, C., Illuminati, S., Scarponi, G. Direct Gravimetric Determination of Aerosol Mass Concentration in Central Antarctica. *Analitical Chemistry*, **83** (2011) 143-151.
8. Annibaldi, A., Illuminati, S., Truzzi, C., Finale, C., Scarponi, G. Soluble/Insoluble (dilute-HCl-extractable) fractionation of Cd, Pb and Cu in Antarctic snow and its relationship with metal fractionations in the aerosol. *EDP Sciences*, **1** (2013) 23006.
9. Argentini, S., Viola, A., Sempreviva, A.M., Petenko, I. Summer boundary-layer height at the plateau site. Dome C, Antarctica. *Boundary Layer Meteorol*ogy, **115** (2005) 409-422.
10. Arrigo, K., Robinson, D., Worthen, D., Dunbar, R., Di Tullio, G., VanWoert, M., Lizotte M. Phytoplankton community structure and drawdown of nutrients and CO_2 in the Southern Ocean. *Science,* (1999) 283-365.
11. Arrigo, R., DiTullio G. R.,. Dunbar R. B, Robinson D. H., van Woert M.L., Worthen D. L. and Lizotte, J M. P. *Geophyical. Research*, **105** (2000) 8827–8846.
12. Arrigo, K., van Dijken G. L. Annual changes in sea-ice, chlorophyll *a,* and primary production in the Ross Sea, Antarctica. *Deep-Sea Research II*, **51** (2004) 117-138.

13. Bargagli, R., Nelli L., Ancora S., Focardi S. Elevated cadmium accumulation in the marine organisms from Terra Nova Bay (Antartica). *Polar Biology,* **16** (1995) 513-520.
14. Bazzano, A., Soggia, F., Grotti, M. Source identification of atmospheric particle-bound metals at Terra Nova Bay, Antarctica. *Environmental Chemistry*, **12** (2015) 245-252.
15. Biesuz, R., Alberti, G., D'Agostino, G. Magi, E., Pesavento, M. Determination of cadmium, copper, manganese, and nichel species in Antarctic seawater with complexing resins. *Marine Chemistry*, **3** (2006) 180-189.
16. Boyle, E. A. Cadmium: chemical tracer of deepwater paleoceanography. *Paleoceanography*, **3** (1988) 471–489.
17. Boyle, M., Wake, B. D., Lopez Garcia, P., Bown, J., Baker A. R., Achterberg E. P. Distributions of dissolved trace metals (Cd, Cu, Mn, Pb, Ag) in the southeastern Atlantic and the Southern Ocean. *Biogeosciences*, **9** (2012) 3231-3246.
18. Boyle, E. and Edmond, J. M. Copper in surface waters south of New Zealand. *Nature,* **253** (1975) 107–109.
19. Boutron, C. Past and present day tropospheric fallout fluxes of Pb, Cd, Cu, Zn and Ag in Antarctica and Greenland. *Geophysical Research Letters,* **6** (1979) 159-161.
20. Boutron, C.F. *Enviromental Reviews,* **3** (1995) 1-28.
21. Brand, L.E., Sunda W.G. and Guillard R.R.L. Reduction of marine phytoplankton reproduction rates by copper and cadmium. *Journal of Experimental Marine Biology and Ecology,* **96** (1986) 225-250.
22. Braune, B.M, Otridge, P.M., Fisk, A.T., Muir, D.C.G., Helm, P.A., Hobbs, K., Hoekstra P.F., Kuzyk Z.A. Kwan, Letcher M., Lockhart R.J., Norstrom R.J., Stern G.A., Stirling I. Persistent organic pollutants and mercury in marine biota of the Canadian Arctic: an overview of spatial an temporal trends. *Science of the Total Environment* **4** (2005) 351-352.
23. Broise, D. and Palenik B. Immersed in situ microcosms: A tool for the assessment of pollution impact on phytoplankton. *Journal of Experimental Marine Biology and Ecology,* **341** (2007) 274-281.
24. Bruland, K. W. and Lohan, M. C. Controls of Trace Metals in Sea-water. *Treatise on Geochemistry,* edited by: Elderfield, H., Else-vier Science Ltd., Cambridge, **6** (2003) 23-47.
25. Bruland, K. W. Oceanographic distributions of cadmium, zinc, nickel, and copper in the north Pacific Earth Planet. *Science Letters,* **47** (1980) 176- 198.
26. Bruland, K.W. Trace elements in seawater. *Chemical Oceanography Academic Press,* **45** (1983) 157-220.
27. Brzezinski, M.A., Dickson M.L., Nelson D.M., Sambrotto R. Ratios of Si, and C uptake by

microplankton in the Southern Ocean. *Deep sea research part II,* **50** (2003) 619-633.

28. Capodaglio,G., Toscano, G., Scarponi, G., Cescon P. Copper complexation in the surface sea water of Terra Nova Bay (Antarctica). *International journal of environmental analytical chemistry,* **55** (2004) 129-148.
29. Capodaglio, G., Turetta C., Toscano G., Gambaro A., Scarponi G., Cescon P.. Cadmium, lead and copper complexation in Antarctic coastal seawater. Evolution during the austral summer. *International Journal of Environmental Analytical Chemistry*, **71** (1998) 195-226.
30. Capodaglio, G., Toscano G., Scarponi G., Cescon P. Copper complexation in the surface sea water of Terra Nova Bay (Antarctica). *International Journal of Environmental Analytical Chemistry,* **55** (1994) 129-148.
31. Cappelletti, A., Picco, P., Peluso, T. Upper ocean layer dynamics and response to atmospheric forcing in the Terra Nova bay polynya, Antarctica. *Antarctic science*, **22** (2010) 319-329.
32. Cassar, N., Bender, M.L., Barnett, B.A., Fan, S., Moxim, W.J., Levy II, H., Tilbrook, B. The Southern Ocean biological response to aeolian iron deposition. *Science,* **371** (2007) 1067-1070.
33. Catalano, G., Povero, P., Fabiano, M., Benedetti, F., Goffart, A. Nutrient utilization and particulate organic matter changes during summer in the upper mixed layer (Ross Sea, Antarctica). *Deep-Sea Research I,* **44** (1997) 97-112.
34. Chance, R., Jickells, D.T., Baker, R.A. Atmospheric trace metal concentrations, solubility and deposition fluxes in remote marine air over the south-east Atlantic. *Marine Chemistry,* **177** (2015) 45-56.
35. Cincinelli, A., Stortini, A.M., Perugini, M., Checchini, L. & Lepri, L. Organic pollutants in sea-surface microlayer and aerosol in the coastal marine environmentof leghorn (Tyrrehenian Sea). *Marine Chemistry,* **76** (2001) 77-98.
36. Colin, J.L, Jaffrezo J.L., Le Bris, N., Bergametti, G., Lim, B., Jickells, T.D. Aluminium solubility in rainwater and molten snow. *Journal of Atmospheric Chemistry,* **17** (1993) 29-43.
37. Comiso, J., McClain C., Sullivan C., Ryan J., and Leonard C. Coastal zone color scanner pigment concentrations in the Southern Ocean and relationships to geophysical surface features. *Journal of geophysical research,* **98** (1993) 2419-2451.
38. Corami, F., Capodaglio G., Turetta C., Soggia F., Magi E., Grotti M. Summer distribution of trace metals in the western sector of the Ross Sea, Antartica. *Journal of Environmental monitoring*, **7** (2005) 1256-1264.
39. Cullen, J.J. The deep chlorophyll maximum: comparing vertical profiles of chlorophyll *a*. *Canadian Journal of Fisheries and Aquatic Sciences,* **39** (1982) 791-803.

40. Dalla Riva, S., Abelmoschi, M.L., Chiantore, M., Grotti, M., Magi, E., Soggia, F. Biogeochemical cycling of Pb in the coastal marine environment at Terra Nova Bay, Ross Sea. *Antarctic Science,* **15** (2003) 425–432.
41. Davolio, S., Buzzi, A. Mechanisms of Antarctic katabatic currents near Terra Nova Bay. *Tellus*, **54 A** (2002) 187-204.
42. Desboeufsa, K.V., Sofikitisa, A., Losnoa, R., Colina, J.L., Ausseta, P. Dissolution and solubility of trace metals from natural and anthropogenic aerosol particulate matter. *Chemosphere* **58** (2005) 195-203.
43. Demayo, A., Taylor M. C., Taylor K. W., Hodson, P. V. Toxic effects of lead and lead compounds on human health, aquatic life, wildlife, and life-stok. *CRC Critical Reviews in Environmental Control,* **12** (1984) 257-305.
44. Dick A.L. Concentration and sources of metals in the Antarctic Penisula aerosol. *Geochimica et Cosmochimica Acta*, **55** (1991) 1827-1836.
45. Dixon, J.L. Macro and micro nutrient limitation of microbial productivity in oligotrophic subtropical Atlantic waters. *Environmental Chemistry*, **2** (2008) 135-142.
46. Donat, P. Häder. Ultraviolet effects on phytoplankton. Germany (2008)
47. Donat, J.R., Lao, K.A., Bruland, K.W. Speciation of dissolved copper and nickel in South San Francisco Bay: a multi-method approach. *Analytica Chimica Acta*, **284** (1994) 547-571.
48. Donat J. R. and Bruland K. W. Trace elements in the oceans. *Trace Elements in Natural Waters (eds. E. Steinnesand B. Salbu*). CRC Press, Boca Raton, FL, (1995) 247-280. .
49. Draxler, R.R., Rolph, G.D., 2015. HYSPLIT (Hybrid Single-particle Lagrangian Integrated Trajectory) Model Access via NOAA ARL READY. NOAA Air Resources Laboratory. College Park, MD Website, Available at htpp://www.arl.noaa.gov/HYSPLIT.php.
50. Dubischar, C.D., Bathmann U.V. Grazing impact of copepods and salps on phytoplankton in the Atlantic sector of the Southern Ocean. *Deep sea research II,* **44** (1997) 415-433.
51. Duce, R. A., Liss, P. S., Merrill, J. T., Atlas, E. L, Buat-Menard, P., Hicks B. B, Miller J. M.,. Prospero J. M, Arimoto, R., Church, T. M., Ellis W., Galloway J. N., Hansen, L.,T. D. Jickells,A. H. Knap,K. H. Reinhardt, B. Schneider, A. Soudine, J. J. Tokos.. S. Tsunogai, R. Wollast, M. Zhou. The atmospheric input of trace species to the world ocean. *Global Biogeochemical Cycles,* (1991) 193-259.
52. Echeveste, P. Agustì, S., Tovar-Sanchez, A. Toxic thresholds of cadmium and lead to oceanic phytoplankton: cell size and ocean basins dependent effect. *Environmental Toxicology and Chemistry,* **31** (2012) 1887-1894.
53. Echeveste, P., Tovar-Sàanchez A., Agusti S. Tolerance of polar phytoplankton communities to

metals. *Environmental pollution,* **185** (2014) 188-195.

54. Ellwood, M. J. Wintertime trace metal (Zn, Cu, Ni, Cd, Pb andCo) and nutrient distributions in the Subantarctic Zone between 40–52° S; 155–160 °E, *Marine Chemistry*, **112** (2008) 107-117.
55. European Commission, Joint Research Centre, Institute for Reference Materials and Measurements BCR-414, Certified Reference Material for plankton (2007).
56. Fabiano, M., Povero, P., Misic, C. Spatial and temporal distribution of particulate organic matter in the Ross Sea. *Ross Sea Ecology:Italianantartide Expeditions (1987-1995),* **11** (1993) 135-150.
57. Falkowski, P.G. Light-shade adaptation in marine phytoplankton. *Primary productivity in the sea,* (1998) 99-119.
58. Fennel K., Boss E. Subsurface maxima of phytoplankton and chlorophyll, Steady-state solutions from a simple model. *Limnology and Oceanography*, **48** (2003) 1521-1534.
59. Finale, C. Distribution of heavy metals in the Antarctic marine environment: possible relationships between aerosol, seawater and phytoplankton. PhD thesis (academic years 2011-2014).
60. Fischer, N., Teyssie, J.L., Krishnaswami, S., Baskaran, M. Accumulation of Th, Pb, U and Ra in marine phytoplankton and its geochemical significance. *Limnology and Oceanography*, **32** (1987) 13l-142.
61. Fitzwater S.E., Johnson K.S., Gordon R.M., Coale K.H., Smith Jr. W.O. Trace metal concentrations in the Ross Sea and their relation ship with nutrients and phytoplankton growth. *Deep sea research Part II,* **47** (2000) 3159-3179.
62. Flegal, A. R. and Patterson, C. C. Vertical concentration profiles of lead in the Central Pacific at 15° N and 20°S. *Earth Planet Science Letters*, **64** (1983) 19–32.
63. Flemming, C.A., Trevors J.T. *Water Air Soil Pollution* (1989) 143-158.
64. Fofonoff, N.P., Millard, J. Specific volume anomaly and density anomaly of seawater. In: Algorithms for Computation of Fundamental Properties of Seawater. UNESCO technical papers in marine science **3** (1983) 15-21.
65. Fonda Umani, S., Accornero, A., Budillon, G., Capello, M., Tuccic, S., Cabrini, M., Del Negro, P., Montia, M., De Vittor, C. Particulate matter and plankton dynamics in the Ross Sea Polynya of Terra Nova Bay during the Austral Summer 1997/98. *Journal of Marine Systems* **36** (2002) 29–49.
66. Fonda Umani, S. and Beran A. Seasonal variations in the dynamics of microbial plankton communities: first estimates from experiments in the Gulf of Trieste, Northern Adriatic Sea.

Marine Ecology Progress Series **247** (2003) 1-16.

67. Fonda Umani, S., Monti M., Bergamasco A., Cabrini M., De Vittor C., Burba N., Del Negro P. Plankton community structure and dynamics versus physical structure from Terra Nova Bay to Ross Ice Shelf (Antarctica). *Journal of Marine Systems* **55** (2005) 31-46
68. Frache, R., Baffi, F., Ianni, C., Soggia, F. Dissolved and particulate metals in the pack ice melting process in the Ross Sea Antarctica. *Annali di Chimica* **87** (1997) 367-374.
69. Frache, R., Abelmoschi M.L., Grotti M, Ianni C., Magi E., Soggia F., Capodaglio G., Turetta C. and Barbante C. Effects of ice melting on Cu, Cd and Pb profiles in Ross Sea waters **79** (2001) 301-313.
70. Fung, I., S. Meyn, I. Tegen, S. C. Doney, J. G. John, and J. K. B. Bishop Iron supply and demand in the upper ocean. *Global Biogeochemical Cycles*, **14** (2000) 281-295.
71. Garcia, V.M.T., Garcia, C.A.E., Mata, M.M., Pollery, R.C., Piola, A.R., Signorini, S.R., McClain, C.R., Iglesias-Rodriguez, M.D. Environmental factors controlling the phytoplankton blooms at the Patagonia shelf-break in spring. *Deep-Sea Research I* **55** (2008) 1150-1166.
72. Giere, R., Xavier, Q. Solid particulate matter in the atmosphere. *Elements,* **6** (2010) 215-222.
73. Giordano, R, Lombardi G, Ciaralli L, Beccaloni E, Sepe A, Ciprotti M, Costantini S. Major and trace elements in sediments from Terra Nova Bay, Antarctica (1999) 29-40.
74. Grammatika, M. & Zimmerman, W.B. Microhydrodynamics of flotation processes in the sea surface layer. *Dynamics of Atmospheres and Oceans*, **34** (2001) 327-348.
75. Grigioni, P., De Silvestri, L., Pellegrini, A., Sarao, R. Some climatological aspects in Terra Nova Bay area, Antarctica. In: Porano, Italy, Colacino, M., Giovanelli G., Stefanutti, L.,(Eds), Conference Proceedings of 4th Workshop on Italian Research on Antarctic Atmosphere. *Italian Research on Antarctic atmosphere*, **35** (1991) 97-121.
76. Grotti, M., Soggia F., Abelmoschi .L., Rivaro P., Magi E., Frache R. Temporal distribution of trace metals in Antarctic coasal waters. *Marine chemistry,* **76** (2001) 189-209.
77. Grotti, M., Soggia, F., Ianni, C., Frache, R. Trace metals distributions in coastal sea ice of Terra Nova Bay, Ross Sea, Antarctica. *Antarctic Science*, **2** (2005) 289-300.
78. Gustavson, K. and Wänberg S.A. Tolerance and succession in microalgae communities exposed to copper and atrazine. *Aquatic Toxicology,* **32** (1995) 283-302.
79. Hong, J.N., Hindle, M., Byron, P.R. Control of particle size by coagulation of novel condensation aerosols in reservoir chambers. *Journal of aerosol medicine,* **4** (2002) 359-368.
80. Jickells, T.D. Global iron connections between desert dust, ocean biogeochemistry, and climate. *Science*, **67** (2008) 67-71.

81. Jones, G.J., Palenik, B.P., Morel, F.M.M. Trace metal reduction byphytoplankton: the role of plasmalemma redox enzymes. *Journal of Phycology,* **23** (1987) 237–244.
82. Illuminati, S., Annibaldi, A., Truzzi, C., Finale, C., Scarponi, G. Square-wave anodic-stripping voltammetric determination of Cd, Pb and Cu in wine: set-up and optimization of sample pre-treatmentand instrumental parameters. *Electrochemical Acta*, **104** (2013)146-161.
83. Illuminati, S., Annibaldi, A., Truzzi, C., Libani, G., Mantini, C. Scarponi, G. Determination of water-soluble, acid extractable and inert fractions of Cd, Pb and Cu in Antarctic aerosol by square wave anodic stripping voltammetry after sequential extraction and microwave digestion. *Journal of Electroanalytical Chemistry,* **755** (2015) 182-196.
84. Illuminati, S., Sebastien, B., Annibaldi, A., Mantini, C. Evolution of size-segregated aerosol mass concentration during the Antarctic summer at Northern Foothills, Victoria Land. *Atmospheric Environment*, **125** (2016) 212-221.
85. Kolb, M., Rach, P., Schaefer, J., Wild, A. Investigations of oxidative UV photolysis. Sample preparation for the voltammetric determination of zinc, cadmium, lead, copper, nickel, and cobalt in waters. *Journal of Analitical Chemistry*, **342** (1992) 341-349.
86. Kim, S.J. Effect of heavy metals on natural populations of bacteria from surface microlayers and subsurface water. *Marine Ecology Progress Series* **26** (1985) 203-206.
87. Kustka, A. B., A. E. Allen, and F. M. M. Morel. Sequence analysis and transcriptional regulation of iron acquisition genes in two marine diatoms. Journal of Phycology **43** (2007) 715–729.
88. Hendrya, K. R., Rickabya, R. E.M., de Hooga, C.M., Westonb, K., Rehkämperc, M. Cadmium and phosphate in coastal Antarctic seawater: Implications for Southern Ocean nutrient cycling. *Marine Chemistry,* **112** (2008) 149-157.
89. Huneeus, N., M. Schulz, Y., Balkanski, J. Griesfeller, S. Kinne, J. Prospero, S. Bauer, O. Boucher, M. Chin, F. Dentener, T. Diehl, R. Easter, D. Fillmore, S. Ghan, P. Ginoux, A. Grini, L. Horowitz, D. Koch, M.C. Krol, W. Landing, X. Liu, N. Mahowald, R.L. Miller, J.-J. Morcrette, G. Myhre, J.E. Penner, J.P. Perlwitz, P. Stier, T. Takemura, and C. Zender. Global dust model intercomparison in AeroCom phase I. *Atmospheric Chemistry Physics*, **11** (2011) 7781-7816.
90. La Fontaine, S., Quinn, J. M., Nakamoto, S. S., Page, M. D., Gohre, V., Moseley, J. L., Kropat, J. & Merchant, S. Copper-dependent iron assimilation pathway in the model photosynthetic eukaryote *Chlamydomonas reinhardtii. Eukaryotic Cell,* **1** (2002) 736–57.
91. Laj, P., Ghermandi, G., Cecchi, R., Maggi, V., Riontino, C., Hong, S., Candelone, J.P., Boutron, C. Distribution of Ca, Fe, K, and S between soluble and insoluble material in the

Greenland Ice Core Project ice core. *Journal of Geophysical Research,* **102** (1997) 26615-26623.

92. Langston, R. F. Metals in sediments and benthic organisms in the Mersey estuary. *Estuarine, Coastal and Shelf Science,* **23** (1986) 239 - 261.
93. Lannuzel, D., Bowie, A.R, Merwe, P.C., Townsend, A.T., Schoemann, V. Distribution of dissolved and particulate metals in Antarctic sea ice. *Marine Chemistry*, **124** (2001) 134-146.
94. Lazarus, D., Caulet J.P. Cenozoic Southern Ocean reconstructions from sedimentologic, radiolarian and other microfossil data. *The Antarctic paleoenvironment; a perspective on global change Antarctic research series,* **60** (1993*)* 145-174.
95. Le Jeune, A.H., Charpin M., Deluchat V., Briand J.F., Lenain J.F., Baudu M. and Amblard C. Effect of copper sulphate treatment on natural phytoplankton communities. *Aquatic Toxicology,* **80** (2006) 267-280.
96. Libes, S.M. *An introduction to marine biogeochemistry* (1992).
97. Longhurst, A.R., Harrison, G.W. The biological pump: Profiles of plankton production and consumption in the upper ocean. *Progress in Oceanography*, **22** (1989) 47-123.
98. Loscher, B. M. Relationships among Ni, Cu, Zn, and major nutrients in the Southern Ocean. Marine Chemistry, **67** (1999) 67-102.
99. Losno, R., Colin, J.L, Le Bris, N., Bergametti, G., Lim, B., Jickells, T.D. Aluminium solubility in rainwater and molten snow. *Journal of Atmospheric Chemistry* **17** (1993) 29-43.
100. Lu, Z. Cai, M., Wang. J. Yin, Z., Yang, H. Levels and distribution of trace metals in surface sediments from Kongsfjorden, Norwegian Arctic. *Environmental Geochemistry and Health* **35,** (2013) 257-269.
101. Lymann, W.J., *Fundamentals of Aquatic Toxicology: Effects, Environmental Fate, and Risk Assessment*, 2nd edition Rand G. M. (ed.) Taylor & Francis, London. Chapt. **15** (1995) 449-492.
102. Macdonald, R.W., Barriel L.A., Bidlemanb T.F., Diamond M.L., Gregor D.J., Semkin R.G., Strachan W.M.J., Lib Y.F., Wania F., Alaee M., Alexeeva L.B., Backus S.M., Bailey R., Bewers J.M., Gobeil C.,. Halsall C.J, Harner T., Hoff J.T., Jantunen L.M.M., Lockhart W.L., Mackay D., Muir D.C.G., Pudykiewicz J., Reimer K.J., Smith J.N., Stern G.A, Schroeder W.H., Wagemann R., Yunker M.B.. Contaminants in the Canadian Arctic: 5 years of progress in understanding sources, occurrence and pathways. *Science of the Total Environment,* **254** (2000) 93-234.
103. Maeda, S., Sakaguki, T. Accumulation and detoxification of toxic metal elements by algae. In: *Akatsuka*, I.(Ed.), Introduction to Applied Phycology. Balogh Scientific Books Academic

Publishing, Tokyo, (1990) 109-136.

104. Maldonado, M. T., Allen, A. E., Chong, J. S., Lin, K., Leus, D., Karpenko, N. & Harris, S. L. Copper-dependent iron transport in coastal and oceanic diatoms. *Limnology and Oceanography* **51, (**2006) 1729–1743 **.**
105. Maring, H.B. and Duce, R.A. The impact of atmospheric aerosols on trace metal chemistry in open ocean surface seawater. *Journal of Geophysical Research 2* **94** (1989)
106. Marino, F., Ghermandi, G.,Cecchi, R., Maggi,V., Riontino, C., Hong, S., Candelone, J.P., Boutron, C., Journal of Geophysical Research **102** (1997) 26725-26734.
107. Martin, J.H. Glacial-interglacial CO_2 change: The iron hypothesis (1990).
108. McLaughlin, M. J., Parker, D. R., Clark, J. M. Metal and micronutrients-food safety issues. *Field Crops Research* **60**, (1999) 143–163.
109. Merchant, S. S., Allen, M. D., Kropat, J., Moseley, J. L., Long, J. C., Tottey, S. and Terauchi, A. M. Between a rock and a hard place: trace element nutrition in *Chlamydomonas. Biochimica et Biophysica acta***, 1763** (2006) 578–94.
110. Middag, R., de Baar, H. J. W., Laan, P., Cai, P. H., and van Ooijen, J. C. Dissolved manganese in the Atlantic sector of the Southern Ocean. *Deep-Sea Research II*, **58** (2011) 2661–2667.
111. Mitchell and Brody. Light limitation of phytoplankton biomass and macronutrient utilization in the Southern ocean. *Limnology and oceanography,* **36** (1991) 1662-1667.
112. Moffett, J.W. The spatial and temporal variability of copper complexation by strong organic ligands in the Sargasso Sea. *Deep-Sea Research I* **42** (1995) 1273–1295.
113. Moore, J.K., Abbott M.R. Phytoplankton chlorophyll distributions and primary production in the southern ocean. *Journal of geophysical research*, **15** (2000) 709-722.
114. Morel, F.M.M., Price, N.M., The Biogeochemical Cycles of Trace Metals in the Oceans Science, **300** (2003) 944-947.
115. National Institute of Standards and Tecnology (NIST), Standard reference material (SRM) 1648a for urban particulate matter, NIST, Gaithersburg, MD, USA, 7 (2012).
116. National Research Council of Canada (NRCC), Seawater Reference Material for Trace metals, NASS-6, (2010).
117. Nolting, R.F., H.J.W. de Baar. Behaviour of nickel, copper, zinc and cadmium in the upper 300 m of a transect in the Southern Ocean. *Marine chemistry,* **3,** (1994) 225-242
118. Nuccio, C., Innamorati, M., Lazzara, L., Mori, G., Massi, L., Ianora, A. (Eds.), *Ross Sea Ecology.* Springer-Verlag, Heidelberg, Berlin **19** (2000) 231-245.
119. Nriagu, J.O, In Copper in the Environment. I. Ecological Cycling, *Interscience New York* (1979) 43–75.

120. Olson, R., H. Sosik, A. Chekalyuk, and A. Shalapyonok. Effects of iron enrichment on phytoplankton in the Southern Ocean during late summer: Active fluorescence and flow cytometric analyses. *Deep Sea Research II*, **47** (2000) 3181-3200.
121. Peers, G. and Price, N. M. Copper-containing plastocyanin used for electron transport by an oceanic diatom. *Nature,* **441** (2006) 341–344.
122. Peers, G., Quesnel, S. A. and Price, N. M. Copper requirements for iron acquisition and growth of coastal and oceanic diatoms. *Limnology and Oceanography,* **50** *(*2005) 1149–1158.
123. Peloquin, J.A., Smith J.R W.O., *Journal of Geophysical Research* (2007).
124. Pérez V., Fernández E., Marañón E., Morán X.A.G., Zubkov M.V. Vertical distribution of phytoplankton biomass, production and growth in the Atlantic subtropical gyres. *Deep sea research,* **53** (2006) 1616-1634.
125. Petrou, K, Trimborn S, Rost B, Ralph P, Hassler C. The impact of iron limitation on the physiology of the Antarctic diatom *Chaetoceros simplex. Marine biology,* **161** (2014) 925-937.
126. Planchon, F.A.M, Van de Velde, K., Rosman K.J.R, Wolff, E.W. Ferrari, C.P., Boutron, C.F. One hundred fifty-year record of lead isotopes in Antarctic snow from Coats Land. *Geochimica and Cosmochimica Acta*, **67** (2003) 693-708.
127. Presley, B.J. A review of Arctic trace metal data with implications for biological effects. *Marine pollution bulletin,* **35** (1997) 226-234.
128. Price, N. M. & Morel, F. M. M. Cadmium and cobalt substitution for zinc in a marine diatom. *Nature,* **344** (1990) 658-660.
129. Priddle, J., Smetacek V., Bathmann U., Stromberg J.O, Croxall J.P. Antarctic marine primary production, biogeochemical carbon cycles and climatic change (1992).
130. Quigg, A., Reinfelder, J.R., Fisher, N.S. Copper uptake kinetics in diverse marine phytoplankton. *Limnology and Oceanography*, **51** (2006) 893–899.
131. Rand, G.M., Wells P.G., McCarty L.S. Effects, Environmental Fate, and Risk Assessment. *Fundamentals of Aquatic Toxicology* (1995) 3-66, 449-492.
132. Raven, J. A., Evans, M. C. & Korb, R. E. The role of trace metals in photosynthetic electron transport in O_2-evolving organisms. *Photosynthesis Research,* **60** (1999) 111-50.
133. Redfield, R., Linton, R. Herskovits, M.J. Memorandum for the study of acculturation. *American Antropologist,* **38** (1936) 149-152.
134. Rivaro, P., Ianni, C., Abelmoschi, M.L., De Vittor, C., Frache, R. Distribution of dissolved labile and particulate iron and copper in Terra Nova Bay polynia (Ross Sea, Antarctica) surface waters in relation to nutrients and phytoplankton growth. *Continental Shelf Research,*

31 (2011) 879-889.

135. Rivaro, P., Abelmoschi, M.L., Grotti, M., Ianni, C., Magi, E., Margiotta, F., Massolo, S., Saggiomo, V. Combined effects of hydrographic structure and iron and copper availability on the phytoplankton growth in Terra Nova Bay Polynia. *Deep-Sea Research I,* **62** (2012) 97-110.
136. Sadiq, M. Toxic metal Chemistry in Marine Enviroment, *Marcell Dekker*, Inc., (1992).
137. Saggiomo, V., Catalano, G., Mangoni, O., Budillon, G., Carrada, G.C. Primary production processes in ice-free waters of the Ross Sea (Antarctica) during the austral summer 1996. *Deep-Sea Research Part II,* **49** (2002) 1787-1801.
138. Santana-Casiano, J. M., Gonzalez-Davila, M., Perez-Pefia, J., Millerob, F. J., Pb^{2+} interactions with the marine phytoplankton *Dunaliella tertiolecta*. *Marine Chemistry,* **48** (1995) 115-129.
139. Santschi, P. H., Li Y. H., Carson S. R. The fate of trace metals in Narragansett Bay, Rhode Island: radiotracer experiments in microcosmos. *Estuarine and coastal marine science journal,* **10** (1980) 635 - 654.
140. Scarponi, G. Capodaglio G., Toscano G., Barbante C., Cescon P. Speciation of Lead and Cadmium in Antarctic seawater: comparision with areas subject to different anthropic influence. *Microchemical Journal,* **51** (1995) 214-230.
141. Scarponi, G., Capodaglio G., Barbante C., Toscano G., Cecchini M., Gambaro A., Cescon P. Concentration changes in Cadmium and Lead in Antarctic Coastal Seawater (Ross Sea) during the austral summer and their relationship with the evolution of biological activity. *Ross Sea Ecology*, (2000) 585-594
142. Scarponi, G., Capodaglio G., Barbante, C., Cecchini, M., Toscano G., Cescon P. Evolution of Cadmium and Lead contents in Antarctic Coastal Sea Water during the Austral Summer. *International Journal of Enviromnta lAnalytical Chemistry,* **66** (1997) 23-49.
143. Schulz, M., J.M. Prospero, A.R. Baker, F. Dentener, L. Ickes, P.S. Liss, N.M. Mahowald, S. Nickovic, C. Pérez, S. Rodríguez, M. Manmohan Sarin, I. Tegen, and R.A. Duce. The atmospheric transport and deposition of mineral dust to the ocean: Implications for research needs. *Environmental Science Technology*, **46** (2012) 10390-10404.
144. Sedwick, P., and G. DiTullio. Regulation of algal blooms in Antarctic shelf waters by the release of iron from melting sea ice. *Geophysical Research Letters*, **24** (1997) 2515–2518.
145. Semeniuk, D., Cullen, J. T., Johnson, W. K., Gagnon, K., Ruth, T. J., Maldonado, M. T. Plankton copper requirements and uptake in the subarctic Northeast. *Deep-Sea Research I,* **56** (2009) 1130-1142.
146. Stiefel, E.I. Bioinorganic chemistry and the biogeochemical cycle. In: Bertini I., Grey, H.,

Stiefel, E., Valentine J. (Eds.). *Biological inorganic chemistry. University Science Books* (2007) 7-30.

147. Shallari, S, Schwartz C, Hasko A, Morel JL. Heavy metals in soils and plants of serpentine and industrial sites of Albania, **209** (1998) 133-142.
148. Shaw G.F. Antarctic aerosols: a review. *Reviews of Geophysics*, **26** (1988) 89-112.
149. Sholkovitz, R.E., Sedwick, N.P., Church, M. T. On the fractional solubility of copper in marine aerosols: Toxicity of Aeolian copper revisited. *Geophysical research letters*, **37** (2010).
150. Smetacek, V., Scharek, R., Gordon, L. I., Eicken, H., Fahrbach, E., Rohardt, G., Moore, S. Early spring phytoplankton blooms in ice platelet layers of the southern Weddell Sea, Antarctica. *Deep Sea Research Part A. Oceanographic Research Papers,* **39** (1992) 153-168.
151. Smith, Jr W.O., Marra, J., Hiscock M.R., Barbere R.T. *Deep-Sea Research II* (2000)
152. Smith, W., Jr., J. Marra, M. Hiscock, and R. Barber. The seasonal cycle of phytoplankton biomass and primary productivity in the Ross Sea. *Antarctica Deep Sea Research II*, **47** (2000) 3119-3140.
153. Smith, W. O., Jr and. Asper V. L, *Deep-Sea Research* Part *I*, **48** (2001) 137-161.
154. Smith Jr., W.O., Dinniman, M.S., Klink. J.M., Hofmann, E. Biogeochemical climatologies in the Ross Sea, Antarctica, seasonal patterns of nutrients and biomass. *Deep-Sea Research II*, **50** (2003) 3083-3101.
155. Sposito, G.A. On distinguishing adsorption from surface precipitation. In Geochemical Processes at mineral surfaces. *ACS symposium Series* (1986) 217-218.
156. Stauber, J.L. and C.M. Davies. Use and limitations of microbial bioassays for assessing copper bioavailability in the aquatic environment. *Environmental Reviews Journal,* **8** (2000) 255-301.
157. Sullivan, C.W., Arrivo K.R, McClain C.R, Comiso J.C., Firestone J. Science (1993).
158. Sunda, W.G. Trace metal interactions with marine phytoplankton. Biological Oceanography, **6** (1989). 411-442.
159. Sunda, W.G., Guillard, R.R.L. The relationship between cupric ion activity and the toxicity of copper to phytoplankton. Journal of Marine Research, 34 (1976) 511-529.
160. Sunda, G W., Huntsman, S. A. Effect of Zn, Mn, and Fe on Cd accumulation in phytoplankton: Implications for oceanic Cd cycling. Limnology and Oceanography, 7 (2000) 1501–1516.
161. Sunda, W.G., Hanson, A.K. Measurement of free cupric ion concentration in seawater by a ligand competition technique involving copper sorption onto C-18 Sep-Pak cartridges.

Limnology and Oceanography, **32** (1987)537–551.

162. Sunda, W. G. and Huntsman, S. A. Control of cadmium concentrations in a coastal diatom by interactions among free ionic Cd, Zn, and Mn in seawater. *Environmental Science and Technology,* **32** (1998) 2961-2968.
163. Sunda, W. G. and Huntsman, S. A. Iron uptake and growth limitation in oceanic and coastal phytoplankton. *Marine Chemistry,* **50** (1995) 189–206.
164. Sunda, W.G, Klaveness, D, Palumbo, A.V. Bioassay of cupric ion activity and copper complexation. *Complexation of Trace Metals in Natural Water* (1984) 399-409.
165. Sunda, W.G., Huntsman, S.A. Interrelated influence of iron, light and cell size on marine phytoplankton growth. *Nature*, **390** (1997) 389-392.
166. Thatje, S. Effects of Capability for Dispersal on the Evolution of Diversity in Antarctic Benthos Integrative and comparative biology. *Integrative and Comparative biology* (2012) 1-13.
167. Thomas, W.H. and D.L.R Seibert. Effects of copper on the dominance and the diversity of algae: controlled ecosystem pollution experiment. *Marine Science bulletin,* **27** (1977) 23-33.
168. Thomas, L.C; Chamberlin, G.J. (Eds) *Colorimentric Chemical Analytical Methods*. The Tintometer Ltd, United Kindom, (1974).
169. Toscano, G., Gambaro, A., Moret, I., Capodaglio, G., Turetta, C., Cescon, P. Trace metals in aerosol at Terra Nova Bay, Antartica. *Journal of Enviromental Monitoring,* **7** (2005) 1275-1280.
170. Truzzi, C., Lambertucci, L., Gambini, G., Scarponi ,G. Optimization of square wave anodic stripping voltammetry (SWASV) fo the simultaneaus determination of Cd, Pb and Cu in seawater and comparision with differential pulse anodic stripping voltammetry (DPAV) *Annali di chimica*, **92** (2002) 313-326.
171. Truzzi, C., Annibaldi, A., Finale, C., Libani, G., Romagnoli, T., Scarponi, G., Illuminati, S. Separation of micro-phytoplankton from inorganic particulate in Antarctic seawater (Ross Sea) for the determination of Cd, Pb and Cu: optimization of the analytical methodology. *Analytical Methods* **7** (2015) 5490-5496.
172. Truzzi, C., Annibaldi, A., Illuminati, S., Bassotti, E., Scarponi G. Square-wave anodic stripping voltammetric determination of Cd, Pb and Cu in a hydrofluoric acid solution of silicieaus spicules of marine sponges (from the Ligurian Sea, Itali and the Ross Sea, Antarctica). *Analytical and Bioanalytical chemistry*, **392** (2008) 247-262.
173. Thuroczy, C., Boye, M., Losno, R. Dissolution of cobalt and zinc from natural and anthropogenic dusts in seawater. *Biogeosciences,* **7** (2010) 1927–2010.

174. UNESCO Background papers and supporting data on the Practical Salinity Scale 1978. UNESCO *Technical papers in marine science*, **37** (1981) 1-140.
175. Ussher, S.J., Achterberg, E.P., Powell, C., Baker, A.R., Jickells, T.D., Torres, R., Worsfold, P.J. Impact of atmospheric deposition on the contrasting iron biogeochemistry of the North and South Atlantic Ocean. *Global Biogeochemical Cycles,* **4** (2013) 1096-1107.
176. Utermohl, H. Zur Vervollkommung der quantitativen Phytoplankton-Methodik. *Mitteilung Internationale Vereinigung fuer Theoretische unde Amgewandte Limnologie*, **9** (1958) 1-38.
177. Van den Berg, C.M.G. Determination of copper in seawater by chatodic stripping voltammetry of complexes with catechol. *Analityca Chimica Acta*, A. **164** (1984) 195-207.
178. Van Hilst, C. and Smith, W. Photosynthesis/irradiance relationships in the Ross Sea, Antarctica and their control by phytoplankton assemblage composition and environmental factors. *Marine ecology progress series,* **226** (2002) 1-12.
179. Van Ho, A. Ward, D.M. and Kaplan, J. Transition metal transport in yeast. *Annual Review of Microbiology,* **56** (2002) 237-261.
180. Walker, O. Smith, Jr. The Seasonal Cycle of Phytoplankton Biomass and Primary Productivity in the Ross Sea, Antarctica. *Deep sea research II*, **47** (2010) 3119-3140.
181. Westerlund, S. and Ohman P. Cadmium, copper, cobalt, nickel, lead, and zinc in the water column of the Weddel Sea, Antarctica. *Geochimica et cosmochimica acta,* **8** (1991), 2127-2146.
182. Whitworth, S. and Peterson ,R. G. Volume transport of the Antarctic Circumpolar Current from bottom pressure meaurements. *Journal of physical oceanography,* **25** *(*1985) 810-816.
183. Zabel, T. F. Current standards and their relation to environmental behaviour and effects: the case of Pb. *Science of Total Environmental*, **78** (1989) 187-204.
184. Zhang, Y., Obata, H., and Nozaki, Y. Silver in the Pacific Ocean and the Bering Sea. *Geochemistry Journal*, **38** (2004) 623–633.
185. Zubkov, M.V., Sleigh, M.A., Burkill, P., Leakey, R.J.G. Picoplankton community structure on the Atlantic Meridional Transect: a comparison between seasons. *Progress in Oceanography*, **45** (2000) 369-386.

Appendix

	Sal	T	Cond	Dens	O2	O%	pH	Eh	Chl-a	NO3	NO2	NH4	DIN	PO4	Si	Cdtot	Cddis	Cdph	Cdpa	Pbtot	Pbdis	Pbpar	Pbph	Cutot	Cudis	Cupa	Cuph
Salinity	1,00	-0,17	**0,94**	**1,00**	0,07	0,21	-0,04	0,00	0,26	-0,12	-0,19	**-0,46**	-0,29	-0,09	-0,14	-0,11	-0,18	-0,11	0,10	0,04	-0,18	0,14	0,02	**-0,57**	0,06	**-0,65**	0,16
T		1,00	0,17	-0,18	-0,11	-0,02	-0,38	**0,49**	-0,07	-0,30	0,10	-0,12	-0,34	-0,27	**-0,69**	**-0,71**	**-0,78**	**-0,71**	0,06	-0,30	-0,14	-0,28	-0,25	-0,18	**-0,63**	0,14	0,22
Cond			1,00	**0,94**	0,03	0,20	-0,17	0,16	0,24	-0,22	-0,14	**-0,50**	**-0,40**	-0,19	-0,38	-0,36	**-0,45**	-0,36	0,12	-0,06	-0,23	0,05	-0,07	**-0,63**	-0,16	**-0,60**	0,24
Density				1,00	0,06	0,20	-0,03	-0,01	0,26	-0,12	-0,19	**-0,45**	-0,28	-0,10	-0,13	-0,10	-0,17	-0,09	0,10	0,05	-0,17	0,15	0,03	**-0,56**	0,05	**-0,64**	0,17
O2diss					1,00	**0,96**	**0,58**	**-0,59**	**0,68**	-0,26	0,04	0,29	-0,15	0,04	-0,13	0,13	0,18	0,12	-0,08	0,36	0,35	0,23	0,20	0,39	0,36	0,23	0,18
O%						1,00	**0,57**	**-0,51**	**0,73**	-0,31	0,01	0,22	-0,23	0,01	-0,20	0,05	0,07	0,04	-0,03	0,33	0,31	0,21	0,15	0,29	0,27	0,17	0,28
pH							1,00	**-0,88**	0,35	-0,37	0,19	0,37	-0,23	0,30	0,04	0,19	0,34	0,18	-0,21	**0,42**	**0,56**	0,19	0,09	0,36	0,16	0,31	0,11
Eh								1,00	-0,39	0,14	-0,23	-0,28	0,03	-0,36	-0,14	-0,29	**-0,43**	-0,28	0,21	**-0,60**	**-0,57**	**-0,40**	-0,28	**-0,42**	-0,29	-0,30	-0,10
Chl-a									1,00	-0,15	-0,29	0,27	-0,05	-0,13	-0,14	0,17	0,14	0,18	0,06	0,30	0,38	0,15	0,19	0,28	0,13	0,23	**0,44**
NO3										1,00	0,03	-0,13	**0,93**	0,22	0,35	**0,41**	**0,40**	**0,41**	0,04	0,19	-0,28	0,37	0,04	0,13	0,31	-0,03	-0,24
NO2											1,00	-0,06	0,01	0,00	-0,06	-0,21	0,01	-0,21	-0,34	0,23	-0,04	0,29	0,10	-0,04	0,05	-0,07	0,02
NH4												1,00	0,23	-0,08	0,18	0,19	0,34	0,19	-0,22	0,11	0,31	-0,04	0,16	**0,42**	0,05	**0,43**	0,15
DIN													1,00	0,19	**0,41**	**0,47**	**0,52**	**0,47**	-0,04	0,22	-0,17	0,35	0,10	0,27	0,33	0,12	-0,19
PO4														1,00	0,21	0,27	0,13	0,27	0,22	0,26	0,29	0,15	-0,06	0,14	0,04	0,13	-0,02
Si(OH)4															1,00	**0,65**	**0,59**	**0,65**	0,12	0,11	-0,10	0,18	0,34	0,25	**0,52**	-0,01	-0,17
Cdtot																1,00	**0,79**	**1,00**	0,37	**0,54**	0,35	**0,45**	**0,46**	**0,46**	**0,66**	0,15	-0,03
Cddiss																	1,00	**0,79**	-0,28	**0,44**	0,33	0,34	0,27	**0,47**	**0,67**	0,16	-0,27
Cdphy																		1,00	0,37	**0,53**	0,35	**0,44**	**0,46**	**0,46**	**0,66**	0,15	-0,03
Cdpart																			1,00	0,18	0,04	0,19	0,32	0,01	0,02	0,00	0,37
Pbtot																				1,00	**0,52**	**0,90**	**0,65**	0,39	**0,41**	0,20	0,35
Pbdiss																					1,00	0,09	0,17	**0,62**	0,10	**0,61**	0,34
Pbpart																						1,00	**0,67**	0,13	**0,42**	-0,09	0,23
Pbphy																							1,00	0,22	**0,40**	0,02	0,29
Cutot																								1,00	**0,40**	**0,87**	0,14
Cudiss																									1,00	-0,10	-0,28
Cupart																										1,00	0,31
Cuphy																											1,00

Tab. A1. Correlation matrix for November the 28th 2013, December the 7th and 17th 2013 and February the 2nd, 2014 data. Boldface $p<0.05$, Underlined $p<0.10$

Regressions: $NO_3^- = 10.7\ PO_4^{3-} + 40$ $r = 0.23$ $p = 0.28$ $Si(OH)_4 = 0.44\ NO_3^- + 37$ $r = 0.35$ $p = 0.008$

	Sal	T	Cond	Den	O2dis	O%	pH	Eh	Chl-a	NO3	NO2	NH4	DIN	PO4	Si	Cdtot	Cddis	Cdph	Cdpa	Pbtot	Pbdis	Pbpar	Pbph	Cutot	Cudis	Cupa	Cuph
Salinity	1,00	-0,14	**0,95**	**1,00**	0,05	0,21	-0,02	-0,02	0,28	-0,17	-0,22	**-0,52**	-0,34	-0,06	-0,21	-0,16	-0,28	-0,16	0,13	0,03	-0,14	0,11	-0,01	**-0,58**	-0,05	**-0,65**	0,23
T		1,00	0,19	-0,15	-0,04	0,04	**-0,48**	**0,58**	-0,09	-0,22	0,17	-0,16	-0,27	**-0,46**	**-0,72**	**-0,70**	**-0,76**	**-0,70**	-0,02	-0,29	-0,30	-0,20	-0,22	-0,19	**-0,59**	0,02	0,14
Cond			1,00	**0,94**	0,03	0,22	-0,17	0,17	0,25	-0,24	-0,16	**-0,57**	-0,43	-0,21	-0,44	-0,39	**-0,52**	-0,39	0,12	-0,06	-0,24	0,05	-0,08	**-0,63**	-0,24	**-0,64**	0,27
Density				1,00	0,05	0,21	-0,01	-0,03	0,28	-0,17	-0,23	**-0,52**	-0,34	-0,05	-0,20	-0,15	-0,26	-0,15	0,13	0,04	-0,14	0,12	0,00	**-0,57**	-0,04	**-0,65**	0,23
O2diss					1,00	**0,96**	**0,67**	**-0,68**	**0,78**	-0,38	0,03	0,32	-0,26	0,00	-0,23	0,07	0,12	0,07	-0,05	0,41	**0,47**	0,26	0,26	0,43	0,29	0,39	0,40
O%						1,00	**0,64**	**-0,57**	**0,82**	-0,41	0,01	0,22	-0,32	-0,06	-0,29	-0,01	0,00	-0,01	-0,01	0,37	0,39	0,25	0,21	0,32	0,21	0,29	**0,48**
pH							1,00	**-0,87**	0,40	-0,37	0,23	**0,45**	-0,20	0,27	0,15	0,27	**0,50**	0,27	-0,27	**0,45**	**0,55**	0,27	0,19	0,39	0,44	0,27	0,09
Eh								1,00	-0,43	0,11	-0,26	-0,34	-0,01	-0,36	-0,24	-0,37	**-0,59**	-0,36	0,25	**-0,63**	**-0,57**	**-0,47**	-0,38	-0,44	**-0,59**	-0,28	-0,08
Chl-a									1,00	-0,10	-0,21	0,19	-0,04	-0,19	-0,25	0,18	0,17	0,18	0,05	0,36	0,38	0,25	0,24	0,28	0,18	0,25	**0,48**
NO3										1,00	-0,06	-0,08	**0,94**	**0,39**	0,38	0,39	0,34	0,39	0,12	0,15	-0,19	0,29	-0,02	0,14	0,19	0,08	-0,16
NO2											1,00	0,11	-0,02	0,02	-0,02	-0,23	-0,01	-0,24	-0,33	0,20	0,05	0,22	0,10	-0,04	-0,01	-0,04	0,06
NH4												1,00	0,25	-0,10	0,08	0,15	0,38	0,14	-0,29	0,18	0,34	0,05	0,07	**0,48**	0,07	**0,53**	0,20
DIN													1,00	0,35	0,39	0,42	**0,46**	0,42	0,01	0,21	-0,08	0,29	0,01	0,29	0,21	0,26	-0,09
PO4														1,00	0,40	**0,48**	0,40	**0,48**	0,17	0,38	0,20	0,36	0,14	0,17	0,40	0,04	-0,09
Si(OH)4															1,00	0,60	**0,53**	**0,60**	0,18	0,12	-0,01	0,15	0,30	0,27	0,50	0,11	-0,14
Cdtot																1,00	**0,76**	**1,00**	**0,47**	**0,56**	**0,52**	0,42	0,44	**0,50**	**0,71**	0,30	0,08
Cddiss																	1,00	**0,76**	-0,22	**0,46**	**0,60**	0,25	0,16	**0,54**	**0,58**	0,39	-0,17
Cdphy																		1,00	**0,46**	**0,55**	**0,51**	0,41	0,43	**0,49**	**0,71**	0,29	0,08
Cdpart																			1,00	0,22	-0,04	0,29	0,44	0,02	0,27	-0,09	0,36
Pbtot																				1,00	**0,62**	0,91	**0,72**	0,40	**0,53**	0,25	0,41
Pbdiss																					1,00	0,25	0,34	**0,67**	**0,49**	**0,58**	0,29
Pbpart																						1,00	**0,72**	0,14	0,40	0,00	0,35
Pbphy																							1,00	0,25	**0,48**	0,10	0,39
Cutot																								1,00	**0,55**	**0,94**	0,15
Cudiss																									1,00	0,25	-0,07
Cupart																										1,00	0,20
Cuphy																											1,00

Tab. A2. Correlation matrix for December the 7th and 17th 2013 and February the 2nd, 2014 data. Boldface $p<0.05$, Underlined $p<0.10$

Regressions: $NO_3^- = 20.7\ PO_4^{3-} + 29$ $r = 0.39$ $p = 0.09$ $Si(OH)_4 = 0.43\ NO_3^- + 35$ $r = 0.38$ $p = 0.10$

	Sal	T	Cond	Dens	O2dis	O%	pH	Eh	Chl-a	NO3	NO2	NH4	DIN	PO4	Si	Cdtot	Cddis	Cdph	Cdpa	Pbtot	Pbdis	Pbpa	Pbph	Cutot	Cudis	Cupa	Cuph
Salinity	1,00	-0,07	**0,96**	**1,00**	-0,01	0,18	-0,17	0,07	0,36	-0,08	-0,29	**-0,77**	-0,30	-0,06	-0,25	-0,16	-0,32	-0,16	0,19	0,05	-0,20	0,15	0,01	**-0,61**	-0,07	**-0,70**	0,33
T		1,00	0,23	-0,09	0,06	0,15	-0,35	0,50	-0,16	**-0,69**	0,32	-0,16	**-0,64**	**-0,73**	**-0,83**	**-0,79**	**-0,79**	**-0,79**	-0,13	-0,38	-0,35	-0,31	-0,31	-0,34	**-0,70**	-0,14	0,09
Cond			1,00	**0,95**	0,01	0,22	-0,27	0,21	0,30	-0,28	-0,18	**-0,80**	-0,48	-0,27	-0,49	-0,39	**-0,55**	-0,39	0,14	-0,06	-0,30	0,06	-0,08	**-0,69**	-0,28	**-0,72**	0,35
Density				1,00	-0,01	0,18	-0,16	0,06	0,36	-0,07	-0,30	**-0,77**	-0,29	-0,05	-0,24	-0,15	-0,31	-0,15	0,19	0,06	-0,20	0,16	0,02	**-0,60**	-0,06	**-0,70**	0,33
O2diss					1,00	**0,95**	**0,74**	**-0,72**	**0,82**	-0,27	0,12	0,08	-0,20	0,27	-0,26	0,11	0,14	0,10	-0,02	0,50	**0,59**	0,34	0,29	**0,57**	0,48	0,50	0,35
O%						1,00	**0,72**	**-0,59**	**0,87**	-0,35	0,09	-0,04	-0,31	0,17	-0,33	0,01	0,00	0,01	0,02	0,44	0,48	0,32	0,22	0,41	0,36	0,35	0,48
pH							1,00	**-0,88**	**0,66**	0,10	0,22	0,47	0,23	0,48	0,27	0,38	**0,55**	0,37	-0,16	**0,66**	**0,65**	0,51	0,37	**0,73**	**0,63**	**0,64**	0,26
Eh								1,00	**-0,60**	-0,25	-0,22	-0,35	-0,32	**-0,61**	-0,27	-0,42	**-0,60**	-0,42	0,17	**-0,77**	**-0,69**	**-0,63**	-0,50	**-0,65**	**-0,73**	-0,50	-0,19
Chl-a									1,00	-0,10	-0,20	-0,18	-0,14	0,25	-0,19	0,23	0,22	0,23	0,06	0,47	0,51	0,34	0,22	0,33	0,48	0,21	0,37
NO3										1,00	-0,03	0,34	**0,96**	**0,65**	0,49	**0,54**	**0,63**	**0,55**	-0,03	0,21	0,01	0,25	-0,12	0,10	0,36	-0,02	-0,22
NO2											1,00	0,39	0,09	0,12	-0,14	-0,26	-0,09	-0,27	-0,29	0,33	0,17	0,34	0,18	0,07	-0,18	0,15	0,40
NH4												1,00	**0,60**	0,26	0,35	0,15	0,46	0,15	-0,40	0,12	0,15	0,08	0,03	**0,54**	0,23	**0,56**	-0,29
DIN													1,00	**0,63**	0,53	0,51	**0,68**	0,51	-0,15	0,22	0,06	0,24	-0,09	0,25	0,37	0,15	-0,27
PO4														1,00	**0,62**	**0,75**	**0,66**	**0,75**	0,25	**0,57**	0,47	0,48	0,35	0,44	**0,72**	0,25	0,33
Si(OH)4															1,00	**0,71**	**0,64**	**0,71**	0,22	0,22	**0,22**	0,17	0,35	0,40	0,52	0,27	-0,02
Cdtot																1,00	**0,77**	**1,00**	0,49	**0,56**	**0,55**	0,43	0,44	0,51	**0,82**	0,29	0,04
Cddiss																	1,00	**0,77**	-0,18	0,49	**0,65**	0,31	0,19	**0,63**	**0,67**	0,50	-0,21
Cdphy																		1,00	0,48	**0,55**	**0,55**	0,43	0,43	0,50	**0,81**	0,29	0,04
Cdpart																			1,00	0,19	-0,04	0,25	0,42	-0,09	0,33	-0,24	0,37
Pbtot																				1,00	**0,64**	**0,94**	**0,74**	0,35	**0,66**	0,17	0,39
Pbdiss																					1,00	0,33	0,41	**0,73**	**0,67**	**0,62**	0,15
Pbpart																						1,00	**0,72**	0,10	0,50	-0,08	0,41
Pbphy																							1,00	0,19	**0,58**	0,01	0,37
Cutot																								1,00	**0,64**	**0,95**	-0,09
Cudiss																									1,00	0,38	0,01
Cupart																										1,00	-0,12
Cuphy																											1,00

Tab. A3. Correlation matrix for December the 17th 2013 and February the 2nd, 2014 data. Boldface $p<0.05$, Underlined $p<0.10$

Regressions: $NO_3^- = 34.5\ PO_4^{3-} + 25$ $r = 0.65$ $p = 0.01$ $Si(OH)_4 = 0.69\ NO_3^- + 18$ $r = 0.49$ $p = 0.07$

	Sal	T	Cond	Den	O2dis	O%	pH	Eh	Chl-a	NO3	NO2	NH4	DIN	PO4	Si	Cdtot	Cddis	Cdph	Cdpa	Pbtot	Pbdis	Pbpa	Pbph	Cutot	Cudis	Cupa	Cuph
Salinity	1,00	**-0,96**	**-0,92**	**1,00**	-0,67	-0,58	-0,04	-0,27	-0,18	**0,87**	**-0,75**	-0,07	**0,86**	**0,84**	**0,95**	**0,95**	**0,84**	**0,95**	0,47	0,18	0,21	0,12	0,35	0,45	**0,77**	-0,21	-0,14
T		1,00	**0,99**	**-0,97**	**0,81**	**0,74**	0,19	0,05	0,34	**-0,89**	**0,82**	0,05	**-0,87**	-0,71	**-0,95**	**-0,84**	**-0,84**	**-0,85**	-0,32	0,01	-0,09	0,09	-0,36	-0,27	-0,69	0,33	0,33
Cond			1,00	**-0,93**	**0,85**	**0,80**	0,26	-0,07	0,43	**-0,85**	**0,84**	0,04	**-0,85**	-0,63	**-0,93**	**-0,77**	**-0,81**	**-0,77**	-0,23	0,12	-0,01	0,20	-0,39	-0,15	-0,63	0,39	0,42
Density				1,00	-0,69	-0,60	-0,06	-0,24	-0,20	**0,87**	**-0,78**	-0,07	**0,86**	**0,82**	**0,96**	**0,93**	**0,84**	**0,93**	0,46	0,14	0,19	0,08	0,36	0,43	**0,77**	-0,23	-0,17
O2diss					1,00	**0,94**	0,34	-0,30	0,63	**-0,82**	0,49	-0,04	**-0,83**	-0,29	-0,67	-0,51	**-0,79**	-0,51	0,15	0,08	-0,14	0,21	0,02	0,11	-0,35	0,41	0,64
O%						1,00	0,65	-0,53	**0,83**	**-0,77**	0,51	0,17	**-0,74**	-0,27	-0,54	-0,44	-0,67	-0,44	0,12	0,13	-0,10	0,26	-0,15	0,29	-0,34	0,58	**0,73**
pH							1,00	**-0,81**	**0,86**	-0,28	0,24	0,53	-0,17	-0,07	0,07	-0,04	-0,07	-0,05	0,03	0,16	0,02	0,23	-0,40	0,57	-0,11	0,66	0,58
Eh								1,00	**-0,81**	0,00	-0,10	-0,04	-0,01	-0,40	-0,27	-0,40	-0,17	-0,39	-0,43	-0,54	-0,34	-0,58	0,25	**-0,83**	-0,16	-0,70	**-0,79**
Chl-a									1,00	-0,51	0,21	0,23	-0,46	-0,09	-0,09	-0,10	-0,29	-0,11	0,20	0,13	0,05	0,17	-0,26	0,51	-0,18	0,66	**0,77**
NO3										1,00	-0,54	-0,11	**0,98**	**0,72**	**0,77**	**0,85**	**0,79**	**0,85**	0,38	0,24	0,26	0,18	0,18	0,32	**0,75**	-0,33	-0,41
NO2											1,00	-0,01	-0,54	-0,54	**-0,82**	-0,59	-0,46	-0,60	-0,39	0,44	0,32	0,45	**-0,72**	-0,09	-0,62	0,44	0,30
NH4												1,00	0,10	-0,28	0,03	-0,22	0,01	-0,22	-0,36	-0,31	-0,26	-0,29	-0,09	-0,09	0,10	-0,18	-0,33
DIN													1,00	0,66	**0,77**	**0,80**	**0,80**	**0,81**	0,30	0,18	0,21	0,13	0,15	0,30	**0,78**	-0,37	-0,48
PO4														1,00	0,70	**0,94**	0,61	**0,94**	**0,74**	0,46	0,27	0,50	**0,49**	0,62	**0,83**	-0,09	0,13
Si(OH)4															1,00	**0,82**	**0,75**	**0,82**	0,38	-0,06	-0,03	-0,07	0,36	0,45	0,64	-0,10	-0,11
Cdtot																1,00	**0,78**	**1,00**	0,64	0,43	0,39	0,38	0,30	0,58	**0,82**	-0,13	0,01
Cddiss																	1,00	**0,78**	0,02	0,37	0,53	0,20	0,01	0,15	0,51	-0,28	-0,27
Cdphy																		1,00	0,64	0,42	0,39	0,38	0,30	0,58	**0,82**	-0,13	0,01
Cdpart																			1,00	0,23	-0,02	0,36	0,45	**0,74**	0,69	0,15	0,36
Pbtot																				1,00	**0,84**	**0,94**	-0,37	0,43	0,19	0,27	0,39
Pbdiss																					1,00	0,61	-0,49	0,09	0,11	0,00	0,12
Pbpart																						1,00	-0,24	0,58	0,21	0,40	0,50
Pbphy																							1,00	-0,03	0,53	-0,48	-0,17
Cutot																								1,00	0,43	0,63	0,63
Cudiss																									1,00	-0,43	-0,26
Cupart																										1,00	**0,86**
Cuphy																											1,00

Tab. A4 Correlation matrix for February the 2nd, 2014 data. Boldface $p<0.05$, Underlined $p<0.10$

Regressions: $NO_3^- = 41.7\ PO_4^{3-} + 22$ $r = 0.72$ $p = 0.04$ $Si(OH)_4 = 1.20\ NO_3^- - 11$ $r = 0.77$ $p = 0.03$